UNIVERSITY OF SASSARI

Department of Biomedical Sciences

International PhD School in Life Sciences and Biotechnologies

Curriculum Biochemistry, Physiology and Molecular Biology

Cycle XXX

Director: Professor Leonardo A. Sechi

The role of mechanical stress in progression of intima hyperplasia associated to vein coronary bypass grafts disease

Supervisor:

Prof. Gianfranco Pintus

Co-Supervisor:

Dr. Gaia Spinetti

PhD Candidate:

Davide Maselli

November 2017

Abstract

Coronary artery bypass grafting is a surgical procedure introduced to restore the blood circulation into the myocardium after an ischemic event. Despite progress in the use of arterial conduits, saphenous vein (SV) remains one of the most used vessels for the bypass. A short time after bypass implantation SV undergoes intima hyperplasia (IH) that progressively reduce its patency. One trigger cause of IH is the hemodynamic changes in the blood flow with higher sheer stress on the endothelial layer a radial deformation on the wall of the vein.

The aim of this project was to understand the role of saphenous vein progenitors (SVP) in the progression of IH. These cells with high differentiation potential are the pericytes of *vasa vasorum* in the tunica adventitia.

By in vitro and ex vivo models of mechanical stress we demonstrated the susceptibility of SVPs to the strain that causes a cytoskeletal reorganization and the acquisition of a potential migratory phenotype. SVPs showed the stimulus-related up-regulation of Amphoterin-Induced Gene And Open Reading Frame 2 (AMIGO2), that may have a role in the mechanical activation via prosurvival and migratory effects.

For the first time has been described the presence of AMIGO2 in SVPs and its relationship with mechanical stress. Migratory phenotype acquisition and AMIGO2 overexpression demonstrate how SVPs are potential targets for further study of IH.

Dr. Davide Maselli, *"The role of mechanical stress in progression of intima hyperplasia associated to vein coronary bypass grafts disease.",* PhD thesis in Biochemistry, Physiology and Molecular Biology of International PhD School in Life Sciences and Biotechnologies, University of Sassari.

Acronyms and Abbreviations

AdvSca1	Sca1-positive vascular progenitor cells population
AMIGO	Amphoterin-Induced Gene And Open Reading Frame
Angpt-2	Angiopoietin 2
BBB	Blood–Brain-Barrier
BM	Basal Membrane
CABG	Coronary Artery Bypass Grafting
CEACAM1	Carcinoembryonic Antigen-Related Cell Adhesion Molecule 1
CNS	Central Nervous System
DMEM	Dulbecco Modified Eagle's Medium
ECM	Extracellular Matrix
ECs	Endothelial Cells
EPCs	Endothelial Progenitor cells
ET-1	Endothelin-1
FGF	Fibroblast Growth Factor
HAECs	Human Aortic Endothelial cells
HEK	Human Embryonic Kidney
HSCs	Hematopoietic Stem cells
HUVECs	Human Umbilical Vein Endothelial cells
ICAM	Intracellular Adhesion Molecule
IGF	Insulin like Growth Factor
IH	Intima Hyperplasia
IMA	Internal Mammary Artery

IPA	Ingenuity Pathway Analysis
LAD	Left Anterior Descending
LCX	Left Circumflex Artery
MAPKs	Mitogen-Activated Protein Kinases
MCP-1	Monocyte Chemoattractant Protein-1
MS	Multiple Sclerosis
MSCs	Mesenchymal Stromal cells
NFATc2	Nuclear Factor of Activated T-cells cytoplasmic 2
NFkappaB	Nuclear Factors kappa B
NG2	Neuron-Glial 2
NI	Neointima
NO	Nitric Oxide
NT	No-touch Technique
NVU	Functional Neurovascular Unit
P/S	Penicillin/Streptomycin
PCs	Pericytes
PDGF	Platelet-Derived Growth Factor
PDGFRβ	Platelet-Derived Growth Factor Receptor β
PIT	Pathologic Intimal Thickening
PVDF	Polyvinylidene Difluoride
RA	Rheumatoid Arthritis
RBC	Red Blood Cell
RCA	Right Coronary Artery
ROS	Reactive Oxygen Species
RTN4	Reticulon 4

Shh	Sonic hedgehog
SLRP	Small Leucine-Rich Proteoglycans
Sp1	Specificity protein 1
SSREs	Shear Stress Response Elements
SV	Saphenous Vein
TdT	Terminal deoxynucleotidyl Transferase
TNF-α	Tumor Necrosis Factor-α
VECAM	Vascular Endothelial Cell Adhesion Molecule
VW-MPSCs	Vascular Wall-resident Multipotent Stem Cells
VZ	Vasculogenic Zone
α-SMA	α-Smooth Muscle Actin

Table of contents

INTRODUCTION

Myocardial infarction occurs when the arteries that surrounded the cardiac muscle are obstructed. The stenosis hampers the oxygenated blood flow to cardiomyocytes that start to die and by the time the necrotic cells are replaced with non-functional scar tissue. Coronary Artery Bypass Grafting (CABG)is a surgical technique introduced more than 50 years ago to restore blood flow in the ischemic area of the heart. Several vessels can be used as a bridge upstream and downstream of the obstruction, one of the most used is the great saphenous vein (SV) even if it is not free from contra-indications. SV bypass, in fact, progressive thickening due to the accumulation of cells in the intima layer. This arterialization process of the vein named intima hyperplasia (IH) starts few hours after the bypass implantation, and in 10-15 years caused the occlusion of 60% of the SV lumen with consequent need of a stent implantation or a re-intervention. IH involves loss of typical cells phenotype in the vessels and the beginning of proliferation, migratory and invasion events. *This project investigates the cellular and molecular basis of IH associated with vein graft disease, using a multidisciplinary approach focused on mechanobiology.*

1.1 Coronary circulation

Coronary arteries are the arteries that supply oxygenated blood to the cardiac cells (cardiomyocytes). Cardiomyocyte metabolism relies almost exclusively on oxidative phosphorylation carried on mitochondria that are abundant in these cells. Oxidative phosphorylation requires oxygen, making cardiac myocytes extremely vulnerable to ischemia. The coronary arteries are distal to the aortic valve, initially running along the external surface of the heart *(epicardial coronary arteries)* and then penetrating the myocardium *(intramural arteries)*. The intramural arteries gradually decrease by diameter, forming a dense network of capillaries enveloping individual cardiac muscle cells. The three major epicardial coronary arteries are the left anterior descending (LAD) and the left circumflex (LCX) arteries, both rising from branches of the left (main) coronary artery, and the right coronary artery (RCA). Branches of the LAD are called “diagonal” and “septal perforators," and those of the LCX is "obtuse marginals." Most of the blood flow to the myocardium during ventricular diastole, when the microcirculation is not compressed by cardiac contraction. Over time, coronaries may undergo an obstructive pathological condition named atherosclerosis, in which heart arteries are occluded by cholesterol deposits. These diseases fall into the broader group of cardiovascular diseases and contribute to making them the leading cause of death in the world.[1]

1.2 Atherosclerosis

Atherosclerosis is a pathological condition in which a plaque builds up in the luminal side of the artery reducing blood flow and lowering the oxygenation of downstream tissues. At the injury site, the arterial wall becomes hard, stiff and swollen due to calcium and fat deposits and heavily infiltrated with inflammatory cells. Atherosclerosis is a dynamic multifactorial process that starts with a pathologic intimal thickening (PIT), which is characterized by the presence of a cellular lipid deposition within the intima, close to the media.[2]Subsequently, inflammatory cells (macrophages and T-lymphocytes) from the blood infiltrate the fat deposit in the attempt to remove it. The more advanced stage of the atherosclerotic lesion, known as fibroatheroma, is characterized by the presence of a lipid-rich necrotic core (mainly cholesterol and cholesterol esters) encapsulated by fibrotic tissue.[3]

Any artery of the body can be affected, and different diseases may develop as a consequence:

Carotid Artery Disease: occurs when atherosclerosis affects the carotid arteries. On each side of the neck, there are two pairs of carotid arteries: the external carotid artery (ECA) supplies blood to the face, scalp, and neck while the internal carotid artery (ICA)supplies the brain. Atherosclerosis involves frequently the ICA at the branching site. and is responsible for strokes when the blood flow is completely blocked or transitory ischemic attacks (TIA) when the blood flow is reversibly blocked.

Peripheral Artery Disease: is a pathological condition in which there is an obstructive lesion located in the arteries of the lower extremities with hypoperfusion of the legs. The consequences range from numbness to pain, infections or gangrene and an increased chance of experiencing a heart attack.

Chronic Kidney Disease: occurs when renal arteries are occluded. Over time such an occlusion causes loss of kidney function that leads to neuromuscular symptoms, peripheral neuropathies, hypertension and metabolic disorder.

Coronary Artery Disease: occurs when an atherosclerotic plaque builds up in one of the coronary arteries. The reduction of blood flow to the heart can cause angina (chest pain or discomfort) or heart attack. A heart attack consists in the death of the cardiac muscle due to prolonged severe ischemia. It can occur at any age, but the probability rises progressively with age and when predispositions to atherosclerosis are present. **The complete coronary arterial occlusion** is a step by step phenomenon which starts with a sudden

change in the atherosclerotic plaque. This may consist of intraplaque hemorrhage, erosion or ulceration, rupture or fissuring. When sub-endothelial collagen is exposed, the platelets start to adhere and aggregate to form micro thrombi. Vasospasm is stimulated by mediators released from platelets and the coagulation pathway is activated. Within minutes, the thrombus evolves to completely occlude the lumen of the vessel.

In most cases, heart attack produces permanent damage to the myocardium. This occurs when its perfusion is severely reduced for an extended time, usually at least 2 to 4 hours. Necrosis begins in a small zone of the myocardium beneath the endocardial surface in correspondence to the ischemic site and it is usually complete within 6 hours. The extent of myocardial damage depends on the heart portion supplied by the occluded artery (**Figure 1**).[1]

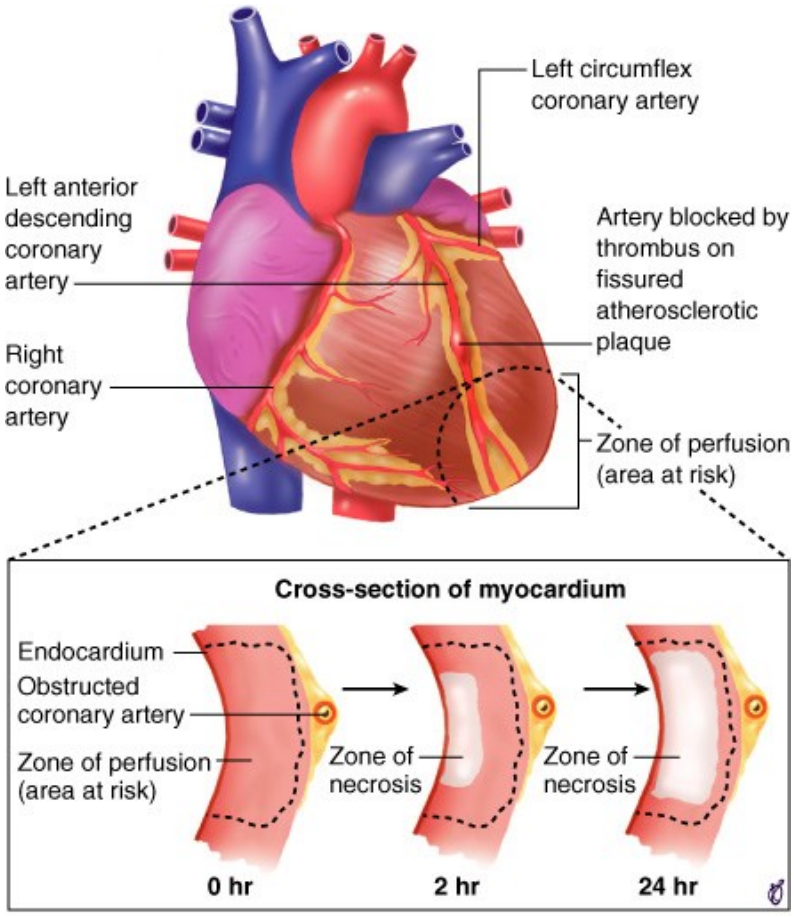

Figure 1 The coronary arteries and their obstruction. *At the top is a schematic representation of the coronary arteries, the left coronary artery is divided into the left anterior descending (LAD) and left circumflex (LCX), and the right coronary artery (RCA). An atherosclerotic plaque in the LAD that has evolved in a thrombus. At the bottom is the scheme of myocardial necrosis progression of the artery. Ischemia starts spreading in the zone of myocardium beneath the obstructed artery. The whole region depends on the occluded vessel for perfusion in the area at risk of necrosis. Image from Pathologic Basis of Disease.6th ed. Philadelphia, WB Saunders, 1999.*

1.3 Coronary artery bypass grafting: arterial and vein conduit

A surgical procedure commonly used to avert a heart attack and restoring blood flow is the Coronary artery bypass grafting (CABG). CABG consists in using vascular grafts as a bridge that connects ascending aorta and one or more coronary arteries, upstream and downstream of a severe lesion with a stenosis of about 70-75%.[4] The severity of the lesion is evaluated by a coronary angiography. With this kind of obstruction, the heart muscle cannot receive the adequate blood or oxygen supply it needs, and this leads to further pathologic conditions such as angina or heart attack, where permanent heart damage occurs.[5, 6]However, not all of the coronary branches can undergo revascularization because of the size limitations: the vessel diameter should be greater than 1-1.5mm. Despite the number of CABG procedures carried out across the majority of industrialized countries between 2000 and 2012 decreased, CABG is still one of the most common types of open-heart surgery to treat coronary disease.[7]

The success of the surgery is related to the choice of the vessel used as bypass arteries as detailed in next paragraphs. Currently, the internal mammary artery (IMA), the radial artery (RA) and gastroepiploic artery (GA) and veins like the saphenous vein (SV) have been used.[8, 9] The conduit evaluation could be based on a combination of clinical, angiographic or other imaging procedures in patients with CABG, but traditionally the graft patency has been a high priority for surgeons.[10]

1.3.1 Internal mammary artery

IMA rises up from the first portion of the subclavian artery, descend below, then transverse the first rib to enter the thorax in the first intercostal space and ends at the 6th intercostal space. The use of IMA as bypass is now the “gold standard” of coronary artery revascularization.[11] The size matches well with most coronary arteries. It needs a single point of anastomosis and both (right and left IMA) could be used as bypass graft.[12] Several studies showed the importance of its use on the longevity of patients who are operated on for coronary artery disease.[13, 14] In general, IMA graft patency is better than SV patency,[15] the main limitations associated with this conduit are an increased incidence of mediastinitis in patients with diabetes mellitus and poorer results, compared to SV, when bypassing target vessels with less than 70% stenosis.[16, 17]

1.3.2 Radial artery

The RA is the lateral branch of the bifurcation of the brachial arteries. It extends from the elbow crease to the palm of the hand. The RA was proposed as a coronary artery bypass for the first time by Carpentier et al. in1973[18] with favorable early results. It was soon abandoned due to short-term occlusion rate (35–50%) and spasm.[19] Currently, with surgical techniques that preserve muscle layer and with an adequate pharmacologic postoperative prophylaxis, most of the limitations can be prevented; and the RA represents the second elective arterial graft after the IMA.[20] The RA is routinely harvested from the non-dominant arm because of concerns that RA harvesting could adversely affect the sensory and motor function of the hand.[21] Some studies suggested comparable patency rates between the RA and SV.[22]

1.3.3 Gastroepiploic artery

The GA derives from the gastroduodenal artery, runs along the greater curvature of the stomach, between the layers of the gastrocolic ligament and ends anatomising with the left gastroepiploic artery, a branch of the splenic artery. GA has been used as CABG since 1986. This conduit has the main advantage of having a coronary-sized fit**.** The issues related with the GA grafting are the postoperative effects due to the laparotomy incision to harvest the artery, the risk of an incisional hernia, the difficulties in obese patients, and the risk of development of atherosclerosis in celiac and gastroduodenal arteries.[23] Randomized controlled trials have shown that the SV has better patency than GA both in early (6 months) and midterm (3 years) results when used for myocardial revascularization.[24]

1.3.4 Saphenous vein

The great saphenous vein is a superficial and subcutaneous vein of the leg, located 2cm anterior to the medial malleolus (where it is easily visible) and ascends posteriorly up to the tibial border before emptying into the femoral vein through the saphenofemoral junction. It receives numerous tributaries and contains 10-20 valves. The vein grafts must be placed in a reversed position to allow free blood flow via the venous valves.

The first use of SV as a bypass conduit dates back to 1967 when Favoloro et al. reported using SV to restore coronary artery blood flow in 171 patients.[25]

The SV is currently the most frequently used conduit in patients undergoing CABG, because it is easy to harvest with minimal side effects, a diameter that fits wits the

coronary arteries and the possibility to be used for multiple. However structural changes occur. The increase in the vein wall thickness, namely intima hyperplasia, lead to the reduction in vein patency in the early months after CABG; an additional 1% to 5% of the bypass occludes each year beyond the first year. Therefore, the early patency rate of SV around 80-90% decreases to 50-60% 10 years after CABG.[26]

The choice of the conduit is still a matter of surgical preference and each surgeon must make decisions considering the balance between risks and benefits for each patient. The difference between the patency of vein and arterial grafts start becoming significant after 7 to 8 years and many surgeons prefer vein grafts over GA and RA due to their medium-term patency.[27] That is why, despite all the associated problems, SV is still an important conduit.

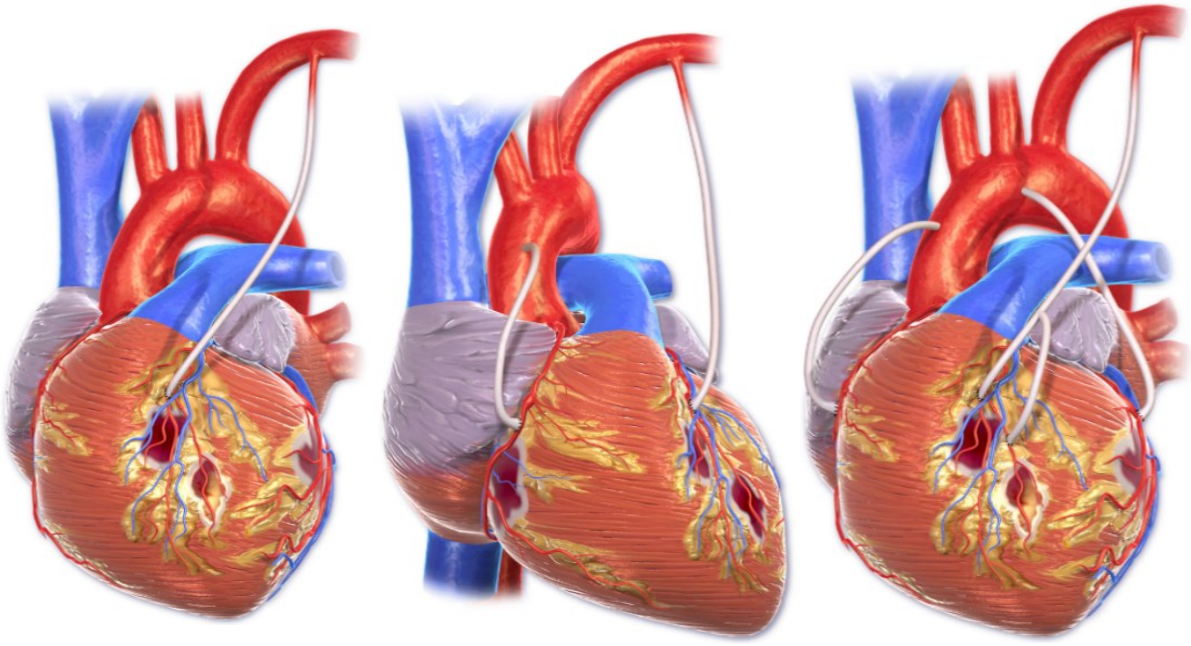

Figure 2 Number of bypass and type of conduit. *These coronaries can undergo a bypass because their diameters are: the LAD, the RCA, the LCX and the first diagonal artery of the LAD. (A) Single bypass performed with left IMA to restore the flux in the LAD. With a single point of anastomosis, IMA represents the gold standard in case of single graft. (B-C) Double and quadruple bypass performed with left IMA and SV, RA or GA: to restore the flow in the LAD and respectively in the RCA (B) and in RCA, in the first diagonal artery of the LAD and LCX (C). Images from en.wikipedia.org*

1.4 Intimal hyperplasia in saphenous vein

Intima hyperplasia (IH) is the formation of a thick layer of neo-intima inside the lumen of SV, which can lead to vessel occlusion. IH is a physiologic healing response to injury of the blood vessel wall. The causes of IH can be traced to the consequence of technical surgical factors occurring during SV harvesting[28] and the influence of the new hemodynamic forces like the pulsatile flow and shear stress.[29] These lead to in situ damage to the endothelial layer, smooth muscle cells, and fibroblast activation and the release of growth factors.[30]

1.4.1 The surgical side: no-touch method

en the vein is stripped out its surrounding tissue, vascular spasm often occurs, the endothelial layer can be particularly damaged.[28] The no-touch technique (NT) for SV graft preparation has been used since the beginning of the '90s,[31] the procedure requires that the SV is extracted from its bed with its perivascular fat pedicle and all its side branches are ligated (**Figure 3**).[32-34] No venous spasm occurs because the perivascular tissue is preserved and neither flushing nor manual dilation is required.[33]With the NT technique, it is possible to avoid direct surgical trauma. The technique also preserves the vein's cushion of perivascular fat and adventitial *vasa vasorum.*[35]

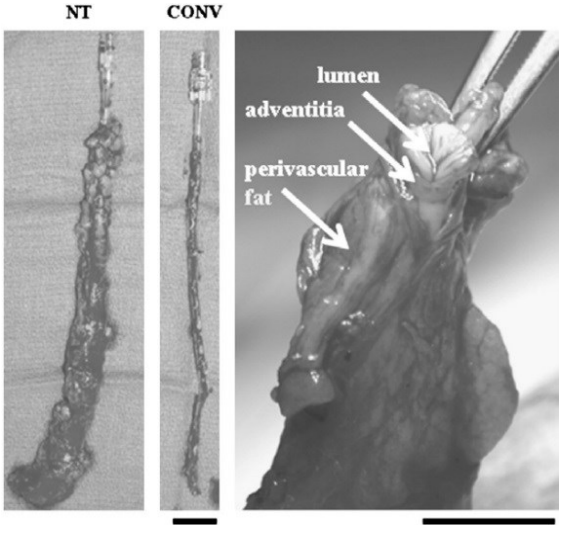

Figure 3 No-touch technique. *Representative image of SV harvesting with the conventional method (CONV) and NT. No venous spasm occurs and the vein's tunica adventitia and cushion of perivascular fat are preserved. Scale bars = 2.5 mm for left panels and 10 mm for right panel. Image from Dashwood et al., 2013.*

1.4.2 Intimal hyperplasia: hemodynamic factors

SV has venous morphofunctional characteristics and is designed to respond to linear flow and low pressure: it has a thin wall and a large lumen that help the venous to accommodate large shifts in volume with minimal change in pressure, the range is usually between 5 and 25 mmHg.[36] Arteries instead have a thick tunica media and a quantity of collagen and elastic fibers that limit their ability to expand but which provides greater resistance to vessels exposed to arterial flow that can change from 70 to 140 mmHg. So when the vein is connected to the arterial circulation in a CABG, the blood flow rate in SV is 5–10 times higher never experienced before.[37] Thus the vein needs to adapt structurally and functionally to the new local biomechanical environment.[38]The higher pressure, causes a shear stress of approximately 3-6 dynes/cm^2, instead of 0.2 dyne/cm^2 normally funded in veins; and the pulsatile flow causes a radial and circumferential deformation (tangential stress) (**Figure 4**),[39] It is known that these forces induce an increase of apoptosis with subsequent cell proliferation at the beginning.[40]

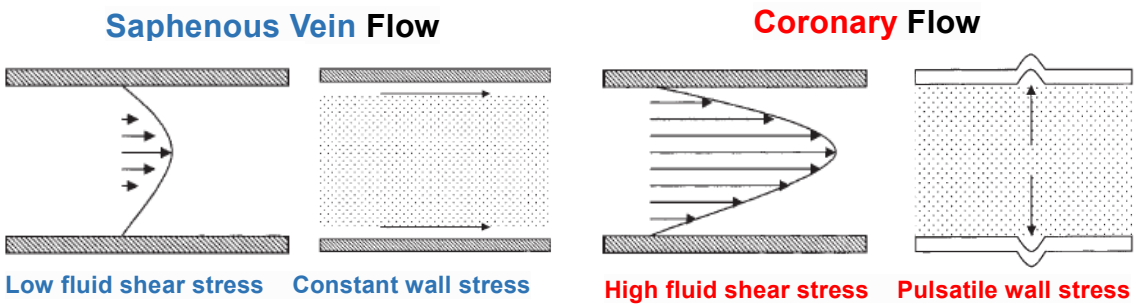

Figure 4 New hemodynamic conditions of SV. *The coronary high pressure and the pulsatile flow leads to two different types of stress on the SV wall: high fluid shear stress that causes mainly ECs damage and pulsatile wall stress which involves the full thickness of the vessel's wall. While the sheer stress has the same direction of flow, pulsatile stress stretches the SV perpendicularly causing a cyclic deformation of the vessel wall.*

1.5 Intimal hyperplasia: cellular factors

Carrell and Guthrie used the SV as a graft for arterial reconstruction in 1906 and for the first time described the IH as a "glistening substance similar in appearance to the normal endothelium".[41] Since then several studies have been carried out to understand the cellular components involved in the IH. Endothelial cell (ECs) damage is considered the first step of the process that leads to IH.[42] It is possible to recognise three different stages in its evolution distributed over time but partly overlapping: inflammatory phase, cellular proliferation phase and remodelling phase (**Figure 5**).[43]

Inflammatory phase (few hours or days after surgery). The single layer of ECs is easily damaged due to the new hemodynamic condition.[44, 45]The damaged endothelium recruits platelets and a deposition of fibrin is observed. The adhesion of platelets and then leukocytes and other inflammatory cells is mediated by selectins as intracellular adhesion molecule (ICAM) and vascular-endothelial cell adhesion molecule (VECAM) expressed by the activated ECs. The endothelial denudation leads to a loss of growth-inhibitory effect of the nitric oxide (NO) produced by EC that normally maintains the quiescence of SMCs and ECs themselves so a phase of intense replication begins.[46]

Cellular proliferation phase (days to weeks after surgery). This phase is marked by the production of growth and chemotactic factors from the activated cells of the injury site. Monocyte adhesion is an early event mediated by monocyte chemoattractant protein-1 (MCP-1). Then monocytes differentiate into tissue resident macrophages under the influence of macrophage colony stimulating factor (M-CSF).[45, 47] Activated SMCs and ECs start to produce interleukins (IL-1, IL-6, IL-8) and tumour necrosis factor-α (TNF-α) that reinforce inflammatory cell recruitment.[48, 49]Other growth factors are induced in SV graft like endothelin-1 (ET-1), platelet-derived growth factor (PDGF), fibroblast growth factor (FGF) and insulin-like growth factor (IGF), all of which promote the proliferation and migration of SMCs.[50, 51]It has also been demonstrated that the transforming growth factor-β_1(TGF-β_1)/connective tissue growth factor (CTGF) pathways mediate a conversion of fibroblasts to myofibroblasts in the adventitia layer.[52, 53]

Remodelling phase (months to year after surgery). This phase involves extra-cellular matrix (ECM) protein degradation and resynthesis. In a physiological condition, elastic fibres and laminae in the vessel wall prohibit SMCs proliferation and prevent intimal hyperplasia.[54]When the endothelial protective factors are lost, NO in particular, metalloproteinases (MMPs) production and proteoglycan synthesis are induced. Inflammatory cells can produce MMPs and other proteases as well, moreover activated

macrophages secrete cytokines that upregulate MMP gene expression in vascular cells.[55] SMCs switch from a quiescent/contractile to a migratory/secretory phenotype that starts to produce MMPs. MMP-3 is considered the protease that supports the SMC-migration the most.[56] It has also been shown that the proliferative SMCs at the superficial layers of the NI have a high concentration ofMMP-9.[57] The lost integrity of the ECM allows the migration of SMCs and myofibroblasts in the intimal layer, in which they subsequentially start the synthesis and deposition of extracellular matrix. The NI grows over the layer of platelets and fibrin resulting in a progressive increase in intimal thickness, which leads to the obstruction of the lumen and the graft failure.[58]

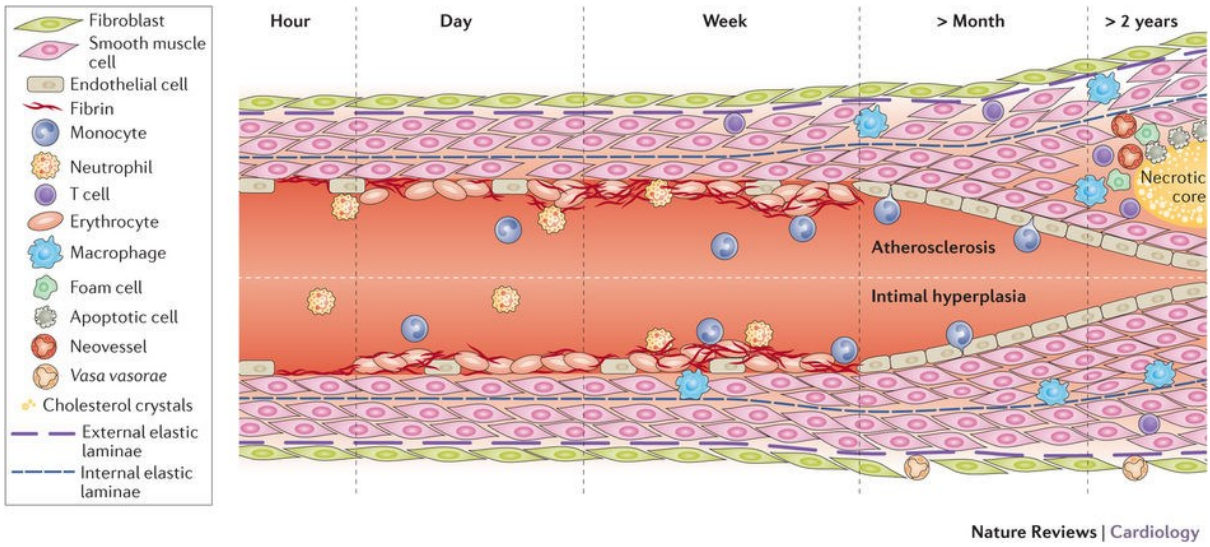

Figure 5 Intimal hyperplasia evolution. *The endothelial layer is easily damaged due to the new hemodynamic condition. Within hours, the luminal surface is covered by platelets, fibrin and white blood cells that start to infiltrate intima. SMCs in the media and fibroblasts in the adventitia are activated and start migrating towards the intima, resulting in formation of IH. Growth factors and cytokines released by cells in the vessel induce ECM protein degradation and resynthesis. That resulting in further growth of the intimal hyperplasia. Under atherogenic conditions, macrophages can uptake lipids and become foam cells. A necrotic core is formed by dying foam cells, apoptosis, and cholesterol deposits. The atherosclerotic process is depicted in the upper part of the illustration. Image from de Vries et al., 2015.*

1.6 Intimal hyperplasia: the layer changes

The SV placed into the coronary circulation is subjected to an increase in wall, sheer and tangential stress due to arterial hemodynamics. All layers are involved, and they respond according to the type of stimulus they receive and the phenotype of their cells.

1.6.1 Tunica intima

The tunica intima is essentially a monolayer of endothelial cells abutting directly on a basal lamina. The basal lamina layer can be divided into two layers due to their different aspects seen by the electron microscope. The clear layer closer to the epithelium is called lamina lucida, while the electro-dense layer is called lamina densa. The lamina densa membrane consists of collagen IV coated with Perlecan, a heparansulfate proteoglycan. The lamina lucida is made up of laminin, integrins, entactins, and dystroglycans.[59]

The conventional technique of harvesting leads to damage of intima integrity, while the NT method, with minimal surgical trauma, retains an essentially normal architecture of the cells.[60] However it has been shown that shear stress is sufficient to activate transcription factors related to the inflammatory response including nuclear factors kappa B (NF kappa B), nuclear factors of activated T-cells cytoplasmic 2 (NFATc2), and specificity protein 1(Sp1).[61] Hemodynamic forces can increase the production of reactive oxygen species (ROS) from NADPH oxidases, nitric oxide synthase (NOS), cytochrome P450, and the mitochondrial electron transport chain.[62] In addition, endothelium-dependent permeability is decreased in a vein under arterial flux.[38] As a result of all these processes inflammation is induced with subsequent endothelial damage or denudation, all mechanisms that trigger IH.

1.6.2 Tunica media

SMCs and elastin are the main component of tunica media. The elastin is arranged in fenestrated sheets (lamellae) between which are collagen fibres (mostly type I and III) and thin layers of amorphous of proteoglycans rich ECM. Thin elastic fibres connect the lamellae into a three-dimensional continuous network and connect the lamellae with the SMCs.[63] The shape of SMCs was observed to be dynamic during the development of the IH and the changes are closely associated with functional modulation. As previously discussed, SMCs under particular conditions can switch their phenotype from quiescent/contractile to migratory/secretory (**Figure 6**). It has been shown that when in IH the SMCs lose their spindle shape and there is a desmin decrease with a contemporary

increase of vimentin expression, which is associated with the secretory phenotype [64] and the reduction of cytoskeleton-associated protein smoothelin, a protein expressed in contractile SMCs.[65]Moreover, physiologically mostly of SMCs are highly aligned in the circumferential direction (perpendicular to the flow of blood), as well as ECM fibres. As a consequence of its passive extension or over-extension, the inner region of the media become straight and co-aligns close to the long axis of the vein; such an event contributes hyperplasia.[66]

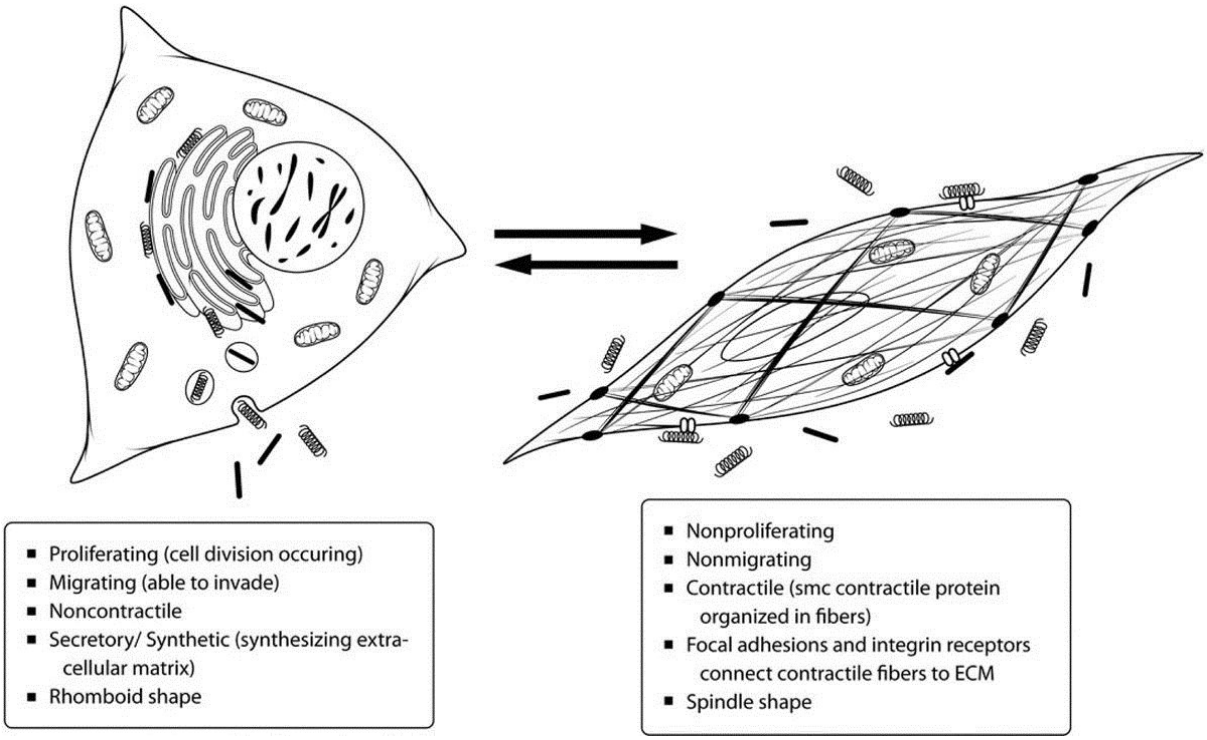

Figure 6 Phenotypic plasticity of SMCs. *Mature SMCs can switch between quiescent/contractile to a migratory/secretory phenotype. The cell on the right represents the quiescent/contractile one, with abundant fibres in the cytoplasm and many focal adhesions to connect to ECM to regulate the tension in the vessel wall. On the left the cell dedifferentiated in the migratory/secretory phenotype, whose main purpose is to repair the vessel wall by proliferation, migration, and synthetic activity. Image from Yuan, 2015.*

1.6.3 Tunica Adventitia

The tunica adventitia is the outer layer of the vascular wall, it consists of loose connective tissue (mostly collagen), fibroblasts and mast cells. There are also small vessels and nerves that serve to provide nutrition and functional molecules to intima and media because the diffusion from the blood through the lumen is inadequate in larger vessels such as the SV.

Several studies describe how the fibroblasts present in adventitia undergo activation by mechanical stimuli. This is an early phenomenon in which the cells start to proliferate and migrate into the neointima by 7–14 days after grafting. Apoptosis occurs simultaneously

with proliferation and migration and in part limits neointimal thickness.[67] The migration is associated with differentiation of fibroblasts to myofibroblasts, which migrate through the injured media of the graft to the neointima. Perivascular fibroblasts transiently acquired α-smooth muscle actin (α-SMA), and some of them expressed desmin during migration toward the vessel lumen in the initial phase of the injury.[68] These processes contribute to remodeling of the graft and the consequent increase in diameter.[69] The adventitia in the SV, like in the other large vessels, is innervated by the autonomic sympathetic, parasympathetic and sensory nerves. There is evidence of neural remodeling being time-related in SV bypass with an increasing number of nerves in the adventitia at 1 month that diminished at 6 months.[70] Many neurotransmitters that possess mitogenic properties may play a role in various stages of graft failure.[71]

1.6.4 Perivascular adipose tissue

The cushion surrounding the SV not only provides postoperative mechanical support to protect the vessel against arterial hemodynamic [72, 73] but it is also a source of adipokines which might contribute to the improved success of the grafts. One of the most important adipokines is Leptin that is demonstrated as a vasodilator in both human SV and internal mammary artery. Leptin-mediated vasodilatation is not dependent on an intact endothelium and is likely to be at least in part due to smooth muscle hyperpolarization.[74] It has been shown that TNF-α is involved in rapid phenotypic changes in adipose tissue surrounding the vessels following endovascular injury and that TNF-α stimulated VSMC proliferation and migration *in vitro.*[75, 76]Little is still known regarding the interaction between the vascular nerves and the perivascular fat although the influence of the sympathetic nervous system on adipocytes is well established with norepinephrine being the predominant neurotransmitter involved.[77]

1.6.5 Vasa vasorum

As mentioned previously, *vasa vasorum* is a complex of small vessels necessary to feed the cells of the media and adventitia. The SV vasa system is extensive and significantly more prolific compared to that in other vessels used for CABG, for example, the IMA and RA.[78] There is also a link between the *vasa vasorum* and the mechanical properties of the vessel wall. Increased luminal pressure causes deformation of the wall, inducing a shape-change, where the initially circular vasa rapidly take on an elliptical shape, causing a reduction in vessel wall irrigation [79] that leads to subsequent loss of elasticity. After the bypass surgery *vasa vasorum* are disconnected from the blood flow but in patients

undergoing CABG using the NT technique of harvesting the SV, this reconnection occurs instantly since filling of the vasa vasorum is observed at the removal of the arterial clamps. It has also been described a proliferation of native *vasa vasorum* after the graft implantation.[80]

Has been described by Campagnolo et al. a population of cells surrounding the SV *vasa vasorum* showing the typical pericytes (PCs) markers and multipotential differentiation capability.[81]Further studies on human samples in an *ex vivo* system showed that these cells undergo activation after 7 days of arterial flow stimulation showing an increase of PCs and vascular progenitor cell markers like NG2, CD44 and SM22α and the acquisition of migratory ability and an increased proliferative rate.[82]

This PhD project tried to describe the effect of mechanical stress on this population of cells around the *vasa vasorum* of the SV. How their activation occurs and how the activate state can have a role in the development of IH. The following chapters will briefly describe the essential characteristics and functions of PCs and the main features about the PCs population in SV discovered in 2010 by Campagnolo et al.

1.7 Pericytes

PCsare SMC-like contractile cells implicated in the regulation of microvasculature tone and vascular permeability.[83]They also play an important role during capillogenesis and angiogenesis, where, under the control of platelet-derived growth factor B (PDGF-B), they control proliferation and differentiation of endothelial buds.[84]PCs' modulation processes include the initial patterning of vascular networks, the regulation EPCs proliferation, and differentiation, regulation of capillary size and ECM synthesis. [85] Studies of genetic knockout mice have demonstrated that lack of pericytes leads to endothelial hyperplasia and abnormal vascular morphogenesis.[86]

1.7.1 Morphology

In 1873 Rouget described cells in frogs as “non-pigmented adventitial cells” that had encircled capillaries with cytoplasmic processes. He detailed their contractile phenotype and their ability to control capillary diameters. In 1923, the anatomist Zimmermann renamed these cells as “pericytes” (peri: around, cyte: cell).[87] Electron microscopy helped to better understand their morphology and position and pericytes have been

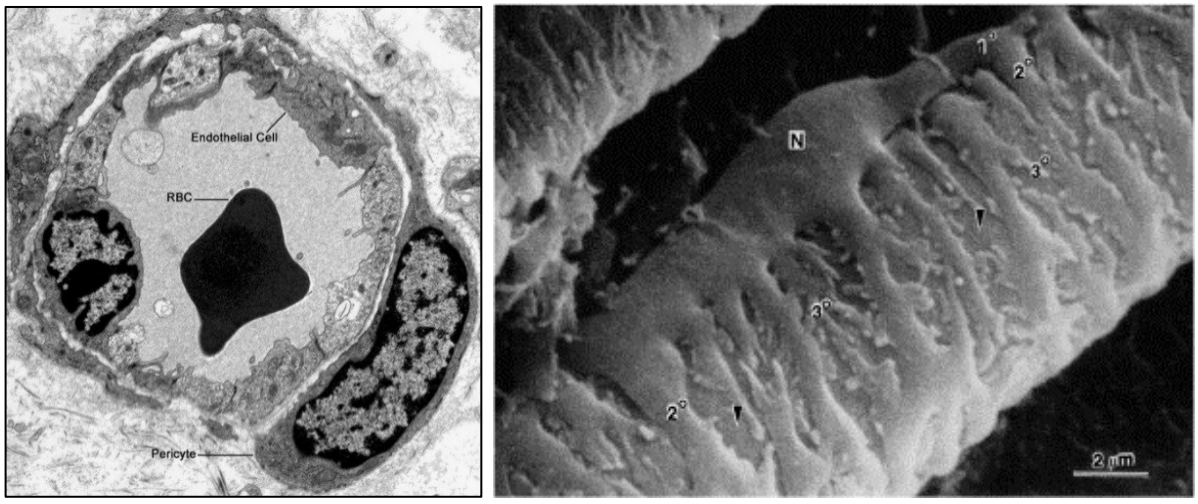

Figure 7 Pericyte morphology. *On the left, electron micrograph scan of a brain capillary with ECs, PCs and red blood cell (RBC). PCs have a prominent nucleus and limited cytoplasm embedded in the basement membrane. Image from PathologyOutlines.com.On the right electron micrograph scan of pericytes attached to the long axis of capillaries, embracing ECs. The plump nuclear area (N)is visible, a primary process (1) of the PCs paralleling the long axis of the capillary, secondary processes (2) encircling the capillary, tertiary processes (3) extending from the secondary process. Image from Shepro et al.,1993.*

described as cells residing around the endothelial layer of capillaries, having a huge nucleus oriented towards the abluminal side of the vessel and with elongated structures used to directly interact with the underneath endothelium (**Figure 7**).[88] Depending on the vascular bed their precise function and organ milieu, PCs can exhibit a wide spectrum of morphologies, from typical flat and stellate shape in the central nervous system to a more rounded shape in the kidneys.[89]PCs are embedded in the same basement membrane of the ECs and they directly contact each other at discrete points of interruption.[90] PCs and ECs interact in different ways. When pericyte protrusions are inserted in invaginations of the endothelial membrane.The interaction is called peg-and-socket. Peg-and-socket contacts contain gap junctions rich in Connexin 43 and N-cadherin- and adherens junctions β-catenin-based,[91] which are mainly involved in ion and molecule exchange.[92] PCs and ECs are also connected by adhesion plaque always in correspondence with holes in the basement membrane. Adhesion plaques anchor PCs to the matrix of fibronectin produced by ECs via integrins with the cytoskeletal actin.[93] It is thought that these junctions may be the mediators of the mechanical signals through ECs and PCs.[92] These basic features cannot be extended to immature, aging or pathological vessels. Changes in morphology and biology of pericytes are known in kidney injury,[94] aging human hippocampus,[95] diabetic ischemia [96] and retinopathy.[97]

1.7.2 Markers

Because of their dynamic expression profile, generally, PCs are identified by a combination of markers, most of them related to a specific organ or type of vessel. The most common membrane markers are platelet-derived growth factor receptor β (PDGFRβ), CD146, aminopeptidases A and N (CD13), endoglin (CD105), and neuron-glial 2 (NG2). The cytosolic markers mostly reflect their contractile activation and are αSMA, non-muscle myosin, desmin, vimentin, and nestin. In general PCs from capillaries are NG2+/α-SMA−, whereas pericytes from arterioles and venules are respectively NG2+/α-SMA+ and NG2−/α-SMA+, but all equally express CD146 and the PDGFR-β.[87]

In 1988 Nayak et al had used what seemed to be a promising membrane marker, 3G5 ganglioside antigen to identify retinal capillary pericytes in humans.[98] The usefulness of this marker was demonstrated also in cardiac muscle and human dermis.[99] Later, studies were performed on granulating tissues from decubitus ulcers and showed that 3G5 antigen-expressing cells exhibited the characteristic structure of mature mast cells. This finding was consistent with the fact that mast cells initially increase in number around blood vessels during inflammation. Further analyses with double immunofluorescent

staining using anti-tryptase and anti-chymase antibodies (tryptase and chymase are serine proteinase contained in mast cells) definitively showed that most 3G5 cells were mast cells even in normal skin.[100]This marker is not used to identify PCs anymore.

Another marker that seems promising is the regulator of G protein signaling 5 (RGS5).[89] This marker may play a role in proliferation and recruitment of SMCs and PCs during vascular remodeling.[16] A limitation for the PCs identification could be its expression on SMCs in larger size vessels.[101]

In the last few years, the use of a single target for pericyte identification has not been the main goal anymore. It is known how the marker expression is dependent on the type of tissue and related to the cells state.

NG2 was reported as a marker of perivascular cells along arterioles and absent in the wall of venules. Thus, NG2 could be considered as a potential marker that differentiates venous SMCs and PCs from other capillary- and arteriole-associated perivascular cells.[102]However, αSMA is still a good marker for the study of PCs when used in combination of additional pericyte markers [103] or to detect their activation state.[104]

1.8 Functions of pericytes

Despite the basic structure and position around the ECs, the morphology, biology and density of PCs vary between organs depending on the stringency of endothelial barrier function. The ratio PCs/ECs changes from 1:100 in the human skeletal muscles up to 1:3 and 1:1 in the central nervous system and the retina, where the para-cellular and transendothelial flow is strictly regulated.[83] PCs density appears to also relate to the rate of endothelial turnover. In tissues where the ECs turnover decreases their coverage is higher. PCs density rise with the increase of orthostatic blood pressure and larger coverage in the lower body parts.[89]

1.8.1 Contribution of pericytes to endothelial barrier

The strict contact of PCs with endothelial cells suggests their role in the development and maintenance of blood barriers. The most stringent endothelial barrier is the blood-brain-barrier (BBB) in the central nervous system (CNS). It consists of physical barriers to the passive transport of proteins and compounds from the blood to the tissue. It has a continuous complex of tight junctions that ensure the isolation from extracellular environment; combined with reduced vesicular exchange; and several specialized transporters for molecular trafficking.[105]The constituents of the BBB include extracellular matrix, astrocytes and pericytes and is mainly formed by direct cell–cell contact. In the CNS, pericytes are in complex structures composed of microglia cells, neurons, ECs, and astrocyte that together form the functional neurovascular unit (NVU).[106] PCs recruitment is necessary for BBB formation during embryogenesis and determines the permeability of CNS vessels during development. PCs regulate the formation of tight junctions and vesicle trafficking. They also have an inhibitory effect on the expression of molecules that increase vascular permeability of ECs. Their integrity also prevents dysfunction and neuroinflammation during CNS injury and disease.[107] PCs secret Wnt and Hedgehog ligands thus contributing to endothelial barrier formation. In particular, Wnt7a and Wnt7b can bind to the endothelial membrane receptor Frizzled 4 (FZD4) and co-receptor LRP5/6, which leads to the induction of claudin-3 expression with an improvement of the tight junctions' formation.[108, 109]As shown in mature BBB, paracrine signalling between pericytes and ECs mediated by TGFβ and angiopoietin 1 (Angpt-1) contribute to endothelial barrier maintenance.[110, 111]

1.8.2 Angiogenesis

PCs contribute to the formation of new vessels and play an important role in their sprouting and stabilization. The initial phase of vascular formation provides the ECM degradation via secretion of matrix MMPs. When both ECs and PCs are activated, they can produce several MMPs like MMP2, MMP3 and MMP9 to support ECs migration outward into the ECM.[112]Angiopoietin 2 (Angpt-2) leads the detachment of PCs from the endothelial layer loosening the EC junctions. In this phase, PCs change their quiescent phenotype, shorten their processes, increase volume and start to proliferate.[113]The sprouting is led by a group of ECs called tip cells. ECs migration following the tip cells forms vascular sprouting by activating proliferating cells. The vessel then undergoes active lumen formation.[112] The ECs release chemokines, such as PDGFβ to recruit PCs from surrounding mesenchymal precursors or from the vessel wall.[114] In order to initiate this vascular stabilization process PCs start to produce ECM, that will form the basement membrane; and start to release paracrine factors as TGFβ and Angpt-1 that promote endothelial maturation, blood-barrier formation, suppress EC proliferation and migratory response.[88, 89] TGFβ is also produced by ECs and may trigger the TGFβ receptor 2 in PCs, inhibiting their proliferation and stimulating the acquisition of a contractile phenotype. Moreover, TGFβ activates Notch pathway and facilitates the pericyte attachment by upregulation of N-cadherin.[93]

1.8.3 Contractile function

PCs may take contractile phenotype, which they probably do not possess physiologically, following activation by ischemic condition or by excess reactive oxygen species (ROS) generation. Their contraction-related proteins αSMA, desmin, and vimentin get in touch with actin filament bundles located on the endothelial side. Activation of endothelin-1 receptors increase the intracellular concentration of ions calcium and lead to constriction of pericytes, which coincides with alignment of F-actin and intermediate filaments.[115]PCs located at the transition of arterioles to capillaries express a high concentration of contractile proteins, which suggests they might be acting as pre-capillary sphincters.[88] PC contraction contribute to increase of vessel wall stiffness in high or increased blood pressure condition. Several ligands can operate a diameter adaptation of PCs: calpain, histamine, serotonin, angiotensin 2, endothelin-1, and α_2-adrenoceptors are known vasoconstrictor. While, nitric oxide, cholinergic agonists, and β_2-adrenoceptors produce vasodilation.[116, 117]

1.8.4 Basement membrane formation

The basement membrane is defined as a thin sheet of ECM located in blood vessels, mainly composed of laminin, collagen type IV, fibronectin and the proteins perlecan and nidogen 1 and 2. During angiogenesis, ECs produce MT1-MMP and MMP14 proteases that digest the surrounded matrix forming vascular guidance tunnels.[118]These are empty spaces within ECM allows the motility of ECs and PCs and used as a guide for angiogenesis. PCs recruitment and allocation upon the abluminal surface of the new forming vessels occurs under the stimulus of PDGF-BB and HB-EGF produced by ECs. ECs-PCs interaction in the site of new vessel formation is crucial for basement membrane production. Deposition of fibronectin and nidogen-1 at the beginning, followed by perlecan and laminin isoforms are the events that start tube maturation.[119] Expression of integrins α5β1, α6β1, α3β1 and α1β1 by both ECs and PCs stabilise the vessel by binding the newly deposited matrix. Finally, TIMP-3 production by PCs inhibits MMPs proteolytic activity and controls collagen type IV deposition and stability, avoiding further morphogenesis processes.[120]

1.8.5 Multipotency of pericytes

PCs are a cell population that share part of their origin with the MSCs,[121] but respect them seems to have a higher differentiation potential. PCs can trans-differentiate into typical cells of mesenchymal lineage like adipocytes, chondrocytes, osteocytes, myocytes, and neural cells [122] which may contribute to regenerative mechanisms following tissue injury. PCs play an important role in mediating inflammation under pathological conditions, several studies have shown that PCs can differentiate into immune cells such as dendritic cells [123] and macrophage-like cells.[124] It is known that there is a strength activated response to ischemia/hypoxia. In the brain, consequentially to an ischemic stroke (cerebral infarction) the PCs can differentiate in neural cells, vascular cells, and microglia and they can produce all the components of NVU.[125]PCs from different types of muscular tissue show wide differentiation potential *in vitro* and *in vivo*, while retaining some specificity of their origin tissue. PCs resident in the skeletal muscle for instance contribute to myofiber regeneration. Dellavalle et al isolated PCs from human skeletal muscle and transplanted them in dystrophic immunodeficient mice. These cells could generate myofibers expressing human mini-dystrophin.[126]Microvascular PCs within human myocardium exhibit angiogenic behaviours in response to hypoxia and seem to have cardiomyogenic potential in pathological and healthy myocardium *in vivo*, although only for a small percentage.[127]It has also been reported that PCs can regenerate human epidermal cells

during skin tissue regeneration.[128] PCs may play a role in bone marrow balance as well. In this tissue PCs are identified as CD34-/CD45-/CD146+ cells, localized around the sinusoids, capillaries and small arterioles. A different role for the two population has been suggested; perisinusoidal cells seem to activate HSCs to egress into vasculature, while the periarteriolar maintain the dormant pool of HSCs in their niche. PCs can recreate bone and marrow stroma in orthotopic and heterotopic transplantation. *Ex vivo* data show that perivascular cells support stemness and differentiation stimuli in human HSC,[129] while *in vivo* data in an immunodeficient mice model demonstrate that /CD271+/CD45-/CD146+ cells from bone marrow are able to induce the formation of bone, adipocyte, fibroblasts and capillaries.[130]

1.9 Vascular progenitor cells in human saphena

In 2010 Campagnolo et al., described a population of progenitor cells present in the tunica adventitia of the saphenous vein, around the *vasa vasorum*. (**Figure 8**) These cells, named saphenous progenitor cells (SVPs), were isolated from aged patients with coronary artery disease by their specific surface markers expression CD34pos and CD31neg. SVPs freshly isolated showed poor expansion capability but because of stimulation with serum, they become proliferating and started to express typical markers of mesenchymal/pericyte lineage. This phenotype might originate from serum-dependent stimulation that induces the expression or expansion of mesenchymal/pericyte clones within the freshly isolated population. Indeed, a vasculogenic zone (VZ) persists in adult veins although the progenitors inside appear more differentiated and with a limited plasticity. In culture, SVPs stop expressing CD34 but maintain the partial stemness as indicated by their expression of Sox2, the clonogenic capacity, and mesenchymal differentiation attitude.[131, 132] SVPs have a strong relation with ECs both in co-culture systems and *in vivo*, establishing multiple interactions. They acquire the migration ability and stimulate angiogenesis and proliferation of ECs. The SVPs transplantation accelerates blood flow recovery of ischemic limbs in a mouse, but this effect is mainly due to paracrine mechanisms. This was hypothesized because no SVP-derived vascular structures were detected but just proliferating SVPs (**Figure 9**). SMCs could be an additional target for the paracrine effect because *in vitro* studies have been documented with increased viability of SMCs exposed to SVPs conditioned medium.[81]

SVPs represent a target of cellular biology with high clinical relevance because they are available during bypass surgery, easily accessible, without additional risk for the patient. However, later studies have opened a new frontier in cellular biology for autologous cell therapy. It has been shown that diversities in the epigenetic profile of SVPs can significantly impact on the recovery outcomes in a model of peripheral ischemia.[133]

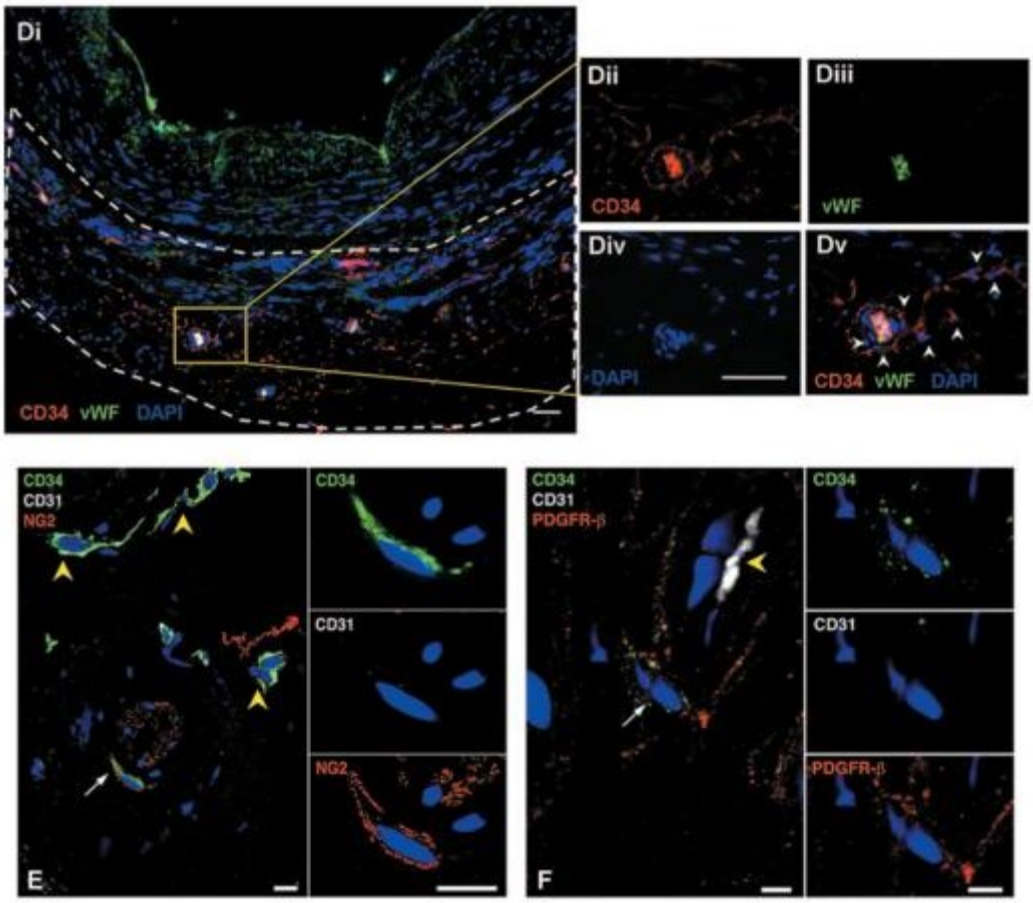

Figure 8 In situ identification of SVPs. *(Di) Low-magnification pictures show a section of saphenous vein with adventitia highlighted by dashed lines. A single vasa vasorum is shown at higher magnification stained for progenitor/EC marker CD34 (red; Dii), EC marker vWF (green; Diii), and nuclei (DAPI, blue, Div). Representative confocal image merge reveals the presence of CD34+vWF- cells located in the perivascular zone of the vasa vasorum (white arrowheads in Dv). Furthermore, few CD34+ cells (green; E and F) coexpressed NG2 (red, E) or PDGFR*β *(red, F). Double-positive cells are indicated by white arrows. Higher-magnification panels in E and F show adventitial CD34+/CD31- cells coexpressing NG2 or PDGFR*β*. Scale bar=50*μm *(D) and 10*μm *(E and F). Image from Campagnolo et al., 2010.*

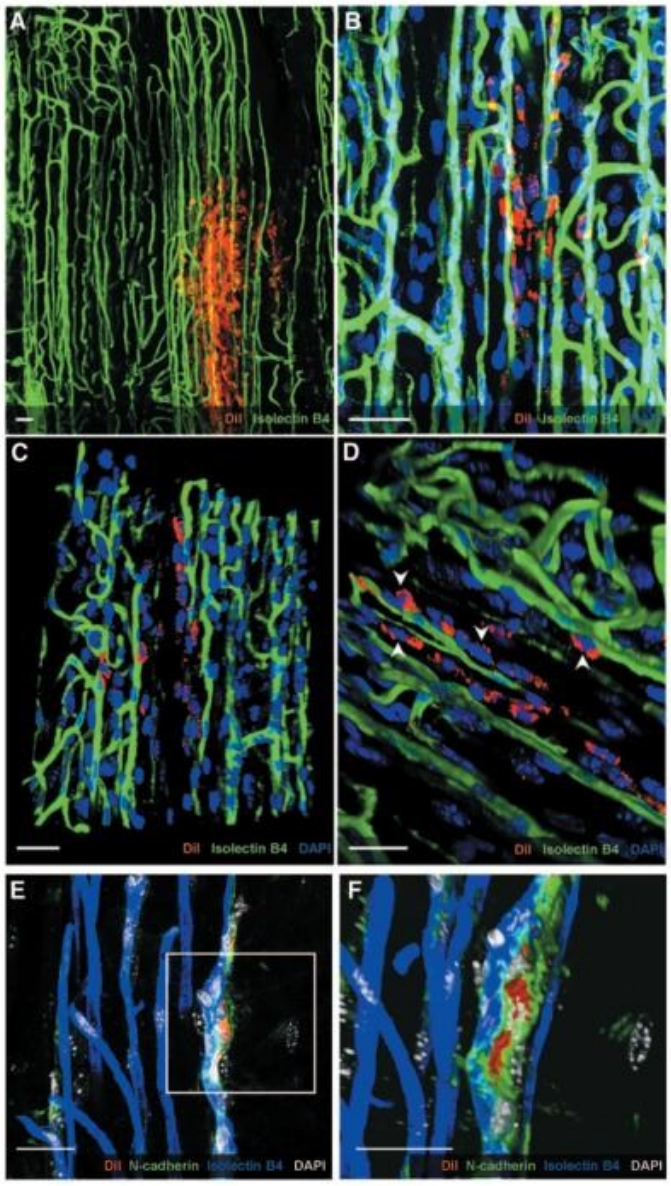

Figure 9 Interaction of SVPs with the host vasculature. *Confocal images showing SVPs (red) surrounding the host vasculature (isolectin B4; green; A and B). 3D reconstruction shows physical contact between SVPs and ECs (C and D; white arrowheads). Direct interaction was also confirmed by N-cadherin staining (green), which accumulated in the junction between SVPs (red) and capillary ECs (blue; E and F). Nuclei were stained with DAPI (blue in A through D; white in E and F). Scale bar=25μm. Image from Campagnolo et al., 2010.*

1.10 AMIGO2, a new modulator of pericytes biology

The Amphoterin-Induced Gene And Open Reading Frame (AMIGO) protein family is described below. In subsequent chapters will be shown as one component of the AMIGO family, AMIGO2, is involved in the SVPs mechano-sensitivity, resulting as a possible marker of the activated PCs status.

1.10.1 The AMIGO family

In 2003 a novel family of transmembrane proteins was described for the first time by Kuja-Panula et al. then named Amphoterin-Induced Gene And Open Reading Frame (AMIGO). This family is composed of three proteins: AMIGO, AMIGO2, and AMIGO3; that shows a clear homology and almost identical length and domain organization (**Figure 10**).[134]

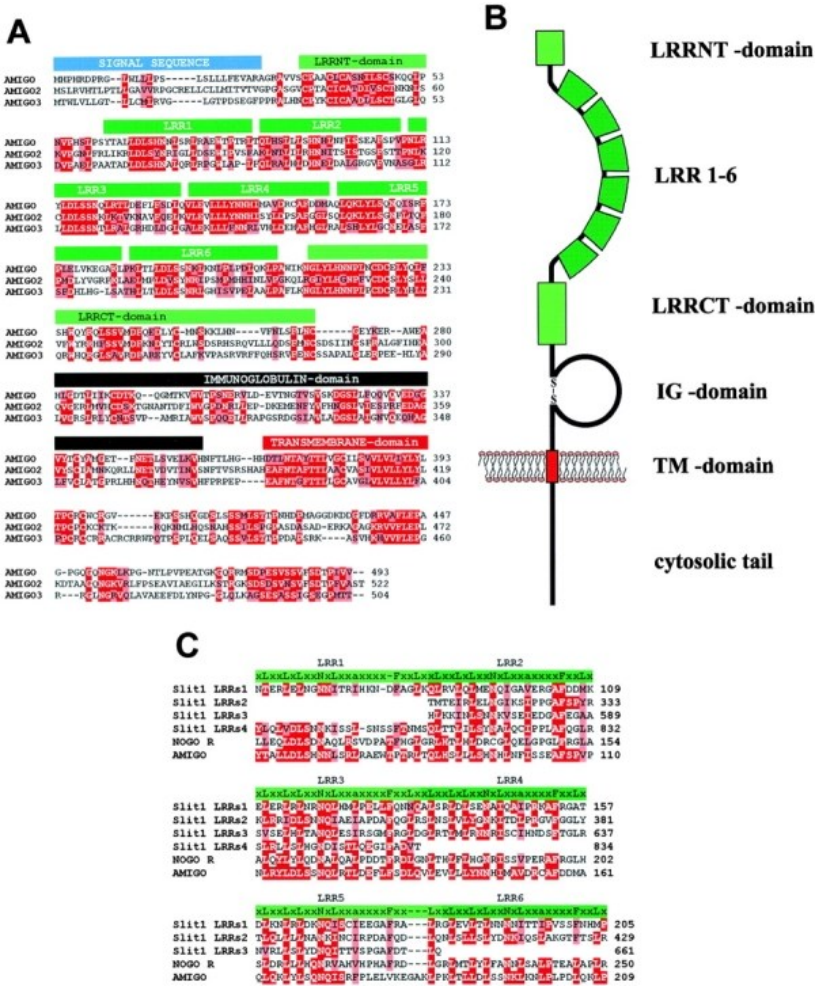

Figure 10 AMIGO proteins. *(A) Alignment of the primary structure of the three AMIGOs. The identical amino acids between all AMIGOs are highlighted in red with white letters and similar amino acids are highlighted in red with black letters (B) The hypothetic tertiary structure of the proteins. (C) Alignment of the LRRs domains of Slit1, Nogo, and AMIGO1. The identical amino acids between Slit1 and Nogo receptor compared with the AMIGO1 are highlighted in red with white letters and similar amino acids are highlighted in red with black letters. Image from Kuja-Panula et al., 2003.*

Dr. Davide Maselli, *"The role of mechanical stress in progression of intima hyperplasia associated to vein coronary bypass grafts disease.",* PhD thesis in Biochemistry, Physiology and Molecular Biology of International PhD School in Life Sciences and Biotechnologies, University of Sassari.

This protein family seems to have a homolog in *Drosophila melanogaster* in the kekkon family, composed, even in this case, of three proteins kek1, kek2,[135]and kek3.[136] They show the same structure in their extracellular parts, with six leucine-rich repeats (LRRs) domains flanked by cysteine-rich LRR NH_2- and COOH-terminal domains and one immunoglobulin-like domain close to the transmembrane region. AMIGOs, as well as kek proteins also have a cytoplasmic part that however does not display any homology. These similarities suggest that the AMIGOs and kekkon family may derive from the same ancestral gene. AMIGO and AMIGO2 have a 48% similarity, AMIGO and AMIGO3 have 50% and AMIGO2 and AMIGO3 share 48% of the amino acid sequence. Their alignment shows that the most preserved region is the extracellular part with the six LRRs domains. They have a basic structure as a motif $LX_2LXLX_2NX(L/I)X_2AX_4(F/L/I)$, in which "A" is an aliphatic residue and "X" is any amino acid. This motif is a typical LRR sequence usually found in the extracellular domain of animal proteins.[134, 137]

1.10.2 AMIGO in central nervous system

The AMIGO family is mostly expressed in the nervous system. Its expression undergoes two peaks of up-regulation during brain development. The first perinatally and the second during myelination and oligodendrocyte maturation.

The first up-regulation occurs while the brain begins to form axonal connections. One mechanism of the nerves growing is fasciculation by which the axons grow along each other by using a pioneer axon as the substratum for the growth cones of the later ones. AMIGO is important for the formation of axons bundles during this phase. The mechanism is still unknown, but two hypotheses can be made. AMIGO displays a homophilic and heterophilic binding mechanism between all the proteins of the family. It is known that homophilic adhesion molecules of Ig superfamily mediate the axons outgrowth and fasciculation during the nervous system development.[138, 139]The LRR sequences of AMIGOs display homology to the Slit1 and to the Nogo extracellular domain. The Slit proteins are secreted molecules identified as a factor involved in the development of midline glia and guidance molecules.[140]Nogo is a family of proteins composed of three isoforms, generated by alternative splicing from reticulon 4 (RTN4) gene. All the three isoforms of Nogo share a 66-amino-acid sequence in their extracellular domain (Nogo-66) by which they inhibit neurite growth in the adult central nervous system (CNS).[141]The similarities found in the LRRs in AMIGO, Slit1, and Nogo suggests an interaction between them. It is known that LRRs promote interaction between LRR proteins [142] or they could share the same binding partner(s).[134]

After birth, the expression is up-regulated again and remains high in the adult brain. The time period of the up-regulation coincides with the onset of myelination. Also the expression of AMIGO and the myelin-specific marker α-CNPasemake a parallel increase during postnatal development. The study of Kuja-Panula et al. suggests that in particular AMIGO and AMIGO2 may have a cooperative role by binding each other from opposing cell membranes, between axons and glial cells, to put the cells in contact.[134]

AMIGOs expression remains high until adulthood, suggesting its possible involvement in regeneration and plasticity of the adult fiber.[134]

Some results obtained during this PhD project showed the AMIGO2 regulation in SVPs subjected to mechanical stress. AMIGO2 is still a little-known molecule, its functions seem to be related to proliferation and migration, but it also plays a role in T cell regulation. Below are some of the functions of AMIGO2 described outside the nervous system.

1.10.3 AMIGO2 and inflammation

Modulation T cell functions

Using a mouse model of multiple sclerosis (MS), Li et al. observed that AMIGO2 played a role in T cell homing in the secondary lymphoid organs and in the CNS, suggesting its direct role as a cell adhesion molecule to regulate T cell trafficking. In this very recent work, Li and coworkers used an AMIGO2-knockout mouse showing the presence of more anti-inflammatory polarized Th cells that produce IL-10 and less polarized pro-inflammatory phenotype producing IL-17A. These cells also had a migratory deficit versus the CNS. Taken together, this data demonstrates that AMIGO2 is involved in the modulation of immune response in a mouse model of MS. They have also shown that AMIGO2-mediates the regulation of NF-kB, which is a critical component in the PI3K-Akt signaling pathway. Akt plays a role in the regulation of cell survival, proliferation, and transcription, such as controlling NF-kB activity. Their results suggest that the Akt activity was enhanced due to AMIGO2-deficiency. This point is in contrast with other studies regarding AMIGO2 operating mechanisms but despite this controversial issue, they propose AMIGO2 as a potential therapeutic target for MS.[143]

Chronic inflammatory disorders

In 2016 Benedetti et al. demonstrated that AMIGO2 expression is up-regulated in human arthritic synoviocytes. Rheumatoid arthritis (RA) is a chronic inflammatory disease characterized by synovium hyperplasia that causes progressive joint destruction and bone

resorption. They discovered that the combination of IL-17A and TNF-α, two pro-inflammatory cytokines in synoviocytes, increased AMIGO2 expression more in RA. The RA synoviocytes in the synovial intimal lining,proliferate excessively and produce cytokines and proteases that perpetuate inflammation and cartilage destruction.

Benedetti et al. also showed that AMIGO2 is tightly regulated by JNK and ERK, two mitogen-activated protein kinases (MAPKs), that can increase or decrease its expression leading to an excessive proliferation or the shift to the invasive phenotype of the synoviocytes. Thus, Benedetti et al. have shed light on the combination of events leading the presence of pro-inflammatory cytokines to AMIGO2 expression enhancing the resistance to apoptosis and the pathogenesis of RA disease.[144]

1.10.4 AMIGO2 and tumorigenesis

The expression of AMIGO2 mRNA in normal tissue is minimal with the only exception of female reproductive tissues as breast, ovary, cervix, and uterus. Lung, colon, and rectum can exhibit significant expression levels but still lower in comparison to the normal breast tissue. Whereas AMIGO2 expression seems to be regulated in tumorigenic cells, it is differentially expressed in 56% of thyroid cancers, 57% of pancreatic cancers, for which represents a biomarker;[145] and 45% of stomach cancers. In patients with gastric adenocarcinoma, the overexpression of AMIGO2 is localized just in the tumor tissue and this may play a functional role in development and progression of the disease. The down-regulation of AMIGO2 in a gastric adenocarcinoma cell line alters their morphology and causes chromosomal instability, leading to an increase in cell size and DNA content (ploidy). The loss of AMIGO2 expression also leads to the lack of adhesive/migratory abilities of these cancer cells.[146]

This data appears to be confirmed by a paper published in 2017 by Kanda et al. in which AMIGO2 seems to be overexpressed in fibrosarcoma cells with high liver-metastatic potential, and its expression is a sufficient condition for metastatic capacity. In these cells, AMIGO2 mediated the adhesion to endothelium by homophilic or heterophilic interactions with the AMIGOs protein present on the endothelial membrane. These results also had a clinical match in the colon and gastric cancers, showing the AMIGO2 presence in primary tumor lesions with an increase in liver metastatic foci, especially on the tumor cell surface. Furthermore, PrognoScan-based Kaplan-Meier survival analysis revealed a correlation between the level of AMIGO2 expression and less life expectancy in 177 colon cancer patients (**Figure 11**).[147]

Thus, AMIGO2 has been found to play a pathological role in tumor growth, endothelial cell adhesion and migration. In particular conditions, its downregulation seems to completely inhibit the tumorigenicity and the *metastatic spread* to the liver.[146, 147]

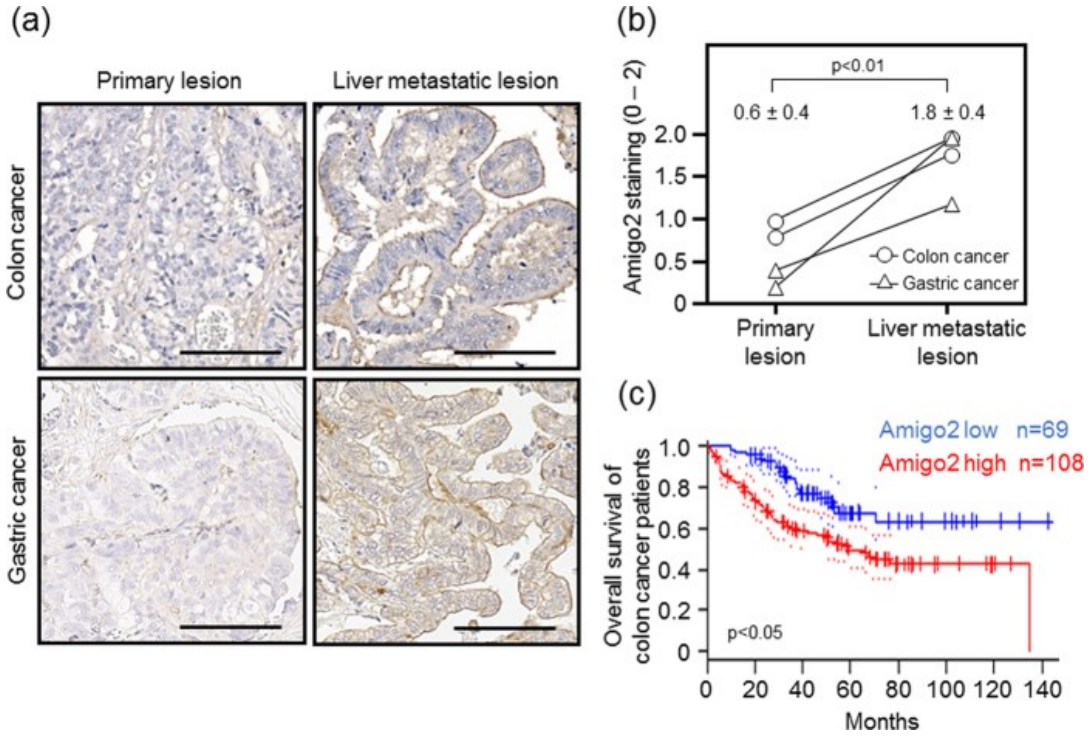

Figure 11 Amigo2 overexpression in cancer. *(a) Immunohistochemical staining of AMIGO2 in primary lesions of human colon and gastric cancers and their liver metastatic lesions. Scale bar: 100 µm. (b) AMIGO2 staining quantification in paired specimens of primary lesions and metastases. Results are shown as means ± SD (n = 4 in each group). (c) Kaplan-Meier analysis of overall survival in colon cancer patients with high versus low AMIGO2 mRNA expression. Dotted lines indicate 95% confidence intervals for each group. This data was obtained from PrognoScan (http://www.abren.net/PrognoScan/). Image from Kanda et al., 2017.*

1.10.5 AMIGO2 activation in endothelial cells

In 2012, for the first time, the expression of AMIGOs in primary culture of human microvascular ECs and PCs was shown. Among the three members, AMIGO2 is the most expressed in the ECs cell line but in human brain PCs the three members expression is essentially equivalent.[148]It has also been demonstrated that hypoxia suppresses the AMIGO2 gene expression in ECs. Because the lack of oxygen is the main cause of angiogenesis, AMIGO2 can have a role in new vessel formation and remodeling due to the homotypical and heterotypic interactions. In a subsequent study Park et al. show that AMIGO2 regulates ECs interactions to ECM and cell viability. The cell–ECM interaction affects the ability to migrate and the tubulogenesis drastically decreases when AMIGO2 is silenced.[149] Experiments conducted on the retinal vessel in mice showed that AMIGO2, plays a pivotal role in the formation of vessels *in vivo*. AMIGO2 was already known for its anti-apoptotic and proliferative activity in neurons [150] and this activity was also shown in ECs. Park et al. have shown that PDK1–Akt signaling pathway is one of the mechanisms regulated by AMIGO2 and involved in cell survival, adhesion, migration, and angiogenesis. They showed AMIGO2 can bind directly the PH domain of PDK1 enhance the activation of PDK1 and Akt in the plasma membrane. They used PTD-A2, a peptide that mimics the C-terminal region of AMIGO2 in the cytoplasmic tail, to interfere with PDK1-Akt activation due to AMIGO2. The result showed the abrogation of the PDK phosphorylation with consequences on cell survival and angiogenesis (**Figure 12**).[149]

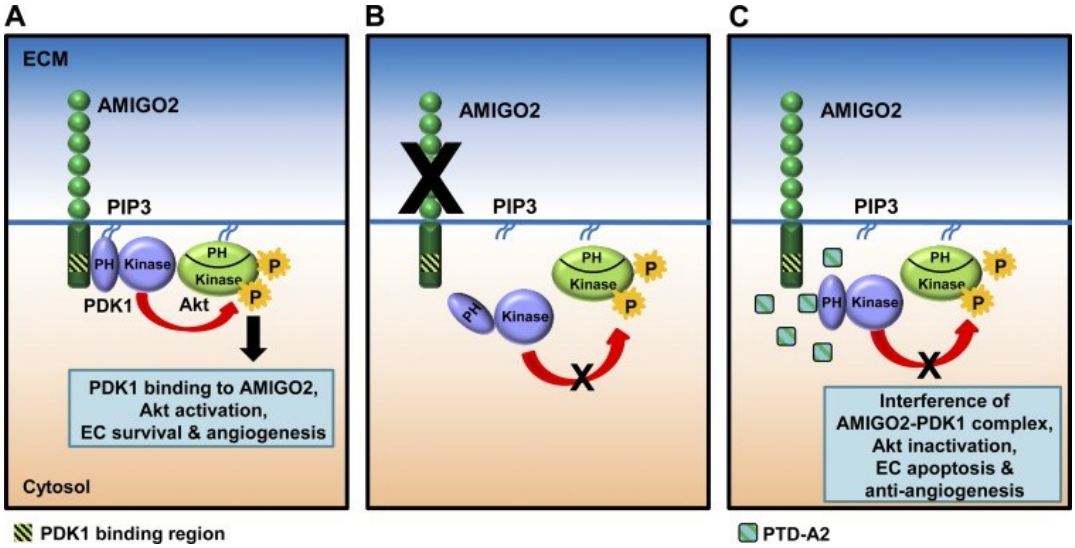

Figure 12 AMIGO2 and PDK1–Akt signaling pathway. *(A) AMIGO2 can bind directly the PH domain of PDK1 and enhance the activation of Akt**pathway** in the plasma membrane, which results in increased ECs viability, adhesion, migration, and angiogenesis. Loss of AMIGO2 function by silencing (B) or by a peptide that mimics the cytoplasmic tail (C) abrogated the phosphorylation of PDK1 and Akt affecting cell survival and angiogenesis. Image from Park et al., 2015.*

AIMS OF THE STUDY

Coronary artery disease is the most common type of heart disease in the industrialized countries. When an atherosclerotic plaque builds up in one of the coronary arteries, the consequent limitation of blood flow to the heart can cause the death of cardiac muscle due to prolonged severe ischemia. CABG is a surgical procedure with the purpose of re-establishing an adequate blood supply to the ischemic myocardium, using an autologous vessel of the patient to connects ascending aorta and the coronary arteries, upstream and downstream a severe lesion.

Since the beginning of CABG surgery, the SV has always been one of the surgical preference as a graft. However, SV graft undergoes to a constant increase of the thickness that starts from the early days after surgery and reduces the patency rate up to 40-50% in ten years. The formation of a thick layer of neo-intima inside the lumen of SV is a physiologic adaptive response of the vein wall to the different hemodynamic forces encountered in the cardiac milieu. Those forces are pulsatile flow and shear stress. It is known that changes in wall strain can activate different cell phenotypes resident in all layers of the vein wall. From the differentiated SMCs in the media, that can switch their phenotype to migratory/secretory; up to the fibroblasts in adventitia that, once activated by mechanical stimuli, start to proliferate and migrate to the intima. In 2010, SVPs were described as an adventitial progenitor cells population with multilineage differentiation ability.

The aim of this project was to understand the SVPs role in intima hyperplasia associated with vein graft disease, using a multidisciplinary approach focused on mechanobiology.

My work is centered on the investigation of the effects of *in vitro* mechanical load on proliferative rate, structural rearrangement and transcriptomic changes of SVPs. By exposing SVPs to uniaxial mechanical strain genome-wide transcriptional differences due to mechanical stress were characterized. Those differences have been analyzed to screen for possible activation of specific functions/single genes, strongly regulated by the stretch. The most upregulated gene turned out to be AMIGO2, a transmembrane protein with six LRRs. Since its expression increases up to 14 times under mechanical strain and it is not modulated in static conditions we hypothesize a role in the mechanobiology of SVPs. We thus overexpressed AMIGO2 in unstrained SVPs to understand its effect on apoptosis and proliferation rate *in vitro*. In addition, we also evaluated the effect of mechanical strain on the entire vein *ex vivo*, using a bioreactor in which an entire portion of saphenous vein underwent cyclic strain under heart like hemodynamic conditions. The tissue sections have

been analyzed by immunohistochemistry to evaluate the AMIGO2 distribution in the vein layers and the morphological changes after mechanical stimulation.

The specific aims of the project are herein summarized. A concise description of the experimental design for each aim is reported:

AIM1: To screen for strain-associated SVPs functional changes

- ✓ SVP isolation by immunomagnetic sorting and their characterization
- ✓ Description of the effects on SVPs of uniaxial cyclic strain *in vitro*: analysis of phenotypic and functional changes

AIM2: To screen for strain associated pathway modulation

- ✓ RNA sequencing and Ingenuity Pathway Analysis: Core Analysis for the analysis of pathways and functions
- ✓ Analysis of top scored modulated genes and technical and biological validation by qPCR
- ✓ Identification of target genes for specific *in vitro* and *ex vivo* analysis

AIM 3: To assess the functional effect of the regulated gene on SVPs *in vitro* and *ex vivo*

- ✓ Optimisation of overexpression protocol for AMIGO2
- ✓ Proliferation and apoptosis rate
- ✓ Immunofluorescence assessment of AMIGO2 expression on *ex-vivo* stimulated SVs, mimicking the hemodynamics of coronary flow

METHODS

3.1 Patients recruitment

Tirth eight patients recruited for the study were all normoglycemic, females or males undergoing surgical removal of saphenous vein because of varicosity or at the occasion of CABG surgery. All tissues used in the study are surgical leftovers Exclusion criteria include concomitant neoplastic, infectious, connective tissue or inflammatory diseases; prolonged hyperglycemia due to glucocorticoid (steroid-related diabetes), pregnancy. The Research Ethics Committee of our institution approved the study which was performed according to the ethical principles recorded in the 1964 Declaration of Helsinki and later amendments. All the subjects gave written informed consent to participate. **Table 1** summarizes their main clinical features.

AGE (Years)	SEX (male %)	BMI	Hypertension (%)	Dyslipidaemia (%)	Smoker (%)	Glycaemia (mg/dl)	Creatinine (mg/dl)
58±4	41.7	25.8±0.5	29.20	8.30	16.7	100±12	0.81±0.06

Table 1 Details of patients involved in the study

3.2 Cell isolation

The vein was washed in PBS containing Penicillin/Streptomycin (P/S) 100 U/mL (Thermo Fisher Scientific, USA) and then processed for cell isolation as follows.

3.2.1 Vein omogenation for cell isolation

Saphenous veins were finely minced with scissors and scalpels in a Petri dish and digested with LiberaseBlendzyme 2 (Roche, Switzerland) diluted 2 mg/ml in Dulbecco Modified Eagle's Medium (DMEMGIBCO Thermo Fisher Scientific, USA) for 4h at 37°C. After the digestion, the cell suspension was sequentially filtered through 70 µm,40 µm, and 30µm cell strainer to remove cell clumps and debris, washed twice in PBS + P/S and centrifuged at 300xg for 10 minutes at room temperature.

3.2.2 Magnetic sorting and culture

The cell pellet was resuspended in DMEM containing P/S 100 U/mL and CD34 positive/CD31 negative cells, i.e SVPs were isolated by two consecutive magnetic beads–assisted cell sorting (MACS, MiltenyiBiotec, Germany) according to manufacturer's instructions (**Figure 13**). The principle of this technique is that the cells expressing a specific antigen will react with the antibody conjugated to the magnetic beads. The cells are then separated using a MACS MS column (MiltenyiBiotec, Germany) placed in a

magnetic field MACS separator (MiltenyiBiotec, Germany), the positive fraction is retained while the negative one passes through.

More in details, the first selection was performed using CD31 magnetic beads (MiltenyiBiotec, Germany). Cells were resuspended in 60µl of DMEM+P/S 100U/mL and treated with 20µlof FcR blocking reagent (to saturate aspecific binding sites) and 20µl of CD31 labeled beads and incubated for 20 min at 4°C. Labelled cells were then washed and resuspended in the same medium. Cells were dispensed on top of a magnetic column and the CD31 negative fraction flowing through the column was retained while the CD31 positive fraction entrapped inside the column was discarded. This step was necessary to remove the endothelial CD31positive component from the cell suspension. Then, the cells were washed and resuspended in 300 µl of cold column buffer (PBS, supplemented with 0.5% of BSA and EDTA 2mM) and incubated with 100µl FCR blocking reagent and 100µl CD34 magnetic beads (MiltenyiBiotec, Germany), and incubated for 30 minutes at 4°C. Cells were then resuspended in 500µl of column buffer and dispensed on top of a magnetic column the CD34 positive population entrapped in the column was thus retained and cultured.

Expansion was performed by seeding CD34 positive/CD31 negative cells obtained on fibronectin/gelatine (5:1; fibronectin 1µg/ml:Bovine gelatine 1%) coated plates in endothelial growth medium EGM-2 (Lonza, Switzerland) that contained 2% foetal bovine serum (FBS, GIBCO Thermo Fisher Scientific, USA). The medium was replaced two times a week and at 80% confluency, the cells were trypsinized with Trypsin/EDTA (GIBCO Thermo Fisher Scientific, USA) and split 1:3.

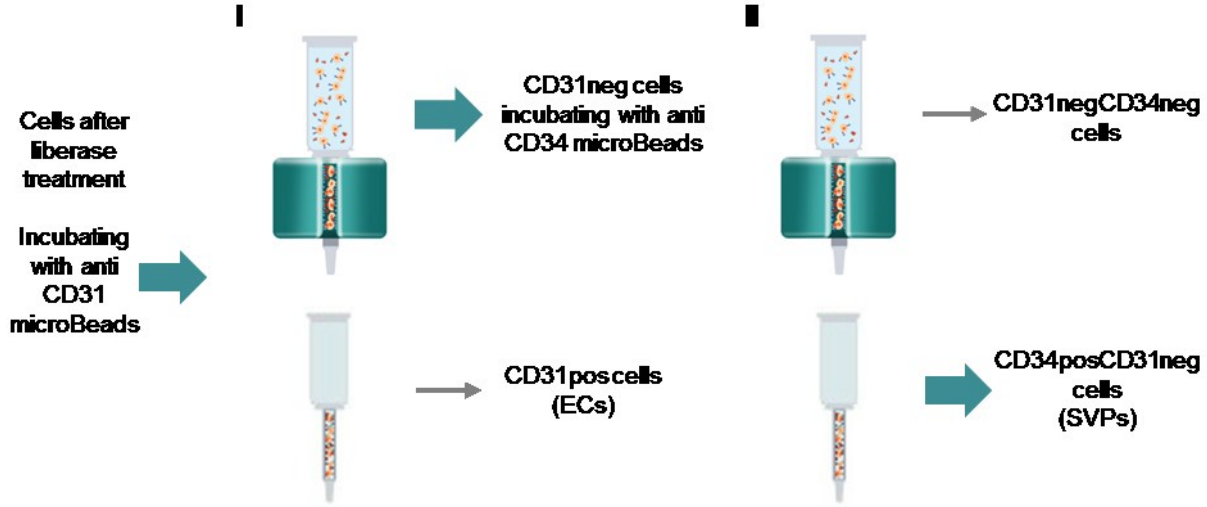

Figure 13 SVP isolation protocol. *Scheme of the double selection with magnetic beads from freshly isolated cells.*

3.3 Cell characterization

Homogeneity of the cell populations were assessed by flow cytometry analysis and immunocytochemistry.

3.3.1 Flow cytometry

Flow cytometry analysis was used to evaluate the homogeneity of the cell population collected with double sorting, after the early passages of in vitro cultures. At the fourth passage in plate the cells were detached with a EDTA (1mM) solution, washed ones with PBS, then every single-cell suspension was divided into six tubes and stained with a single fluorescence-labeled antibody against CD31, CD44, CD90, CD105 (**Table 2**).

Cells were incubated for 15 minutes at RT in staining buffer PBS, supplemented with 0.5% of BSA), then washed and resuspended in staining buffer.

Data were acquired in a flow cytometric sorting Canto II (BD Biosciences, Franklin Lakes, NJ) flow cytometer and analyzed with flow cytometric sorting Diva software (BD Biosciences).

Antibody	Supplier	Dilution
PE Mouse Anti-Human CD90	BD Biosciences (555596)	5 µl for 1×10^6 cells
PE Mouse anti-Human CD105	BD Biosciences (560839)	5 µl for 1×10^6 cells
FITC Mouse Anti-Human CD31	BD Biosciences (557508)	20 µl for 1×10^6 cells
PE Mouse Anti-Human CD44	BD Biosciences (550989)	20 µl for 1×10^6 cells

Table 2 Details of FACS antibodies

3.3.2 Immunocytochemistry

Cells at the fourth passage were analyzed by immunocytochemistry for expression of CD31, CD146, PDGFRβ, α-SMA, GATA4 and NG2 (**Table 3**).

$5x10^3$ cells were seeded in each well of an 8 wells glass chamber slides (Thermo Scientific Nunc, Thermo Fisher Scientific, USA). The day after the cells were washed with PBS three time and then fixed with 4% PFA in PBS for 15 minutes RT. When required, the cells were permeabilized with 0.1% Triton X-100 (Sigma-Aldrich, USA) in PBS for 10 minutes at RT. Nonspecific staining was blocked with 5% FBS (GIBCO Thermo Fisher Scientific, USA) in PBS for 30 minutes at RT. Following the elimination of excess serum, the cells were

exposed to the unconjugated primary antibodies at 4°C O/N. After three washes with PBS, to develop the reaction was used the appropriate fluorescent secondary antibody (Alexa Fluor Dyes ThermoFisher Scientific, USA) diluted 1:200, for 60 minutes at 37°C. Nuclei were stained with DAPI（*Thermo Fisher Scientific, USA*） 1µg/ml for 10 minutes at RT. The slides were mounted with Fluoromount G （*Thermo Fisher Scientific, USA*） *and* stored at 4°C in the dark. Pictures of random fields were taken at 20x magnification with Zeiss Observer Z1 inverted microscope.

Primary Antibody	**TritonX**	**Supplier**	**Dilution**	**2nd *Antibody***
GATA4	*yes*	*Abcam (ab 61767)*	*1:100*	*Alexa488 Goat anti-Rb*
CD146	*no*	*Abcam (ab75769)*	*1:100*	*Alexa488 Goat anti-Rb*
CD31	*no*	*R&D (BBA7)*	*1:100*	*Alexa488 Goat anti-ms*
PDGFRβ	*no*	*Santa Cruz (SC-339)*	*1:50*	*Alexa488 Goat anti-Rb*
NG2	*no*	*Millipore (AB-5320)*	*1:100*	*Alexa488 Goat anti-Rb*
α-SMA	*yes*	*Dako (M0851)*	*1:100*	*Alexa488 Goat anti-ms*
β-Actin	*yes*	*Sigma-Aldrich (AC-15)*	*1:400*	*Alexa568 Goat anti-ms*

Table 3 Details of Immunocytochemistry antibodies

3.3.3 Doubling time

SVPs population doubling time has been calculated between the first passage (P1), after the isolation, and the fourth passage in cloture (P4), while routine subculturing. At 80% confluence, the cells were washed three times with PBS, trypsinized with Trypsin/EDTA, centrifugated at 300xg for 5 minutes and then resuspended in EGM-2 medium. 10 µl of the cell suspension was mixed with 10 µl of Trypan Blue Solution 0.4% (GIBCO Thermo Fisher Scientific, USA). The Trypan Blue Solution test is based on the concept that only the dead cells are permeable and take up the dye. Viable cells were counted and the doubling time was calculated with the following formula:

$$DT = T\frac{\ln 2}{\ln\left(\frac{P4}{P1}\right)}$$

T = incubation time in days
P1 = cell number at the first passage in culture
P4 = cell number at the fourth passage in culture

3.4 In vitro stretching

To assess the effects of mechanical strain on SVP monolayer aFlexcellTension Plus FX-5000T system (Flexcell international corporation, USA) was used This device can apply a defined controlled tensile strain on adherent cells using Arctangle Loading Stations (Flexcell international corporation, USA) via vacuum deformation of the membrane at the bottom of 6-well BioFlex culture plates (Flexcell international corporation, USA). The flexible-bottom culture plate provides a soft substrate for cell growth of 1.5 cm x 2.42 cm (3.68 cm^2), located in a rectangular region at the center of each well (**Figure 14**).

The plates were coated with fibronectin/gelatine after the membrane surface has been made hydrophilic with Sulfo-SANPAH (Thermo Fisher Scientific, USA） solution 50 mM in HEPES (Sigma-Aldrich, USA) pH 8.5. This reagent needs a photolysis to form a crosslink of *N*-Sulfosuccinimidyl-6-hexanoate, that cover the surface of the plate. The crosslinking was carried out by 365 nm UV light for 20 minutes at RT. Then, fibronectin/gelatine coating was performed O/N at RT, followed by another incubation under UV light for 20 minutes at 254 nm. SVPs were then seeded on the bottom of each well and cultured in EGM-2 at 37°C for 24. The day after a uniaxial strain with a frequency of 1 Hz and amplitude of 10% of deformation was applied. The culture system was placed in a standard incubator at 37° C in a 5% CO2 atmosphere, and the mechanical stress was prolonged for 24 or 72 hours, a static control was run in parallel for each time point. After the stimulation, the cells were resuspended in 700 µl of QIAzolLysis Reagent reagent (Qiagen, UK) for RNA isolation, or fixed in formalin solution neutral buffered at 10% (Sigma-Aldrich, USA) for immunocytochemistry analyses.

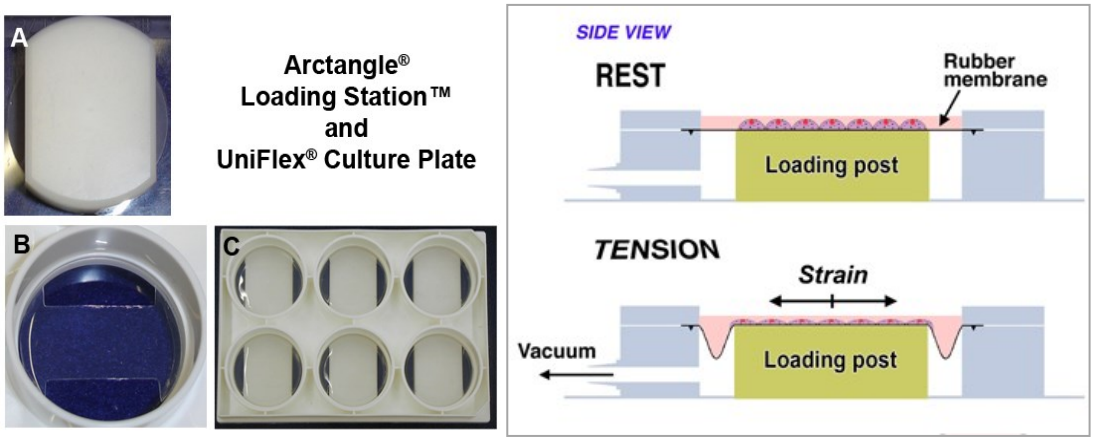

Figure 14 Flexcell operation. *At left A) Arctangle loading post. B) UniFlex well. C) 6-well BioFlex culture plates resting atop Arctangle Loading Station. At right equiaxial strain application to cells plated on the device. Images from flexcellint.com*

3.5 Gene expression analysis

Molecular biology techniques were used to prepare the samples for RNA-sequencing, verify sequencing data by technical and biological validation, and to check the overexpression of AMIGO2 in infected cells.

3.5.1 Total RNA isolation

RNA was isolated using RNeasy Mini kit (Qiagen, UK) following manufacturer instruction. Cultured cells were resuspended in 700 µl of QIAzolLysis Reagent reagent (Qiagen, UK) for 5 minutes at RT. Then, were added 140 µl of chloroform and after an incubation of 3 minutes at RT, the samples were centrifuged for 15 minutes a 12,000xg at 4°C. After the centrifugation, the mixture separates into a lower red phenol-chloroform phase, contain soluble proteins; an interphase, containing denaturating proteins; and a clear upper aqueous phase with the RNA and DNA. The upper part carefully recovered, and the RNA was precipitated with 1.5 volumes of cold absolute ethanol. Samples were centrifuged in RNeasy Mini column (Qiagen, UK) that restrain RNA. After one washing with RWT Buffer (Qiagen, UK), and two with RPE Buffer (Qiagen, UK), total RNA was eluted with 32 µl of RNAase-free water.

To obtain better quality RNA for the sequencing after the resuspension with QIAzol the RNA was extracted using Direct-zol RNA Miniprep Columns (Zymoresearch,USA) according to the manufacturer's advice. Briefly, an equal volume of ethanol 100% was put in the cells lysate. The mixture has been transferred into a Zymo-Spin IIC Column (Zymoresearch,USA), washed two times and eluted with 30 µl of RNAse free water.

3.5.2 RNA quantification

The concentration and the quality of RNA were determined by Nanodrop (*Nanodrop 1000* Thermo Scientific, USA). A blank reading was taken with the same RNAase-free water use to dilute the samples. The ratio between the absorbance values at 260 and 280 nm were used to assess the purity of RNA for each sample. Nucleic acids absorb UV light at 260 nm due to the aromatic base moieties of their structure, proteins and phenolic compounds have a strong absorbance at 280 nm; phenol and TRIzol absorb the light around 230 nm. Thus, 260/280 absorbance ratio is used to determine protein contamination and 260/230 for the other organic contaminants. Samples with 260/280 ratio smaller than 1.7 and 260/230 ratio smaller than 1.8 were discarded.

3.5.3 RNA reverse transcription

RNA was reverse transcribed using the High-Capacity RNA-to-cDNA (Applied Biosystems, USA). Briefly, 400 ng of RNA were mixed with 10 µL of 2X RT Buffer Mix (contain dNTPs blend oligo-dT and random primers) and 1 µL of 20X RT Enzyme Mix (containing the reverse transcriptase) and made up to 20 µl with RNAase-free water. cDNA transcription was performed incubating the samples for 60 minutes at 37°C, then 5 minutes at 95°C, to inactivate the reverse transcriptase. The cDNA samples obtained were frozen at -20 until their use.

3.5.4 RNA-sequencing analysis

RNA-sequencing is a recently developed deep-sequencing analysis. In brief, a whole population of RNA from a sample is converted to a library of cDNA fragments with adaptors attached to one or both ends. Each molecule is then sequenced using high-throughput, short-read sequencing methods; to obtain short sequences from one end (single-end sequencing) or both ends (pair-end sequencing). These short sequences are named reads and their typical length is around 30 to 400 bp, depending on the DNA-sequencing technology used. After sequencing, the reads can be analyzed in two different way. Can be aligned to a reference genome or assembled *de novo* without the genomic sequence. Usually, this second method is used when the genome is unknown, incomplete, or altered compared to the reference. The aim is to produce a genome-scale transcription map, that contains information about both transcriptional structure and level of expression for each gene. The reads are classified as exonic reads, junction reads, and poly(A) end-reads. These three types are used to generate a base-resolution expression profile for each gene.

RNA-Seq experiments, comprising samples quality control and bioinformatics analysis, were performed by Genomix4life S.R.L. (Baronissi. Italy).

RNA collected from 20 samples (24 and 72 hours in static and stretched condition, 5 SVPs samples each) was extracted using Direct-zol RNA miniprep columns according to the manufacturer instructions. RNA was eluted with 30 µl of RNAse free water and quantified with Nanodrop Spectrophotometer (*Nanodrop 1000* Thermo Scientific, USA). Libraries were prepared from 500 ng purified RNA with TruSeq Stranded total RNA Sample Prep Kit (Illumina, USA) according to the manufacturer's instructions. Libraries were quantified using the Agilent 2100 Bioanalyzer (Agilent Technologies) and Qubitfluorometer (Invitrogen Co.), then pooled so that each index-tagged sample was present in equimolar

amounts. With the final concentration of the pooled samples of 2nM. The pooled samples were subject to cluster generation and sequencing using an IlluminaHiSeq 2500 System (Illumina, USA) in a 2x100 paired-end format at a final concentration of 8pmol.

The raw sequence files generated (.fastq files) underwent quality control analysis using FastQC (http://www.bioinformatics.babraham.ac.uk/projects/fastqc/) and the quality checked reads were trimmed with cutadapt v.1.10 [151] and then aligned to the human genome (hg38 assembly) using STAR v.2.5.2 [152], with standard parameters. Differentially expressed mRNAs were identified using DESeq2 v.1.12 [153]. Firstly. Gene annotation was obtained for all known genes in the human genome, as provided by GenCode (GRCh38.p7 release 25). Using the reads mapped to the genome has been calculated the number of reads mapping to each transcript with HTSeq-count v.0.6.1 [154]. These raw read counts were then used as input to DESeq2 for calculation of normalized signal for each transcript in the samples, and differential expression was reported as Fold Change along with associated adjusted p-values (computed according to Benjamini-Hochberg).

3.5.6 Gene ontology

Gene Ontology analysis was performed on differentially expressed mRNAs using the module Comparison Analysis of Ingenuity Pathway Analysis (IPA. QIAGEN, USA www.qiagen.com/ingenuity). IPA is a web-based application for the analysis of omics experiments. Data are analyzed using algorithms integrated with literature to predict regulation, relationships, direct or indirect interactions. Four different study group (24h Static, 24h Dynamic, 72h Static and 72h Dynamic) allow distinguishing the altered canonical pathways and biological functions associated with *in vitro* condition and mechanical stress per se.

3.5.7 Real-time qPCR

Real-timeqPCR was performed to verify the regulation of the genes highlighted by RNA-sequencing. SYBR Green PCR Master Mix (Applied Biosystems, USA) fluorescent dye was used. The SYBR Green probe intercalates just double-stranded DNA. The Increasing of fluorescence intensity is proportional with the increasing of double-stranded DNA molecules produced during the PCR reaction, performed with specific primers for the genes analyzed (**Table 4**).

Gene	Forward	Reverse
AMIGO2	GTGGTCTGACTCCAGGCACT	TGATGCTGTAGAGCAATTCAT
ARHGAP6	GAAGCCCCAGCTGCACTA	GAGAGACTCTGGATGGGGACT
CHRNA9	GGCCATGACTGTATTTCAGCTA	GGCCATCGTGGCTATGTAGT
PMEPA1	ATACAAAAAGCGGAGCTGGA	GTGATCACCACCACCATCAC
STEAP4	GATTGGGAAACTTAACCGTTACC	CAAAGCCACATATGAATCACTGAG

Table 4 Details of primer sequences

3.6 Overexpression

To set the protocol for an efficient overexpression of AMIGO2 in SVP cell lines have been tested two different protocols: a lipo-mediated transfection and a lentiviral transduction.

These methods require different steps and use different techniques described below: bacterial transformation and selection, DNA isolation, lentiviral preparation, and infection.

3.6.1 Lipo-mediated transfection

To overexpress AMIGO2 by lipid was necessary to amplify the number of plasmid (circular DNA) copies by bacterial transformation. The expression efficiency of the plasmid was headed by transfection of HEK 293T cells and verified by Western blot. When the ability of the plasmid to produce the protein has been verified, overexpression in SVPs was performed.

3.6.1.1 Bacterial transformation and selection

Bacterial transformation is the introduction of a plasmid or other types of DNA, into bacterial cells chemically treated to increase the permeability of their membrane. The plasmid contains several genes, not just the one to overexpress. One of these genes provides antibiotic resistance which allows bacteria to survive in the presence of a specific antibiotic. In that way, just the bacteria that took up the plasmid can live and proliferate. Each bacterium plated will give rise to a colony of identical bacteria, all carry the plasmid.

The plasmid pCMV6-AMIGO2 (OriGene, USA), contains AMIGO2 carrying 8 amino acids of the protein c-Myc as TAG and the plasmid pCMV6-entry (OriGene, USA) used as a control, were introduced in a strain of Chemically Competent *E.coli*One Shot Stbl3 (Thermo Fisher Scientific, USA) using heat shock protocols.

Briefly, competent *E. coli* Stbl3 cells were removed from the –80 °C and allow to warm at RT. 20 µl of the cells and 2 µl of the plasmids were mixed in 1.5 ml tube and then incubated on ice for 30 minutes. Heat shock was performed in a water bath at 42°C for 45 seconds and then back in ice for 2 minutes. 300 µl of SOC medium (Corning, USA) were added and the mixture was incubated at 37°C in constant shaking a for 90 minutes. 100 µl of the transformed bacterial cells were transferred to an agar plate containing Luria Broth Base (Miller's LB Broth Base) (Thermo Fisher Scientific, USA), 1.5% agar and 50 µg/ml of kanamycin, for bacterial selection. Plates were incubated inverted O/N at 37°C. The day after the plates with the colonies were putted at 4°C to avoid overgrowth. Then, singles colonies were picked with 200 µl tips and putted in 5 ml of LB Broth medium with 50 µg/ml

of kanamycin O/N at 37°C in constant shaking. The next day, 3 ml of the cells grown were incubated with 150 ml of LB Broth medium with 50 µg/ml of kanamycin O/N at 37°C in constant shaking. O/N cultures were centrifuged at 5000xg for 10 minutes to isolate plasmid DNA.

3.6.1.2 DNA isolation

Plasmid DNA isolation from transformed *E. coli* has been performed using GenElute High Performance (HP) Plasmid Maxiprep Kit (Sigma-Aldrich, USA) following manufacturer instruction. Briefly, the bacterial cells harvested by centrifugation were lysed with an alkaline-SDS solution for 3 minutes. DNA purification was carried out onto a silica membrane column in high salts concentration solution. Contaminants were removed by two wash steps. Finally, DNA bound to the membrane has been eluted 1.5 ml of ultrapure water.

3.6.1.3 Cell transfection

Have been used SVPs isolated at the Bristol Heart Institute of Bristol Royal Infirmary between P4 and P6. $8x10^4$ cells were seeded in 6-well plate. The day after were prepared the solutions for the cell transfection as shown in **Table 5,** using serum-free OptiMEM medium (GIBCO Thermo Fisher Scientific, USA), Lipofectamine 2000 (Thermo Fisher Scientific, USA) and plasmids previously isolated.Tubes wereIncubate for 5 minutes at room temperature, then mixed and incubated at room temperature for 20 minutes. SVPs were washed with PBS once to remove FBS and antibiotics from the cultures. Finally, 1100 µl of antibiotic-free medium was dispensed to each well and the content of the appropriate tube was added. SVPs were incubated for 6 hours, then the transfection medium was replaced by EGM-2.

Treatment	Tube	Reagent
Control	Tube 1	200ul serum-free OptiMEM
	Tube 2	200ul serum-free OptiMEM
Vehicle	Tube 1	200ul serum-free OptiMEM
	Tube 2	2ul lipofectamine 2000 197ul serum-free OptiMEM
pEmpty	Tube 1	25 to 500 ng of pCMV6-entry 190ul serum-free OptiMEM
	Tube 2	2ul lipofectamine 2000 197ul serum-free OptiMEM
pAMIGO2	Tube 1	25 to 500 ng ofpCMV6-AMIGO2 190ul serum-free OptiMEM
	Tube 2	2ul lipofectamine 2000 197ul serum-free OptiMEM

Table 5 Details of transfection solutions

3.6.2 Lentiviral transduction

Viral particles that induced SVPs to overexpress AMIGO2 have been produced through a triple transfection using HEK293T cells. The amounts of plasmids for triple transfection were increased by cloning in Stbl3 competent bacteria.

3.6.2.1 Bacterial transformation and selection

The plasmids pLVhAMIGO2 (VectorBuilder, USA) contains AMIGO2 (**Figure 15**); psPAX.2 that contains Gag, Pol, Rev, and Tat genes for the virus packaging; pVSV carrying the virus' envelope gene and pLVX-GFP with GFP gene (plasmids gently provided by Dr Asthon Faulkner), used as control, were introduced in a strain of Chemically Competent *E.coli*One Shot Stbl3 (Thermo Fisher Scientific, USA) using heat shock protocols as above described.

E. coli Stbl3 cells transformed were platedin agar plates containing LB Broth Base, 1.5% agar and 100 µg/ml of ampicillin to be selected. Four singles colonies were picked with 200 µl tips and putted in 5 ml of LB Broth medium with 100 µg/ml of ampicillin O/N at 37°C in constant shaking. The next day, 3 ml of the cells grown were incubated with 150 ml of LB Broth medium with 100 µg/ml of ampicillin O/N at 37°C in constant shaking. O/N cultures were centrifuged at 5000xg for 10 minutes to isolate plasmid DNAby GenElute High Performance (HP)Plasmid Maxiprep Kit as previously described.

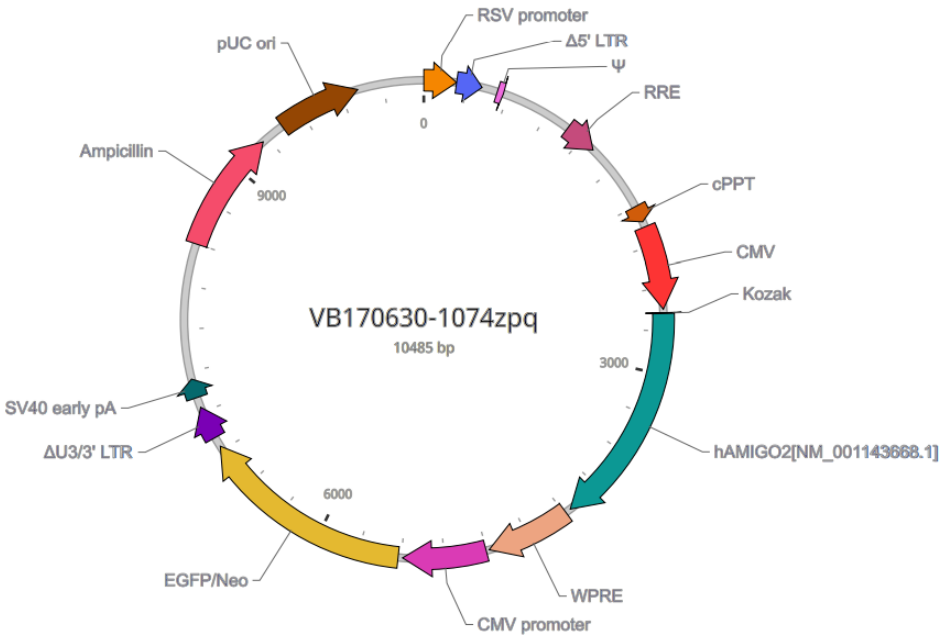

Figure 15 Map of AMIGO2 overexpression plasmid.

3.6.2.2 Lentivirus preparation

Lentiviral particles for cells infection were produced using purified plasmids and human embryonic kidney HEK 293T cell line, gently provided by Dr Graciela Sala-Newby.

3.6.2.3 Cell culture

HEK 293T is a highly transfectable cell line, derivative from HEK 293 cells, that express the SV40 T-antigen. Due to the expression of SV40 large T antigen, the plasmid that carries the SV40 origin of replication can replicate in the cells. This increase the copy number of the plasmid in the cells and the amount of retrovirus that can be produced.

One vial contained frozen HEK 293T has been thawed in a water bath for few seconds and then centrifugated with 5 ml of PBS at 300xg for 5 minutes. Cells were grown in DMEM normal glucose supplemented with 10% of FBS, 1% penicillin-streptomycin (Life Technologies, USA) and 2 mM L-glutamine (Life Technologies, USA). When cells reached 60% of confluence, they were split 1:3 with Trypsin/EDTA solution.

3.6.2.4 HEK 293T transfection

HEK 293T were seeded into a 6-well plate at $2x10^5$ cells per well. The day after the medium was replaced with 2 ml of full growth medium and the transfect mixes were prepared:

For each well: 125 µl of Opti-MEM (GIBCO Thermo Fisher Scientific, USA)

0.55 µg of psPAX2

0.075 µg of pVSV

0.625 µg of pAMIGO2 or pGFP

10 µl ViaFect Transfection Reagent (Promega, USA)

After 10 minutes of incubation at RT the transfection mixes were added above the medium. After 24h the media, that contain the viral particles, were filtered through 0.45 µm filter (Millipore, USA), labeled as V_1 and freeze down at -80°C. Fresh media were added to the cells for the next day virus collection. The day after, the media were filtered with 0.45 µm filter labeled as V_2 and freeze down at -80°C.

3.6.2.5 Cell infection

Have been used SVPs isolated at the Bristol Heart Institute of Bristol Royal Infirmary, at the third passage in culture. The cells were seeded at the density of 9000 cell/cm^2 in 24-well plate. The day after the media V_1 were thawed a 1 ng/ml of polybrene infection/transfection reagent (Millipore, USA) were added. 500 µl of V_1 on each well of SVPs and incubated for 24h. After that, virus media were removed and replaced with EGM-2 for 5 hours to allow the cells to recover. Then, the V_2 media with 1 ng/ml polybrene were added O/N. SVPs, permanently infected, were grown until they have reached sufficient numbers for RNA collection, WB, apoptosis, and proliferation assays.

3.7 Western blot

Western blot analyses were used to quantify the expression of AMIGO2 in the naïve and overexpressing SVPs.

3.7.1 Protein extraction and quantification

Adherent SVPs cell were washed two times with cold PBS. Lysis buffer (50 mM HEPES pH7.5, 150 mMNaCl, 1.5 mM $MgCl_2$, 1 mM EGTA, 1% NP-40, 10% glycerol, protease and phosphatase inhibitors) was added directly in the dish, and cells were mechanically scraped off using a cold plastic cell scraper on ice. The cell suspension was collected in 1.5 ml tube and incubated for 30 minutes in ice, vortex every 10 minutes. Lysate was then centrifuged for 15 minutes at 4°C at 15,000xg, the supernatant was collected and stored at -80°C.

The concentration of protein extracts was measured using Pierce BCA Protein Assay （Thermo Fisher Scientific, USA） following manufacturer instructions. The two-step reaction leads samples to form a purple-colored reaction product that is strongly influenced by four amino acid residues (cysteine or cystine, tyrosine, and tryptophan) in the amino acid sequence of the sample's protein. The absorbance was measured at 570 nm with a microplate spectrophotometer.

3.7.2 Gel electrophoresis

After quantification, 40 µg of protein extracts were resuspended in water and 6X loading buffer (with 10% of β-mercaptoethanol). Samples were heated at 70°C for 10 minutes. Proteins were separated by their molecular weight by SDS-PAGE gel at 10% of polyacrylamide, with stacking gel at 4%. SDS is ionic detergent that denatures and applies a negative charge to the protein in proportion of their molecular weight, so they migrate from the cathode (+) to the anode (-) side. The voltage of the electrophoresis run was set at 60 V for 30 minutes and then 120 V for 60 minutes performed in Tris/Glycine/SDS buffer (Bio-Rad Laboratories, USA). Once the proteins were separated on the gel they were transferred into polyvinylidenedifluoride membranes PVDF (Bio-Rad Laboratories, USA). The proteins were transferred in wet condition in Tris/Glycine Buffer (Bio-Rad Laboratories, USA) for 75 minutes at 90 V, with a stirring magnet to help dissolve the heat and mix the buffer. To check if proteins were correctly transferred into the membrane Red Ponceau staining (Ponceau S solution, Sigma-Aldrich, USA)were applied.

3.7.3 Antibody hybridization

After blocking nonspecific binding with 5% milk in TBST buffer for 60 minutes in agitation, membranes were probed with primary antibodies anti-AMIGO2 (451-463) antibody produced in rabbit (Sigma-Aldrich, USA) 1:1000 at 4°C, O/N or with Anti-Beta Actin antibody [mAbcam 8226] (Abcam, UK) 1:5000 at RT for 60 minutes. Membranes stripping was obtained using restore PLUS Western blot stripping buffer （Thermo Fisher Scientific, USA). Detection was carried out using ECL Western blotting detection reagent (Amersham, UK).

3.8 In vitro scratch assay

In vitro scratch assay has been used to quantify cell migration. Cells were seeded in a 96 well plate at $9x10^4$ cells/cm^2 density and grown until confluence in EGM-2. The cell monolayer was scratched sterile P10 tip to create a gap in cell monolayer. After scratching, the cells were washed two times with PBS to remove debris. The assay has been performed using EBM medium (Lonza, Switzerland) supplemented with 2 mMhydroxyurea (Sigma-Aldrich, UK) to avoid cell growth. As positive control was used EGM-2 with 2mM hydroxyurea. Cells were incubated at 37°C and 5% CO2.

Images were taken at 0 and 24 hours at 5X magnification using a bright field inverted microscope and analyzed with ImageJ.

3.9 Bioreactor for vein stimulation

The *ex vivo* culture system utilized for veins stimulation has been designed by our collaborators from Dipartimento di Elettronica, Informazione e Bioingegneria, Politecnico di Milano and Unità di IngegneriaTissutale of Centro CardiologicoMonzino-IRCCS in Milan (**Figure 16**).

The system is provided with a double chamber, to have a physical separation of the intra-luminal vessel compartment from the extra-adventitial region, with two fluidic independent circuits and reservoirs. The environment of the two chambers can have a different setting to expose the intimal or the adventitial layers to distinct oxygen conditions. The SV samples were mounted into the system as shown in **Figure 16**. The arterial stimulation flux or consisted in 4 independent phases: (I) a loading step, (II) a pulsatile stimulation step, (III) an unloading step and (IV) a recirculation step. In the first phase, the vessel is filled with DMEM, supplemented with 10% (FBS), 1% L-Glutamine, and 1% P/S. During the pulsatile step the medium is put under oscillating pressure between 80 and 120 mmHg and in the third phase, the medium flows out of the vessels. These three phases have an entire duration of 10 minutes. The fourth phase, 2 minutes long, serves to replace the medium inside the vein with the medium contained in the external chamber. The vein flux stimulation doesn't have the second pulsatile phase.

Veins were harvested with a NT method and a 5-cmlong vein segment was mounted in the culture system, placed in a standard incubator at 37° C in a 5% CO_2 atmosphere for 14 days. A piece of the remnant tissue was kept as native vein control. This strategy allowed to have a sample with a flux stimulation, arterial or venous, and native conditions of the same vessel. During the culture period, the medium was partially replaced every 4 days. SV segments were un-mounted from the ex-vivo culture system and put in formalin 37% and then embedded in paraffin for immunohistochemical analyses.

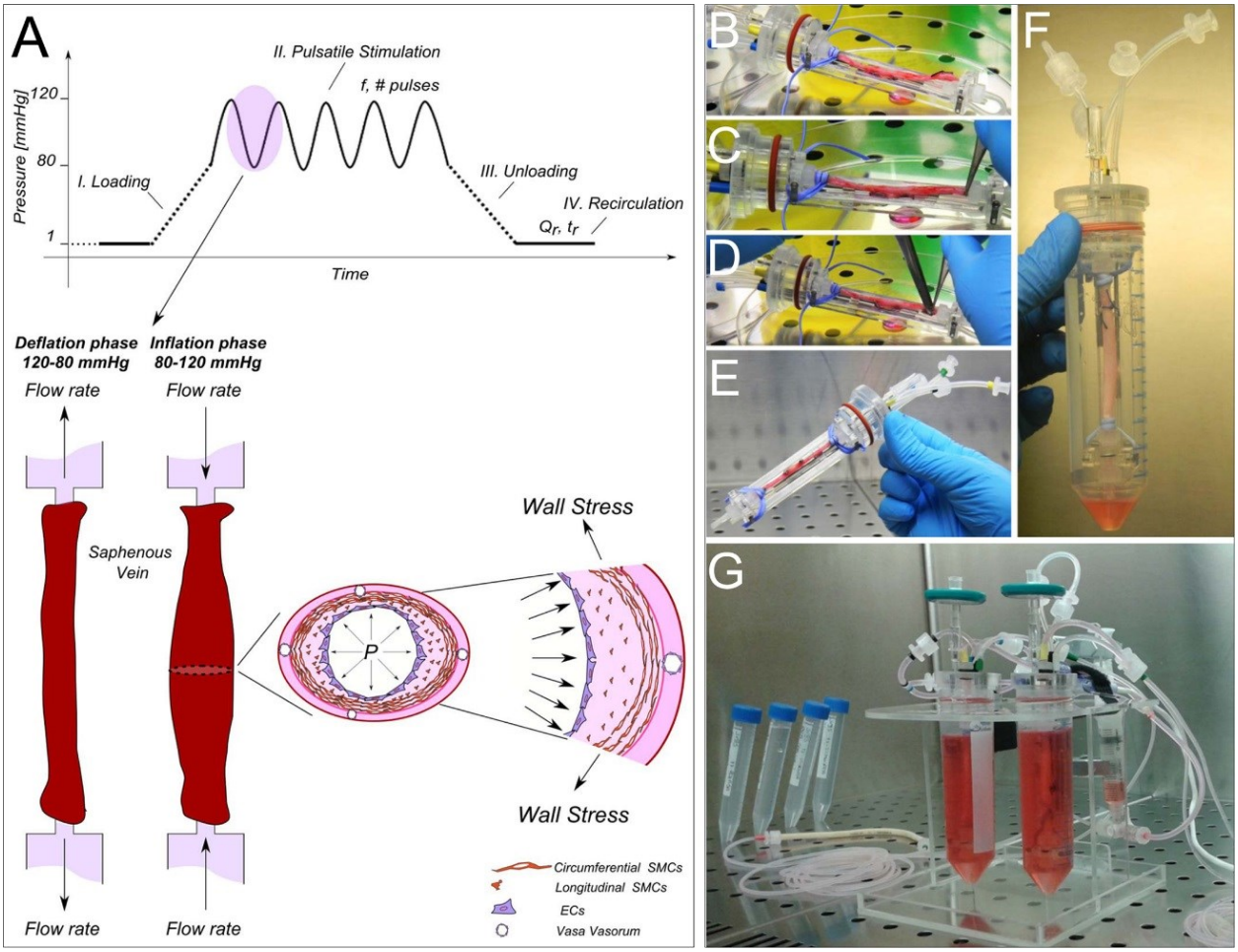

Figure 16 Ex vivo vessel culture system. *(A) The arterial stimulation cycle consists of: I) a loading phase, the vessel is filled with medium. The luminal pressure reaches 80 mmHg at the end; II) a pulsatile stimulation phase with oscillating pressure between 80 and 120 mmHg; III) an unloading phase in with the medium flows out of the vessels and the pressure is lowered to zero; IV) a recirculation phase. The pulse frequency (f), the number of cycles (# pulses), the duration (tr) and the medium flow rate (Qr) can be set through PRESSURE VALUES software interface During the pulsatile phase, the cells of the vessels are subjected to circumferential stress typical of the arterial circulation. (B-G) The ex vivo vessel culture system during assembling under laminar flow hood.*

Dr. Davide Maselli, *"The role of mechanical stress in progression of intima hyperplasia associated to vein coronary bypass grafts disease.",* PhD thesis in Biochemistry, Physiology and Molecular Biology of International PhD School in Life Sciences and Biotechnologies, University of Sassari.

3.10 Immunohistochemistry

Native vein samples were collected after surgery and put in 4%formalin for 24 h. Fixed native and treated veinswerethen processed to be included in paraffin. Sections of 2 µm were collected on glass slides coated with silane and let dry O/N at 37°C. The slides were dewaxed at 65°C for 30 minutes and xylene for 10 minutes, then hydrated in alcohol scale with descending concentration up to distilled water.

The antigen retrieval was performed by microwave in citrate buffer at pH 6, 3 time for 5 minutes. For the staining performed with AMIGO2 and ApopTag In Situ Apoptosis Detection Kit, to visualize the apoptotic cells *in situ*, a double antigen retrieval was necessary. Thus, after microwave the section were incubated with Proteinase K 20 µg/ml in Tris-EDTA Buffer pH 8 (50 mM Tris Base, 1 mM EDTA) for 10 minutes at RT. Nonspecific binding was blocked with 20% goat serum (Sigma-Aldrich, USA) for 30 minutes at RT. After elimination of serum, without washing, the primary antibody solution was added and incubated O/N at 4°C. After 3 washes of 5 minutes the slides were incubated with the secondary antibody diluted 1:200 for 60 minutes at 37°C. After 3 washes of 5 minutes was added the DAPI solution 1µg/ml in PBS for 15 minutes at RT, to stain the nuclei. Slides were mounted with Fluoromount G.

Primary Antibody	Supplier	Dilution	2nd Antibody
AMIGO2	Abcam (ab 84416)	1:200	Alexa568 Goat anti-Rb
PCNA	DAKO (PC10)	1:200	Alexa647 Goat anti-Rb

Table 6 Details of Immunohistochemistry antibodies

RESULTS

4.1 SVPs isolation and characterization

Twenty-seven different SVPs line have been isolated from patients undergoing surgery for varicose veins or cardiac bypass grafting. The isolation protocol requires two cell magnetic-activated sorting performed respectively for CD31, collecting the negative fraction and CD34. Depending on the size of the veins up to $1x10^6$ cells were obtained from the selection. SVPs were expanded until the fourth passage, then the homogeneity of the population was assayed by immunocytochemistry and FACS analysis. Doubling time has been calculated from P1 to P4.

SVPs primary culture *in vitro* show a spindle-shaped morphology similar to fibroblasts and mesenchymal cells (**Figure 17A**).The global mean of the different population is 4.8±0.6 days for a duplication (**Figure 17B**). Immunocytochemistry characterization (**Figure 17C**) shows that the SVPs express pericytes markers as PDGFRβ and NG2, as well as the transcription factor GATA4 related to proliferation. SVPs are negative for CD146 and α-SMA. The absence of cells CD31 positive shows the efficiency of the magnetic sorting.

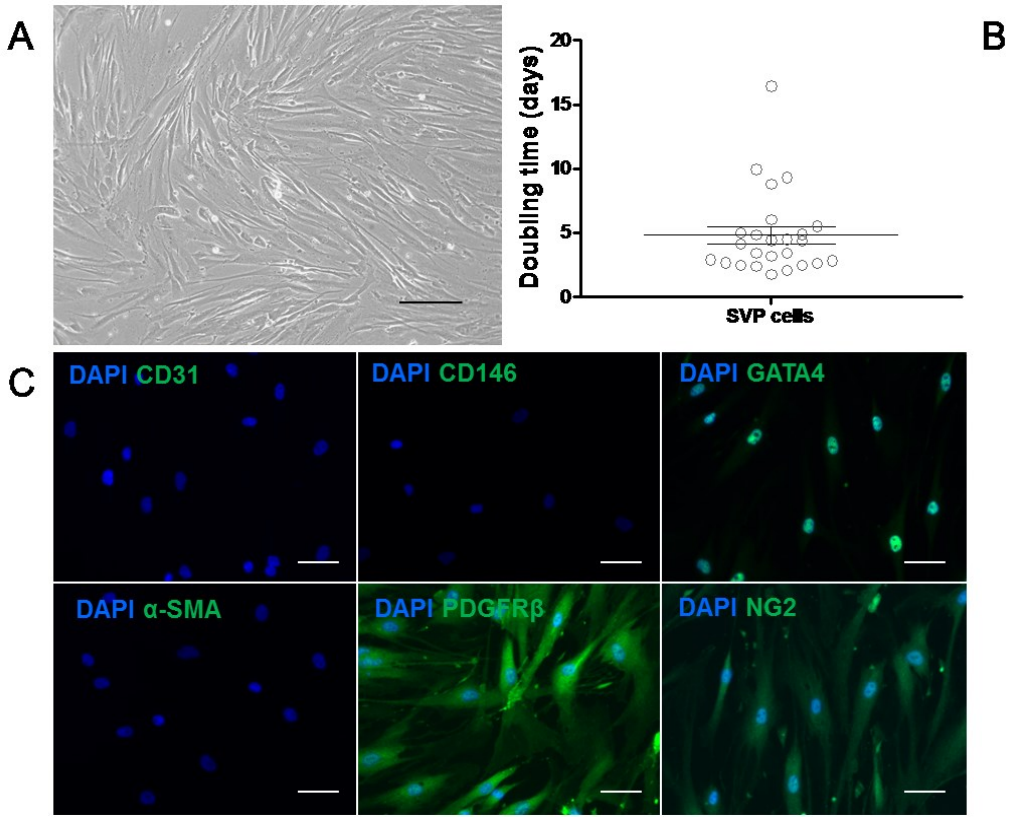

Figure 17 SVPs morphology and phenotype. *SVPs sorted from patients undergoing surgery for varicose veins or cardiac bypass grafting. An SVPs spindle-shaped morphology (scale bar=100 µm).B SVPs doubling time between P1 and P4 after isolation (Graph shows mean and SEM).C Immunocytochemistry characterization of SVPs shows their pericytes phenotype. They are negative for EC markers CD31 and SMC markers α-SMA (scale bars=20 µm).*

Dr. Davide Maselli, *"The role of mechanical stress in progression of intima hyperplasia associated to vein coronary bypass grafts disease.",* PhD thesis in Biochemistry, Physiology and Molecular Biology of International PhD School in Life Sciences and Biotechnologies, University of Sassari.

4.2 FACS analysis

After the fourth culture passage SVPs were characterized also by FACS analyses (**Figure 18**). the efficiency of the magnetic sorting has been analyzed based on the negativity for the CD31 antigen. To examine also the mesenchymal phenotype of SVPs, as previously demonstrated,[81] we measured the expression of CD44, CD90, CD105. Results denote the high efficiency of the sorting, just one of the 27 SVPs lines express CD31 around 50%. This cell line is not being further used. Similarly to the literature, SVPs express high-level of mesenchymal markers CD44 (98.45±0.23%) CD90 (94.55±2.55%) and CD105 (73.88±3.79%). CD105-endoglin expression is variable within the cell populations but just a few samples have a low expression of the marker.

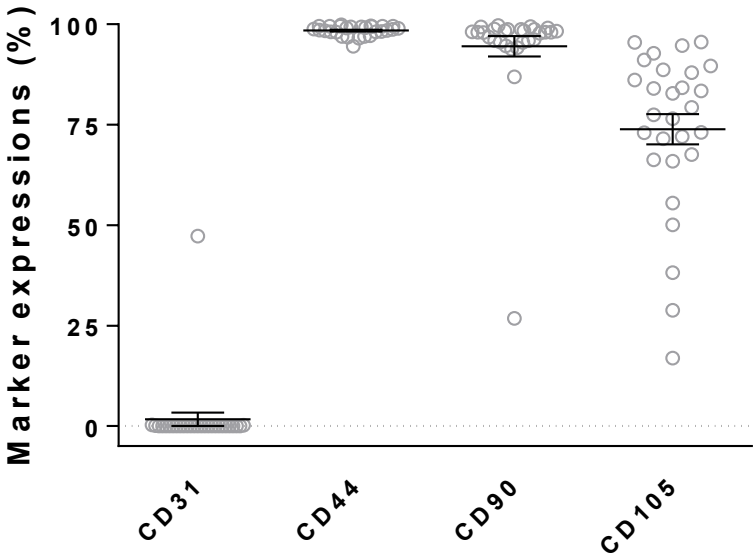

Figure 18 SVP express mesenchymal markers. *SVPs at fourth passage were detached with a EDTA solution and stained for endothelial and mesenchymal markers. The cells populations are negative for CD31, with the only exception of one cell line. Mesenchymal markers are highly expressed in SVPs. More than 90% of SVPs are positive for CD44 and CD90. CD105 have a more heterogeneous expression with few samples under the 50% of positivity (Graph shows mean and SEM).*

4.3 Growth curve in static conditions

To assess the effect of stretching on SVPs they were seeded in 6-well BioFlex culture plates. Their flexible-bottom allow to transmit the vacuum-mediated deformation to the cells plated in monolayer. The rubber bottom of the plate was made hydrophilic with Sulfo-SANPAH solution under UV light to let the polymer to crosslink. Fibronectin/gelatine coating was performed under the UV light as well. In order to evaluate the effect of the different coating protocol and culture condition on the proliferative rate of the cells, a growth curve in static condition of SVPs has been performed.

SVPs at fourth passage were trypsinized, counted and respectively $5x10^4$, $1x10^5$ and $2x10^5$ cells were seeded in duplicate in 6-well BioFlex culture plates. The plates have been put-on Flexcell Tension Plus FX-5000T system in static condition, at 37° C in a 5% CO_2 atmosphere. After 24 hours one of each well with different cells density was trypsinized and the living cells were counted with trypan blue using a Neubeauer chamber. The same has been done after 72 hours. 5 SVPs line were analyzed, and the results show that they are able to adhere, growth and duplicate on the BioFlex coated membrane. At 72 hours the population was three times greater with a low amount of cell death (**Figure 19**).

To ensure the dynamic transmission of the stimulus across the cellular layer and a number of cells sufficient for the assays after the stimulation, we decided to seed $1x10^5$cells per well. At higher density indeed, the confluence of the cells can affect the efficiency of the stretching.

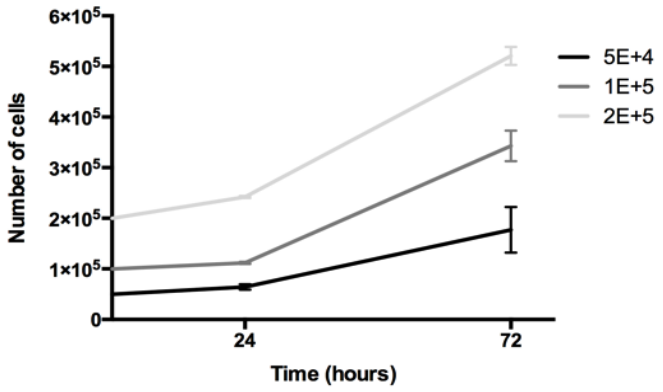

Figure 19 SVPs are adapted to the BioFlex membrane culture. *Growth curve of 4 SVPs line was measured in static condition on the coated BioFlex membrane. Living cells were counted after 24 and 72 hours. The choice to plate $1x10^5$cells for the stretching experiments guarantee that the deformation can act homogeneously across the cells' monolayer and ensure also enough amount of sample to perform several assays (Graph shows mean and SEM).*

4.4 Stretching affects orientation and proliferation rate of SVPs

Five SVPs lines were seeded on BioFlex 6-well culture plate and the mechanical strain was applied with 1 Hz frequency and 10% deformation for 24 and 72 hours in a standard incubator at 37°C in a 5% CO_2 atmosphere. After the stimulus, the cells were analyzed to assess the effect of the strain on their number and their phenotype

After 24 hours of strain, SVPs number seemed unaffected compared to the static control. After 72 hours the cell number was significantly lower than the not strained control, suggesting that the dynamic stimulus can affect the proliferation rate (**Figure 20A**).

During the 24 and 72 hours stimulation, cells were observed under a phase-contrast microscope showing a gradual, time-related shape remodeling. To assess the phenotypic changes SVPs were fixed with PFA 4% and stained for β-Actin. Cell reorientation was quantified using ImageJ. Results show that under dynamic conditions the direction of the major axis of the cytoplasm and nuclei re-oriented. After 24 hours and much more after 72 hours, SVPs were oriented perpendicularly to the direction of the tensile force, acquiring a less dynamic deformation morphology **(Figure 20B)**.

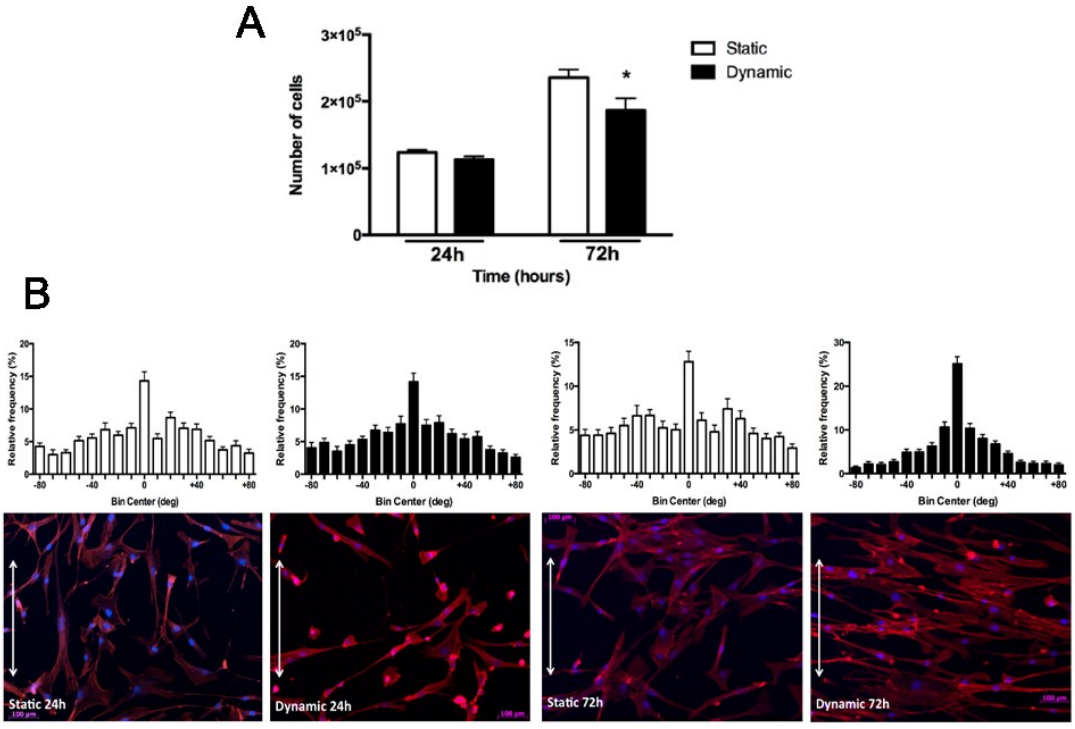

Figure 20 Strain alter proliferation rate and orientation of SVPs. *The number of cells and cell phenotype are affected by mechanical strain. (A) The graph shows that after 72 hours the number of the SVPs growing under dynamic conditions is significantly decreased compared to the static control (Graph shows mean and SEM). Similarly, panel B shows the reorientation of the cells which are arranged perpendicularly to the direction of the deformation. * p<0.05 vs. 72hstatic (Graphs show mean and SEM). SVPs stained with β-Actin and nuclei counterstained with DAPI*

4.5 Mechanical strain change SVPs transcriptome

To understand if mechanical stress modifies gene expression of SVPs, stimulating their passage to an activated state, transcriptome analysis has been performed through RNA-Seq. To perform RNA-seq, samples were checked for purity and integrity using NanoDropSpectrophotometer and Bioanalyzer. The mean concentration of the samples was 38.39±5.6 ng/µl, with a 260/280 ratio around 2, indicating a good purity for the RNA. RNA Integrity was expressed as RNA Integrity Number (RIN) a value spanning from 2 (degraded RNA) to 10 (intact RNA). The sample had a mean RIN of 9.7 indicating a high integrity level. Following the reads, the library was aligned to a reference human genome (Genome Reference Consortium Human Reference 38-GRCh38). The percentage of alignment on unique regions ranged between 32% and 88% with a mean coverage of 61.7%. For each identified gene a differential expression value was calculated using DESeq2 software, giving the adjusted p-value (adjp-value) and a Fold Change (FC) for each gene expressed. Four comparisons were made: 24hDYN vs. 24hSTAT; 72hDYN vs. 72hSTAT; 72hSTAT vs. 24hSTAT; 72hDYN vs. 24hDYN. The first two comparisons show which genes are regulated by the mechanical stimulus. Comparisons based on time include the effects due to the time of culture.

The numbers of genes expressed in all datasets was 29000, and 6192 were the genes co-expressed by all SVPs tested. For each comparison significantly differentially expressed genes, i.e. with values of padj$\leqslant$0.05, were considered up-regulated when FC$\geqslant$1.5 and down-regulated when FC$\leqslant$-1.5. The highest number of differently expressed genes was found in 72hDYN vs. 72hSTAT comparison. Such a result highlights that mechanical stress strongly affects the transcriptional level of SVPs. Heatmap analysis was used to visualize sample clusterization. for either time or treatment in the different comparisons using a hierarchical clustering algorithm (**Figure 21**).

Comparison	genes with padj ≤ 0.05 Total	genes with padj ≤ 0.05 FC ≥ 1.5	genes with padj ≤ 0.05 FC ≤ -1.5
24hDYNvs24hSTAT	1287	388	304
72hDYNvs72hSTAT	3791	899	1186
72hSTATvs24hSTAT	2595	759	390
72hDYNvs24hDYN	1889	565	319

Table 7 Differentially expressed genes. *The table shows the differences found in the four datasets. In the first column, the numbers of differentially expressed genes in the comparison are listed. In the other columns, the up-regulated and down-regulated genes are shown. The sum of up and down regulated genes does not match the total number of differentially expressed genes because differentially expressed genes cannot be considered regulated with FC's values comprised within 1.5 and -1.5.*

Genes in 24hDYN vs. 24hSTAT; 72hSTAT vs. 24hSTAT; and 72hDYN vs. 24hDYN comparisons do not segregate. A gene clusterization on the basis of treatment was observed in 72hSTAT vs.72hDYN. Results of cluster analysis show that after 72 hours mechanical stress the transcriptome of the SVPs changes, causing the differential expression of 3791 genes and the regulation of 2085 of them (**Table 7**).

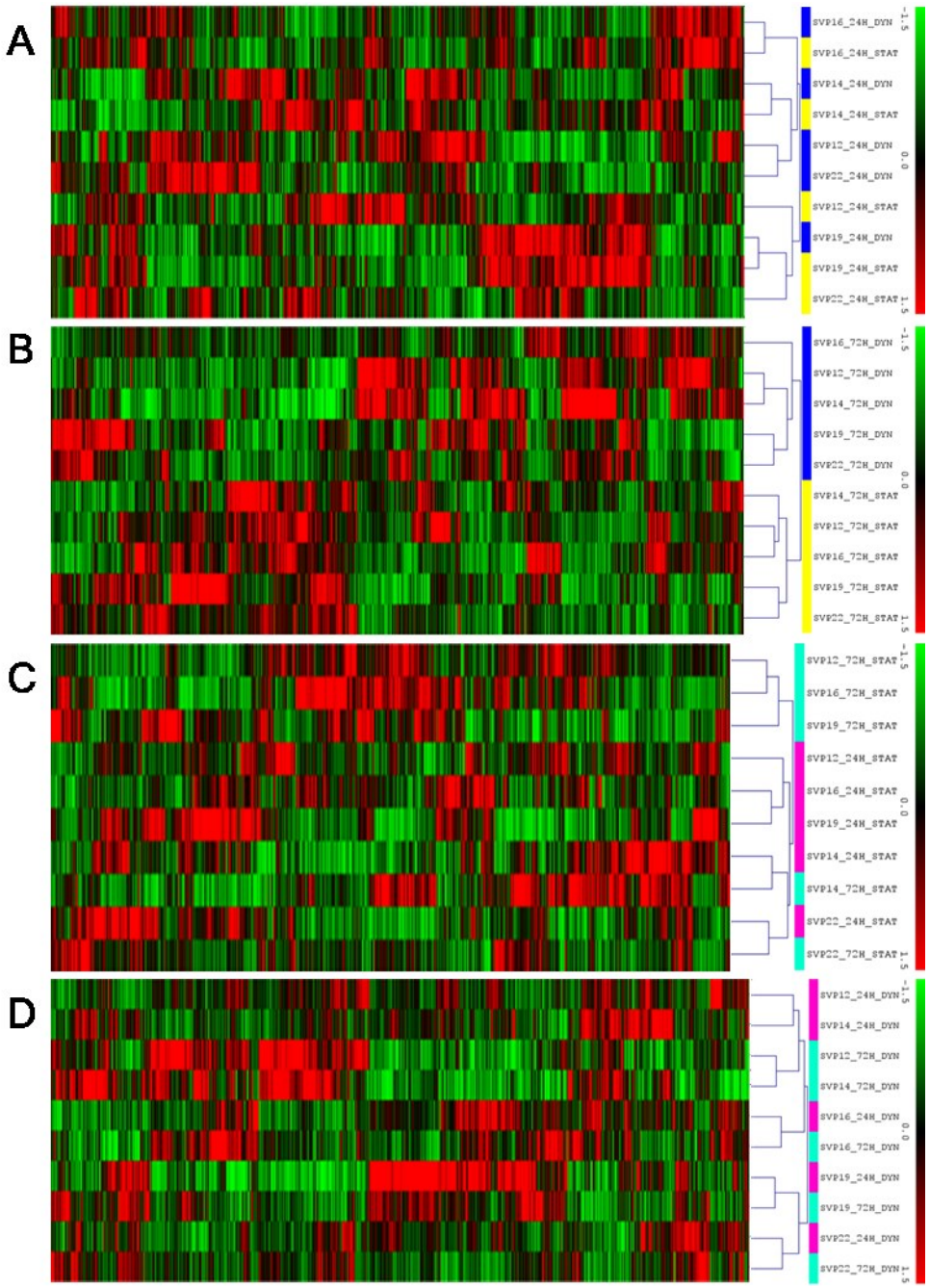

Figure 21 Samples clustering after 72 hours of stress. *Heat maps showing the pair comparison of the samples for each treatment. A and B compare the dynamic and static conditions for the time points: 24hDYN vs. 24hSTAT; 72hDYN vs. 72hSTAT. After 72 hours treatment the samples clustered due their transcriptomic profile. In C and D the comparison 72hSTAT vs. 24hSTAT and 72hDYN vs. 24hDYN show that only the time of culture both in static and dynamic conditions does not lead to clustering, highlighting the importance of mechanical stimulus.*

4.6 Mechanical stress induces migratory phenotype in SVPs

Ingenuity Pathway Analysis was used to investigate if the differentially expressed genes were involved in specific pathways and biofunctions that could be regulated due to the mechanical stress. The four comparisons were loaded restricting the species specificity to human and using an FC cut-off of 1.5. Using the "Comparison Analysis" tool, differences in the activation/inhibition of functions or pathways between the four datasets were simultaneously observed. The activation/inhibition state was defined through a Z-score, a statistical index that expresses how many standard deviations a single value is below or above the mean of all data. A Z-Score$\geqslant$2 was considered a good predictor of a significant activation of specific pathway or function while a z-Score$\leqslant$-2 was a predictor for the inhibition. Most of the differentially expressed genes fell into cancer-related pathways or functions because they are the most annotated in literature with a high degree of overlap with "non-cancer" pathways, thus we decided to not take them in account.

4.6.1 Canonical Pathways

IPA analysis was performed to run a Canonical Pathway analysis. 22 canonical pathways were significantly modulated in the four datasets. 9 out 22 pathways were modulated by time of culturing conditions but not by mechanical stress (in the 72hSTAT vs. 24hSTAT comparison) and were not considered for further analysis.

The analyses show a high prediction of regulation for 4 pathways in 24hDYN vs. 24hSTAT and 7 in 72hDYN vs. 72hSTAT conditions (**Table 8**). One of the most regulated pathways significantly activated in dynamic condition was the *Planar Cell Polarity (PCP) pathway*. This is a highly conserved pathway from insects to vertebrates, known to be involved in many processes in polarized cells and tissues. PCP pathway is involved in oriented cell division, acquisition of asymmetric cellular morphology, and directional cell migration and each process representing a vectoral behavior.[155] Migration, proliferation and cytoskeletal reorganization are mechanisms related to the development of intimal hyperplasia, already know for other phenotypes like SMCs and myofibroblasts, and linked to the PCP pathway. The activation of PCP pathway suggests that also the SVPs can be activated by mechanical stress.

Canonical Pathway	24hDYN vs. 24hSTAT	72hDYN vs. 72hSTAT	72hSTAT vs. 24hSTAT	72hDYN vs. 24hDYN
Interferon Signaling	-2.24	-1.73	0.00	0.00
cAMP-mediated signaling	-2.12	-1.67	0.00	0.00
GNRH Signaling	-1.13	-2.52	0.00	-0.45
Dendritic Cell Maturation	-1.00	-2.29	2.89	2.00
Corticotropin Releasing Hormone Signaling	-0.82	-1.81	2.24	1.00
HMGB1 Signaling	-0.71	-1.89	2.11	1.63
PTEN Signaling	-0.63	1.15	-2.45	0.71
Aryl Hydrocarbon Receptor Signaling	0.00	0.00	0.00	2.00
Cell Cycle: G2/M DNA Damage Checkpoint Regulation	0.00	0.00	2.71	1.67
Cyclins and Cell Cycle Regulation	0.00	-1.34	-2.89	-2.33
Integrin Signaling	0.00	-0.20	2.12	0.38
Mitotic Roles of Polo-Like Kinase	0.00	0.00	-1.94	-2.65
Mouse Embryonic Stem Cell Pluripotency	0.00	0.50	2.24	1.89
Role of BRCA1 in DNA Damage Response	0.00	0.00	-2.12	-1.13
Sperm Motility	0.00	-2.98	1.67	0.82
NRF2-mediated Oxidative Stress Response	0.45	-0.69	2.24	1.41
Coagulation System	1.00	2.00	-1.00	0.00
PCP pathway	1.13	2.32	1.41	2.83
Role of Wnt/GSK-3β Signaling in the Pathogenesis of Influenza	1.34	2.71	0.00	2.00
Colorectal Cancer Metastasis Signaling	1.50	0.63	1.15	2.00
Glioblastoma Multiforme Signaling	2.11	1.40	0.00	1.15
Basal Cell Carcinoma Signaling	2.12	2.32	-0.38	0.82

Table 8 Significantly regulated Canonical Pathway in the four comparisons. *The color gradient is used to visualized the intensity of Z-Score. A positive Z-Score (orange) indicates that pathway expression is upregulated, while a negative score (blue) represents downregulated expression.*

4.6.2 Specific functions

IPA analysis was performed to explore the modulated functions. Unexpectedly the comparisons that showed the strongest regulated functions were 24hDYN vs. 24hSTAT and 72hSTAT vs. 24hSTAT i.e., the dynamism after 24 hours in culture and the long-term effect of the culture system without dynamism. Taking aside again the cancer-specific functions, the comparisons showed the activation of opposite functions (**Table 9**). In long-term static condition lipid metabolism and cell death, related mechanisms like necrosis, apoptosis, and autophagy were activated. In cells exposed to dynamic stress for 24 hours, the activation of cell movement, migration, secretion and mitogenesis was observed. Thus, the mechanical stress after 24 hours seems to improve key functions for cell activation in IH, while the long-term culture inhibits cell proliferation probably due contact inhibition. On the contrary, after 72 hours dynamic stimulus cells shut down functions related to cell proliferation, migration, and differentiation. There is also a decrease in cell survival and

viability. This may indicate that long-lasting mechanical stress has negative effects on SVPs. Otherwise, the detrimental effect on cell viability could be a consequence of prolonged culture, that have negative effects in terms of cells proliferation both in dynamic and static conditions after 72 hours.

Deseases and Bio Functions	24hDYN vs. 24hSTAT	72hDYN vs. 72hSTAT	72hSTAT vs. 24hSTAT	72hDYN vs. 24hDYN
cell movement	3,61	-1,53	0,98	0,39
migration of cells	3,21	-1,82	0,52	-0,04
secretion of molecule	2,56	0,09	0,00	0,00
invasion of cells	2,51	0,67	0,42	1,47
mitogenesis	2,31	1,18	0,00	0,00
activation of vascular endothelial cells	2,18	0,00	0,00	0,00
tubulation of cells	2,12	-0,95	0,00	-0,25
cell spreading	2,12	-0,43	0,00	0,00
leukocyte migration	2,02	-0,93	0,00	0,00
concentration of lipid	2,00	0,32	0,00	0,81
proliferation of cells	1,48	1,04	-4,27	-1,36
cell survival	0,76	-2,94	0,48	0,26
cell viability	0,57	-3,05	0,42	0,46
alignment of chromosomes	0,00	0,00	-2,70	-2,44
autophagy	0,00	0,00	2,25	0,00
chromosomal congression of chromosomes	0,00	0,00	-2,35	-2,24
cytokinesis	0,00	0,00	-2,86	-1,45
differentiation of blood cells	0,00	0,00	2,02	0,00
DNA recombination	0,00	0,00	-2,47	0,00
fatty acid metabolism	0,00	-2,77	3,59	1,77
homologous recombination	0,00	0,00	-2,44	0,00
M phase	0,00	0,00	-2,33	-0,62
recombination	0,00	0,00	-2,63	0,00
repair of DNA	0,00	0,00	-2,71	0,00
S phase of bone cancer cell lines	0,00	0,00	-2,21	0,00
transport of sterol	0,00	0,00	2,08	0,00
binding of cells	-0,09	-2,12	1,28	-0,92
apoptosis	-0,71	-0,07	2,50	0,85
necrosis	-0,82	-0,15	3,15	1,48
cell death	-0,86	-0,38	3,27	1,58
synthesis of lipid	-1,14	-3,28	3,68	0,94
neuromuscular disease	-1,34	-2,83	0,00	0,00

Table 9 Modulated functions under static and dynamic conditions. *A positive Z-Score (orange) indicates that function expression is upregulated in the comparison, while a negative score (blue) represents downregulated expression.*

4.6.3 Regulated genes

The analysis of the top 10 up or down regulated genes into different comparisons showed a few number of common modulated genes under dynamic condition, both after 24 and 72 hours (**Table 10**). Some of them showed also an increasing regulation of time-dependent stimulation. There are no shared genes in the comparisons 72hSTAT vs. 24hSTAT and 72hDYN vs. 24hDYN; and ST6GAL2 is the only gene that has been modulated in both 72hDYN vs. 72hSTAT and 72hDYN vs. 24hDYN comparison. This gene codifies for a protein involved in protein glycosylation in Golgi apparatus.

24hDYN vs. 24hSTAT

Top Analysis-Ready Molecules

Exp Fold Change ↑

Molecules	Value
AMIGO2	↑6,384
PMEPA1	↑5,411
CLDN14	↑5,177
SLC46A3	↑5,002
MURC	↑4,361
KIAA1755	↑4,228
F2RL1	↑4,178
CHRNA9	↑4,016
LBH	↑3,772
TBX21	↑3,653

Exp Fold Change ↓

Molecules	Value
GALNT15	↓-4,888
STEAP4	↓-4,700
GUCY1A2	↓-4,209
ACKR4	↓-3,939
ARHGAP6	↓-3,575
ADH1B	↓-3,477
FAM107A	↓-3,436
FAM65B	↓-3,395
APLN	↓-3,326
ANKRD33B	↓-3,242

72hDYN vs. 72hSTAT

Top Analysis-Ready Molecules

Exp Fold Change ↑

Molecules	Value
AMIGO2	↑14,071
PMEPA1	↑9,781
NOX4	↑8,515
CHRNA9	↑8,425
CLDN14	↑7,948
TGM2	↑7,873
P4HA3	↑7,788
LRRC15	↑7,379
ST6GAL2	↑6,893
SAMD11	↑6,618

Exp Fold Change ↓

Molecules	Value
PPL	↓-15,325
STEAP4	↓-11,653
ADH1B	↓-11,557
SCARA5	↓-11,359
GALNT15	↓-11,342
GUCY1A2	↓-10,456
SLC7A14	↓-8,736
ARHGAP6	↓-8,071
MRVI1	↓-7,160
GDF5	↓-6,810

72hSTAT vs. 24hSTAT

Top Analysis-Ready Molecules

Exp Fold Change ↑

Molecules	Value
C10orf10	↑4,803
MAN1C1	↑4,483
LMOD1	↑4,079
XPNPEP2	↑3,864
FAM65C	↑3,783
C3	↑3,638
NR0B1	↑3,550
GDF5	↑3,548
PDPN	↑3,422
FABP3	↑3,365

Exp Fold Change ↓

Molecules	Value
LINC00161	↓-4,092
ERCC6L	↓-3,439
PF4	↓-2,796
CDCA5	↓-2,768
ANXA10	↓-2,768
CDC45	↓-2,756
MMP3	↓-2,650
CDCA8	↓-2,601
GTSE1	↓-2,542
CKAP2L	↓-2,514

72hDYN vs. 24hDYN

Top Analysis-Ready Molecules

Exp Fold Change ↑

Molecules	Value
ALOX15B	↑5,252
MFAP4	↑5,189
COL10A1	↑4,963
ST6GAL2	↑4,061
TRIL	↑3,640
FBXO32	↑3,574
LINC01503	↑3,544
CYP1A1	↑3,529
DPT	↑3,394
PCSK9	↑3,102

Exp Fold Change ↓

Molecules	Value
RELN	↓-4,295
LY6K	↓-3,682
DHRS9	↓-3,493
SBSPON	↓-3,455
MALL	↓-3,187
MMRN2	↓-2,986
INSC	↓-2,976
TSPAN8	↓-2,934
IL7R	↓-2,682
TMEFF2	↓-2,625

Table 10 Lists of the top 10 up- and down- regulated genes.

AMIGO2, PMEPA1 and CHRNA9, as common up-regulated genes, STEAP4 and ARHGAP6 as common down-regulated genes, have been chosen based on the literature available for the further investigations (**Table 11**)

Gene	Main functions	References
AMIGO2	Enhance ECs survival and adhesion to ECM	*Park*, 2015[149]
CHRNA9	Involved in immune response due the regulation of several populations of human lymphocytes	*Peng*, 2004[156]
PMEPA1	Regulate the expression of TGF-β signaling	*Fournier*, 2015[157]
STEAP4	Improve glucose uptake, mitochondrial function and increase insulin sensitivity	*Chen*, 2014[158]
ARHGAP6	Involved in fatty acid metabolism	*Puig-Oliveras*, 2016 [159]

Table 11 Main function of the regulated genes

4.6.4 Validation of genes expression

The overexpression of AMIGO2, PMAPA1 and CHRNA9 and the down-regulation of STEAP4 and ARHGAP6 were validated by real-time qPCR. For each gene, a single couple of primers was designed using online informatics tools. Real-time qPCR validation was important to confirm the regulation using a different technique from RNA-seq. As housekeeping has been used the eukaryotic 18S ribosomal RNA (rRNA) gene, with the primers designed by Exiqon, Denmark.

Technical validation has been performed on the same samples used for RNA-Seq. Real-time qPCR data confirmed the overexpression of AMIGO2 for 72hDYN vs. 72hSTAT comparison. The down-regulation of STEAP4 were confirmed for both 24 and 72 hours time points (**Figure 22**)

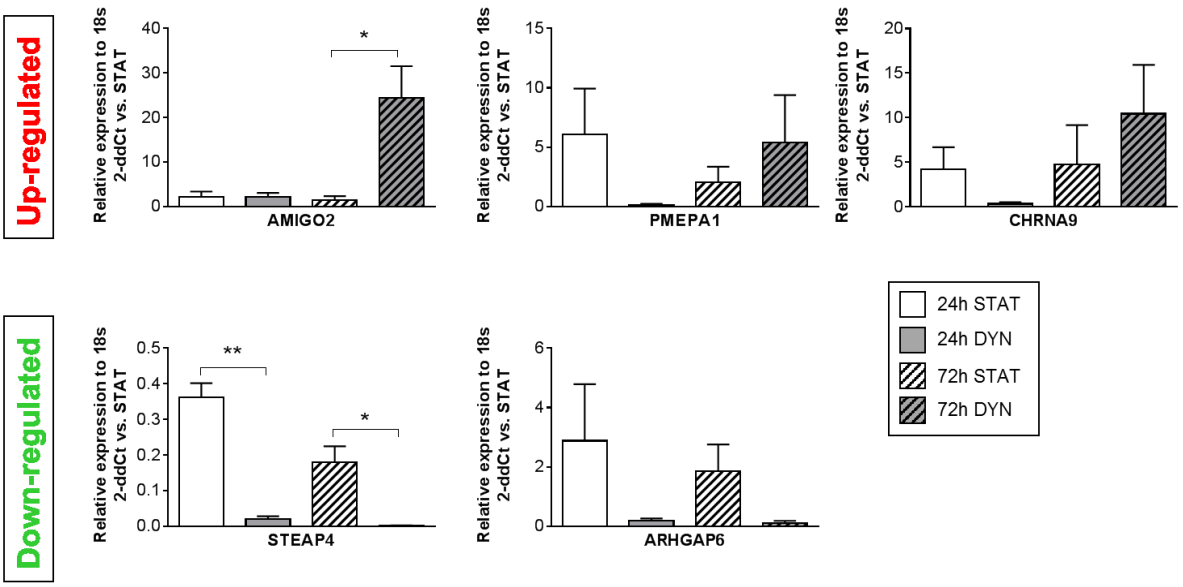

Figure 22 Technical validation. *Expression of AMIGO2, PMAPA1, CHRNA9, STEAP4 and ARHGAP6 analyzed by real-time qPCR(Graphs show mean and SEM). STEAP4 is the only gene validated for both time points. AMIGO2 overexpression has been confirmed after 72 hours of mechanical stimulation. * p<0.05 ** p<0.01.*

Biological validation was performed on 7 SVP lines undergoing mechanical stimulation in the same conditions as the samples used for the RNA-Seq. **Figure 23** confirms the regulation for AMIGO2, CHRNA9, STEAP4, and ARHGAP6. Differences between technical and biological validation may be attributable to RNA damage of samples used for sequencing due to repeated freeze-thaw cycles.

AMIGO2 is known to be involved in the proliferation of ECs as well as migration and adhesion mechanisms,[149] but no data are still available on the potential role of AMIGO2 in SVPs. Therefore, to study whether AMIGO2 regulate SVPs biological functions, we proceeded with its overexpression in SVPs and with the analysis of proliferation, apoptosis, and migration.

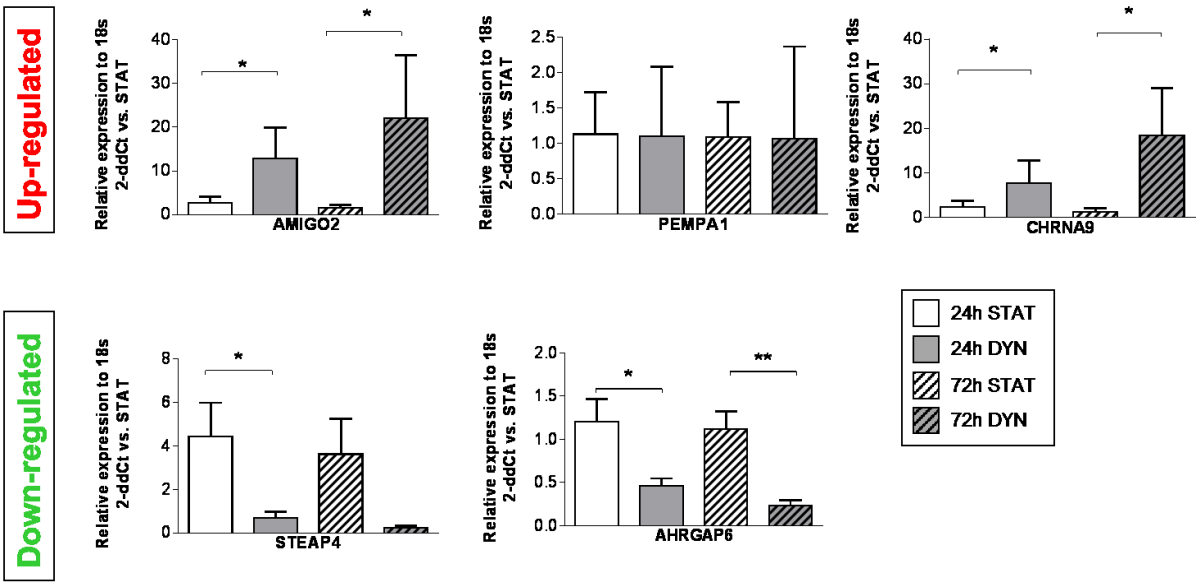

Figure 23 Biological validation. *Real-time qPCR performed on 7 different lines of SVP confirmed the regulation observed with RNA-Seq for AMIGO2, CHRNA9, STEAP4 and ARHGAP6 (Graphs show mean and SEM).* p<0.05 ** p<0.01.*

4.7 AMIGO2 Overexpression

To dissect the potential role of AMIGO2 in SVP functions known to be up-regulated due to the stretch and related to IH, we attempted to overexpress the receptor and test its effects by *in vitro* assays. In order to find the most efficient method for gene overexpression in SVPs we first tested the efficacy of a lipo-mediated transfection with Lipofectamine 2000, and we then moved to a lentivirus transduction. Two different type of plasmids with two different reporters have been tested.

4.7.1 Lipo-mediated transfection

The first method utilized was the lipo-mediated transfection with a plasmid carrying a c-Myc TAG in the AMIGO2 sequence. The plasmid was tested by transfection of HEK 293T cells with Lipofectamine 2000 and the protein expression was verified by western blot analysis performed for both TAG epitope (Myc) and AMIGO2 (**Figure 24A**). In order to understand the adequate amount of plasmidic DNA (pDNA) for the overexpression a curve dose experiment with 25, 50, 100 and 500 ng of pDNA has been performed in SVP lines and the transcription of AMIGO2 was analyzed after 24 and 72 hours by real-time qPCR. As **Figure 24B** shows, AMIGO2 was overexpressed even with the smallest amount of pDNA at both time points. However, this method of transfections was really damaging for the SVPs that massively started dying few hours after the transfection. The effect was dose-dependent i.e. related to pDNA amount, and not caused by the concentration of Lipofectamine 2000 (**Figure 24C**). For this reason, a different approach for overexpress AMIGO2 was used. We designed a different plasmid transduced through a lentiviral vector to produce stable lines of SVPs overexpressing AMIGO2 as herein discussed.

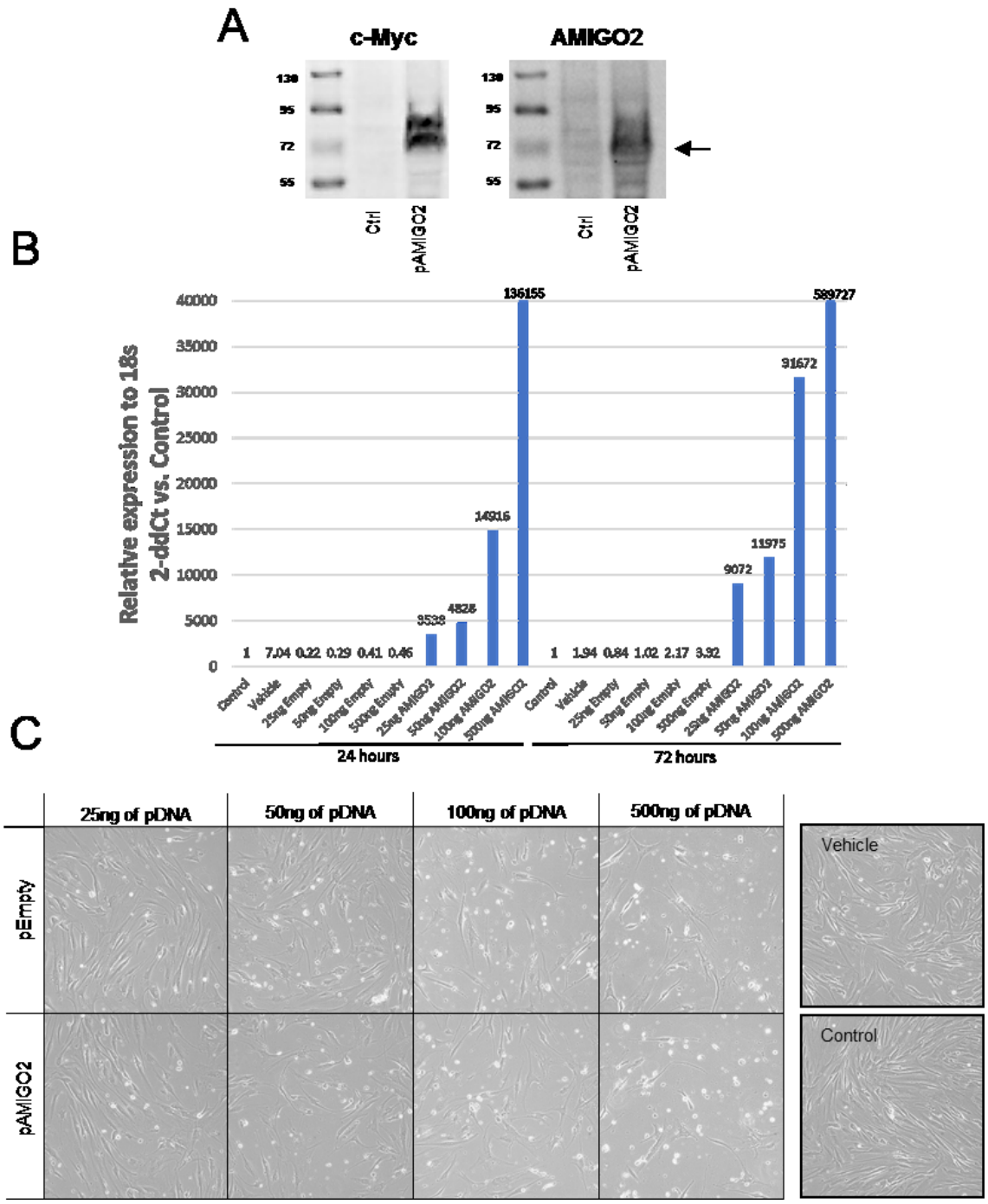

Figure 24 Lipo-mediated transfection. *A Western blot analysis of AMIGO2 overexpression in HEK 293T performed for the TAG c-Myc and AMIGO2. B AMIGO2 mRNA levels after transfection performed with different amounts of pDNA. C SVPs affected by transfection procedure compared to SVPs treated only with Lipofectamine 2000 (vehicle) and untreated (control).*

4.7.2 Lentiviral transduction

SVP lines between P3 and P5 were transduced with lentivirus to produce a stable line of cells overexpressing AMIGO2. Plasmids used for the overexpression had an EGFP as a reporter gene. Detection of green fluorescence by microscopy examination revealed that the SVPs started to express the plasmid 36 hours after infection. Plasmid expressions efficiency was comparable between control plasmid with EGFP and AMIGO2 plasmid. The morphology of the SVPs was not affected by the lentiviral infection and the treatment with polybrene (**Figure 25A**).

Overexpression was checked at mRNA level by real-time qPCR showing an increase of 36 times compared to the control expression of AMIGO2 16 days after infection at P6 (**Figure 25B**).

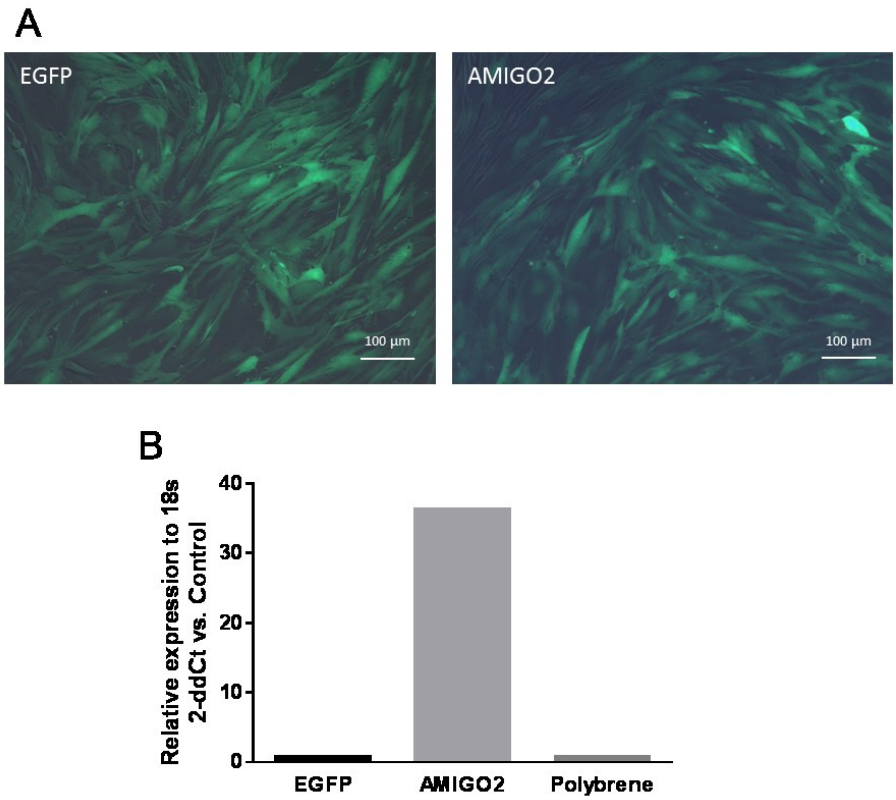

Figure 25 Exogenous DNA expression. *An SVPs 36 hours after infection. In the upper panels, the expression of EGFP and AMIGO2 plasmids is shown. The morphology of the cells does not differ due to the treatments required for the overexpression protocol. B relative expression of AMIGO2 in SVPs after infection at P6.*

4.8 AMIGO2 affects doubling time and migration of SVPs

Two cell lines of SVPs were used to calculate the doubling time and to assess the migration ability after AMIGO2 overexpression in SVPs. Results do not show significant differences, but they show a trend consistent with the literature that we want to further deepen in the future. As shown in **Figure 26A**, the doubling time of AMIGO2 overexpressing cells is lower than doubling time of the cells treated with EGFP and polybrene. Scratch assay in **Figures 26B-C** shows a trend that suggests how AMIGO2 can improve the migration ability of the SVP.

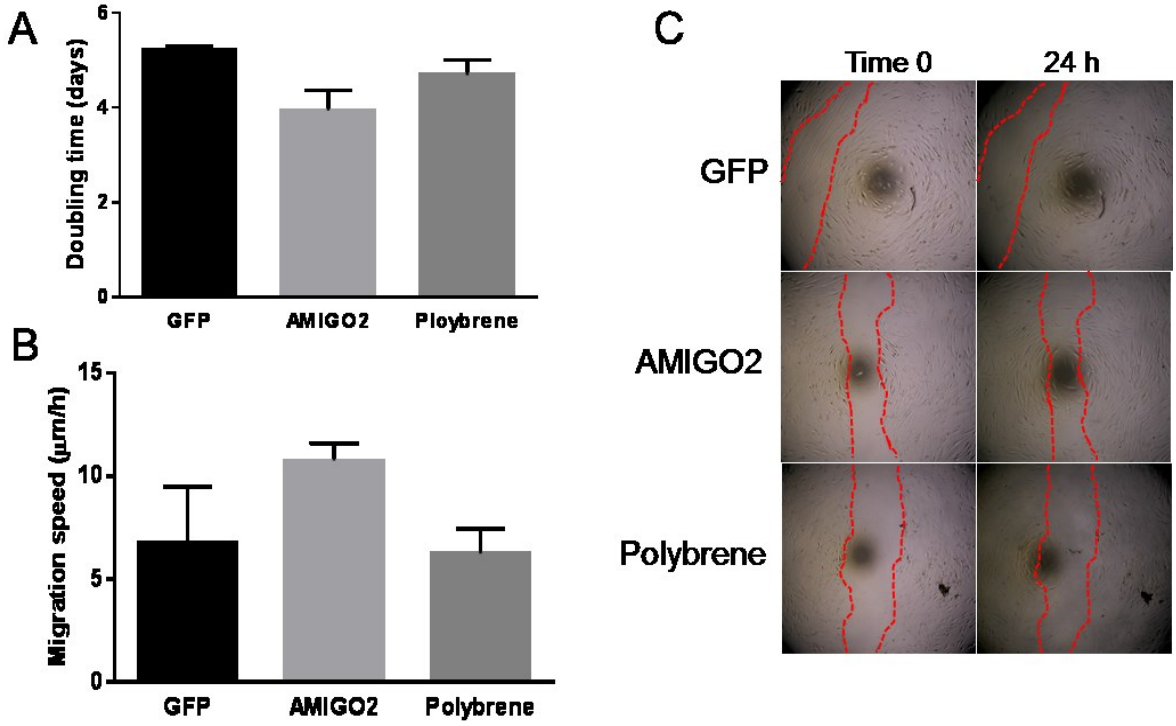

Figure 26 Doubling time and Migration. *A Doubling time of two cell lines of SVP infected with lentivirus or treated with polybrene between passage P4 and P6. Infection was performed at P4. B and C Scratch assay performed with two cell lines at P6. The assay was performed in basal medium EBM (Graphs show mean and SEM).*

4.9 AMIGO2 in situ analysis of ex vivo strain-treated veins

The expression of AMIGO2 was analyzed *in situ* by immunohistochemistry on veins subjected *ex vivo* to arterial stimulation venous stimulation in a bioreactor. Veins from patients undergone bypass grafting were harvested with an NT method and 5cm long vein segments were mounted in the system, while the remaining portion was processed for immunohistochemistry analysis representing the time zero (T0). Veins in the bioreactor were stimulated for 14 days (T14) with pulsatile flux that mimic the arterial circulation or with a continuous flow that mimics the venous condition. This *ex vivo* culture model allows having vein samples that undergo a pulsatile stimulus comparable to the arterial flow. Changes due to mechanical stress can thus be understood regardless of other physiological factors that contribute to IH.

During the analysis of the tissues a high variable baseline expression of AMIGO2 has been observed between samples. This variability does not reflect the clinical differences among patients and there is no evidence in the literature of any relation between AMIGO2 and anamnestic data. In this context, however, an increase of AMIGO2 expression has been observed in many cell types from intima to adventitia after the stretching of the veins. When well preserved in the samples, the endothelial layer in the intima showed a strong positivity for AMIGO2. SMCs in the media showed a high expression of the marker, as well as the cells in the adventitia, the *nerva* and *vasa vasorum* (**Figure 27**). All these phenotypes increased the AMIGO2 expression after 14 days of stretching under arterial flow. AMIGO2 expression in tunica adventitia parallels an increase in proliferation rate. Data show that after the pulsatile stimulation, the number of proliferative AMIGO2 cells increase significantly compare to the venous stimulation (**Figure 28A-B**).

SVP identification around the *vasa vasorum* was based on AMIGO2 expression and morphological aspects. Classical markers of SVPs were not possible because of the lack of CD34 antigen during the *ex vivo* culture and the difficulties to preserve antigens such as NG2 and PDGFRβ in paraffin-embedded tissues. SVPs around the *vasa vasorum of the arterial stimulated vein* show a positive trend for cell proliferationwith a contemporary decreasing of apoptotic cells. These trends have an opposite direction compare to venous stimulation (**Figure 28C-D**).

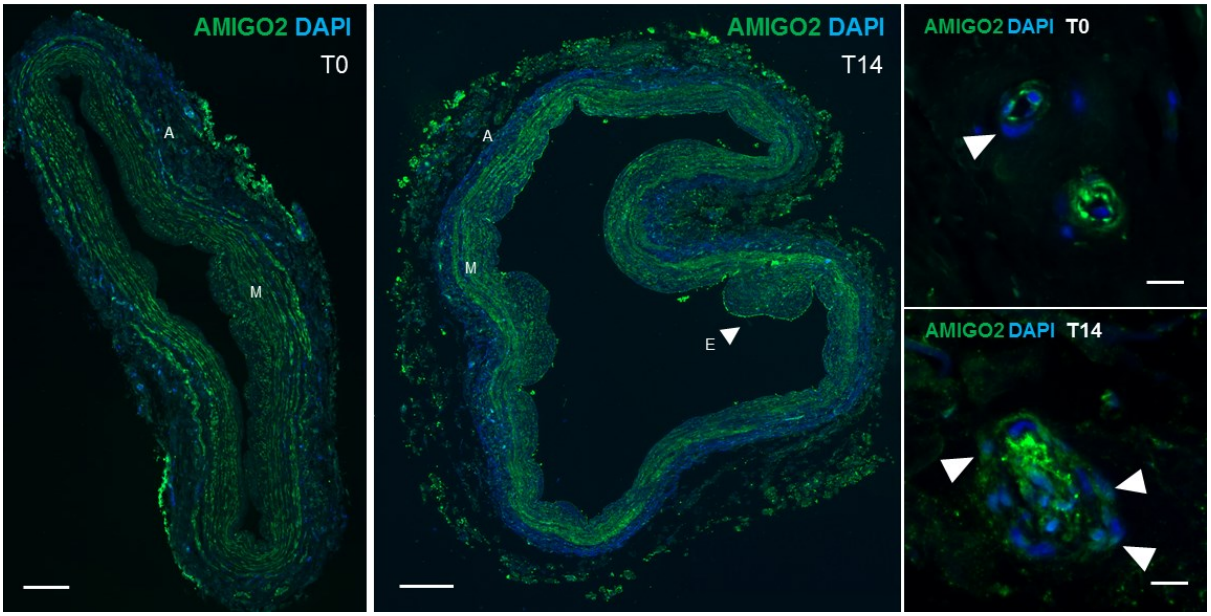

Figure 27 AMIGO2 expression in situ. *Morphological analysis of AMIGO2 expression in native vein and after 14 days of pulsatile flow performed by immunohistochemistry. The vein reconstructions show AMIGO2 expression pattern. Amigo2 increases its expression in Endothelial layer (E) tunica media (M) and adventitia (A) after arterial stimulation (scale bar=100 µm) Right magnifications show that Vasa vasorum AMIGO2 expression at T0 is mostly confined on the ECs, SVPs show just a weak positivity (arrowhead). After 14 days of pulsatile flow, the SVP number increases around vasa vasorum with also a stronger positivity for AMIGO2 (arrowheads) (scale bar=20 µm).*

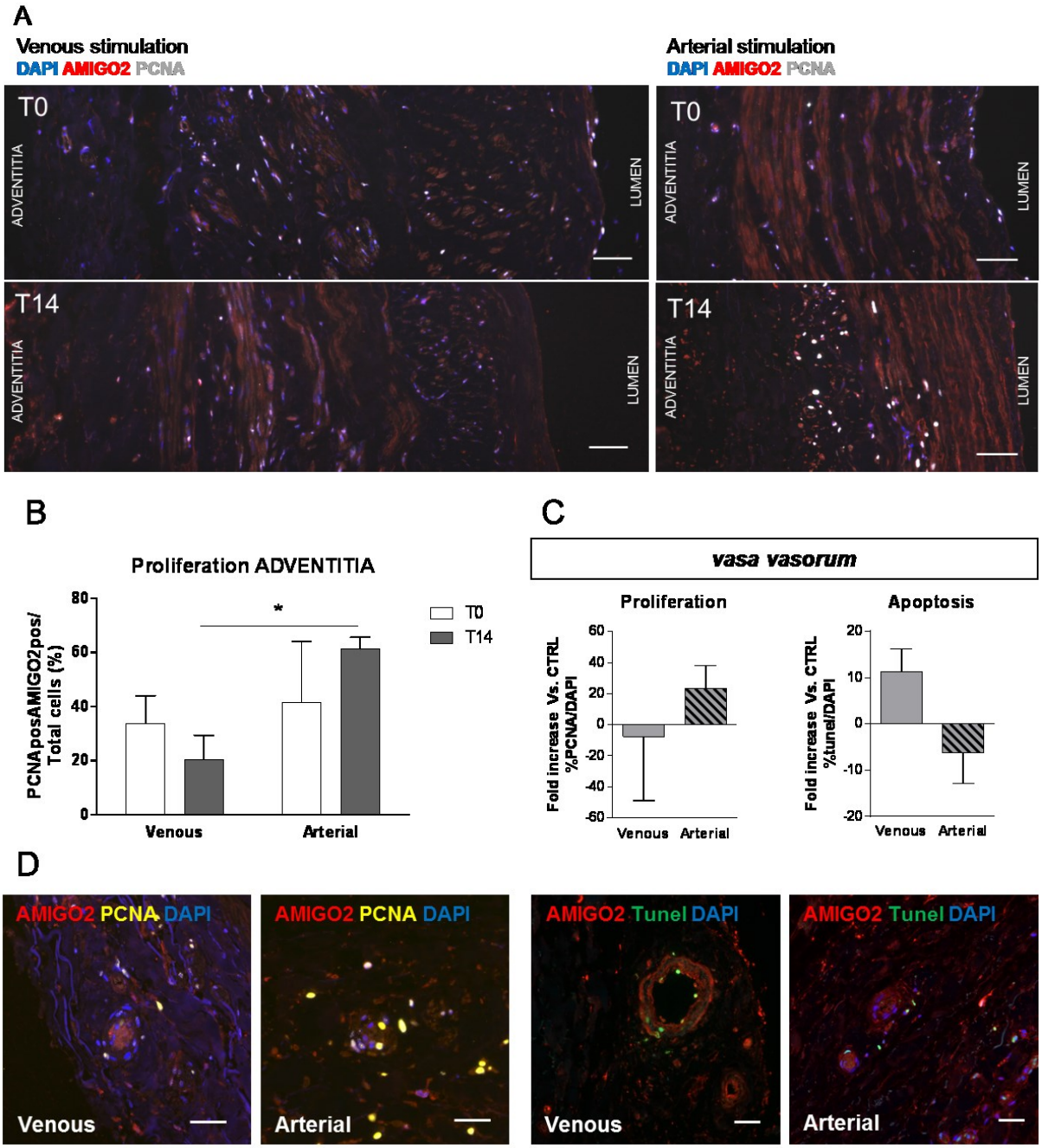

Figure 28.Tunica adventitia after mechanical stress. *A and B show the immunohistochemistry performed for AMIGO2 and PCNA in veins exposed to venous or arterial flow for 14 days. Despite the variability of the samples, the percentage of proliferating cells at T0 in adventitia was comparable. After stimulation ex-vivo, pulsatile flow significantly increases the number of AMIGO2 positive-proliferating cells, while venous mimic flow causes a decrease (scale bar=100 μm * p<0.05). C and D show the quantification of proliferative cells (PCNA positive) and apoptotic cells (Tunel positive) around vasa vasorum after stimulation. Data are expressed as fold change versus native vessels proliferation/apoptotic rate. Graphs in C show a trend of the prosurvival behavior of the perivascular cells in arterial stimulation, opposite to venous flow. Images (D) of the vasa vasorum after 14 days of different ex vivo stimulation (scale bar=50 μm) (Graphs show mean and SEM).*

DISCUSSION

Coronary artery bypass grafting (CABG) is a surgical procedure that has the aim to restore the blood flow to the heart after an ischemic event. This is a consolidated surgical procedure that started to be used in 1967[15] by which an autologous vessel is used to connects the aorta with one or more coronary arteries. The choice of the vessel can make the difference in terms of surgical success. The saphenous vein (SV) has been the first conduit utilized as bypass; and despite the surgical technique permits the use of several arterial vessels, SV is still the most frequently used.However, few days after bypass implantation the thickness of the tunica intima start to increase with the consequent reduction of its patency, that 10 years after CABG decrease to 50-60% and another surgery is often required. Intima hyperplasia (IH) major triggers are the damage of the veins vessel during the surgical procedure and the new hemodynamic environment.[28, 29] To minimize the manipulation of the vein during the harvesting at the beginning of '90s has been introduced the no-touch technique that well preserves the vessels integrity. The hemodynamic changes due to the blood flow rate 5-10 time higher and the pulsatile flow cause an increase of the shear stress on the endothelial layer and a radial deformation on the wall of the vein [38, 39]. Intimal hyperplasia is a disease that involves all the tunics of the vein. Endothelial layer damage is considered the first step, with a consequent activation of the smooth muscle cells in tunica media and fibroblast in tunica adventitia.[42, 43]

This project aimed to enlighten the role of the saphenous vein progenitors (SVP) in the in the progression of IH. SVPs are a population of progenitor cells present in the tunica adventitia around *vasa vasorum*, characterized for the first time in 2010 by Campagnolo et al. that has a profound influence on the endothelium. SVPs can acquire migration ability and stimulate the proliferation of ECs *in vivo* and *in vitro* systems. SVPs can also increase the viability of SMCs by the production of paracrine factors [81]. For these reasons, SVPs could contribute to the mechanisms leading to IH, where the production of chemotactic factors, the migration and the activation of cells represent the preparatory steps for the wall vessel remodeling. Prandi et al., in addition, showed that cells NG2 positive around *vasa vasorum*can be activatedthrough mechanical stimulation. These cells after activation modulate the expression of specific genes and micro-RNA related to epithelium(endothelium)-mesenchymal transition and vascular stress.[82]

This project aimed to enlighten the role of the saphenous vein progenitors (SVP) in the in the progression of IH.

First, we assessed the effect of the different mechanical load on the SVPs, in particular, the effect of the tangential stress that causes a circumferential deformation into the wall of the vessel.

To study the effect of the mechanical stress, SVPs were isolated from SV of patients undergone bypass grafting surgery and stretched by an *in vitro* system (FlexCell). A pulsatile tensile strain was applied on the cell monolayers with a uniaxial deformation of 10% with 1 Hz of frequency for 24 and 72 hours. We found that mechanical pulsatile strain causes a decrease in the proliferation rate of the cells after 72 hours of culture. Meanwhile, SVPs change their cytoskeleton structure assuming an orientationperpendicular to the direction of the strain. Similar morphological modifications affectSMCs in the inner region of the media of SV used as bypass. Cause of this different alignment has been identified in the passive extension that affects venous SMCs when connected to arterial flow.[160]

To understand if the mechanical stress could activate the SVPs through the regulation of gene transcription, the stretched cell lines were analyzed by RNA-Seq. Heatmap analysis revealed that the dynamic stimulus exertedfor 72 hours changed SVPs transcriptome causing theclusterization of the samples. Ingenuity pathway analysis (IPA) helped us to discover pathways and functions modulated in our dataset. After 24 hours of mechanical strain, the cells up-regulated functions linked with the migratory phenotype like cell movement, migration, and invasion; with strong up-regulation of secreting function and mitogenesis as well. Nonetheless, a longer mechanical stimulus seems to inhibit migration and differentiation with a reduction of cell survival and viability. These data do not show the negative effect of prolonged stress, a detrimental consequence of prolonged culture is evident in the time comparisons both in static and dynamic conditions. As well as functions as apoptosis, necrosis and cell death are strong up-regulated in the static time comparison, while the dynamic conditions don't show regulation for these functions. Thus, mechanical strain seems to carry SVPs trough an activation process that causes a cytoskeletal reorganization and lead migratory phenotype also acting as a mitogenic stimulus for cells. Interestingly, a similar fate has been described for SMCs that under strain reorganize their cytoplasm, change cell shape [161] and proliferate. SMCs proliferation seems to be a specific characteristic of cells in SV but not for the ones in IMA, validating the idea that venous cells are sensitive to pulsatile flow.[162] Dynamic culture carried out for 72 hours activate the Planar Cell Polarity (PCP) pathway that leads the cells to acquire a polarization. Functionally, cell polarization is required for each mechanism that needs a directional behavior. Although is known that membrane tension due mechanical cues leads to a polarized actin polymerization with a consequent cell asymmetric morphology.[163]

This different phenotypic asset could induce vectoral activities in SVPs such as migration, orientated cell division and impaired adhesion to extracellular matrix.

Moreover, we investigated the most regulated genes due to the mechanical stress. Membrane receptor Amphoterin-Induced Gene And Open Reading Frame 2 (AMIGO2) was the gene with the strongest time-related up-regulation to the strain, and we decided to further investigate its functions in SVPs. The characteristic extracellular portion of AMIGO2 has six leucine-rich repeats (LRRs) domains and an immunoglobulin-like domain close to the transmembrane region[134]. AMIGO2 is known to be involved in neurite outgrowth. The hypotheses about its functioning mainly concern the homophilic or heterophilic binding mechanism between the other proteins of the family (AMIGO and AMIGO3) or proteins with homolog LRR sequences [140].Recently AMIGO2 has been studied in microvascular cells showing that its expression regulates ECs interactions to ECM with consequents effects on migration and tubulogenesis ability of the cells.[149]

Our attention then has been focused on the function of AMIGO2 in the SVPs. To establish an efficient overexpression protocol, Lipofectamine 2000 transfection was tested. Due to the toxic effect on cells, has been decided to move to a lentivirus transduction to create stable lines of SVP overexpressing AMIGO2. Our data show trends consistent with the literature about the proliferative and adhesion ability improved by AMIGO2 also in the SVPs.

Immunohistochemically and morphological analyses for the *in situ* expression of AMIGO2 have been performed on SV native and subjected to an *ex vivo* model of flow for 14 days. The *ex vivo* systemthat we used allows having SV samples stimulated with the arterial pulsatile flow and venous steady flow. With various gradations, ECs in the intima, SMCs in the media and *nerva* and *vasa vasorum*in the adventitia showed a positivity for AMIGO2. Despite the high variability of AMIGO2 expression in the native non-stretched veins, our results show an increase of proliferating AMIGO2 cell in the adventitia of arterial flow stimulated veins in comparison to the venous stimulation. Standard markers for SVPs identification were not useful in these samples because CD34 has been lost during the *ex vivo* culture and antigens as NG2 and PDGFRβ are not preserved well in paraffin-embedded tissues. For these reasons, SVPs were identified by AMIGO2 positivity and their morphological characteristics. The results show that there is a pro-survival trend in the *vasa vasorum*of thearterial stimulated veins compare to venous stimulation, with an increase of proliferating and a decrease of apoptotic cells.

All these results show that SVPs are sensitive to mechanical stress and if stimulated they can react by rearranging the cytoskeleton, acquiring migratory phenotype and expressing genes related to survival and proliferation. This links them to the underlying IH development mechanisms. AMIGO2 overexpression under strain enhance these abilities and can involve them in another mechanism that occurs in the progression of IH, i.e. the extracellular matrix remodeling. It is known that one of the early metabolic events that contribute to intimal thickness is the increasing of proteoglycan (PG) synthesis.[164] They are extracellular matrix proteins with small leucine-rich repeat domains and their production, mainly from SMCs, has initial defense function against mechanical stress.[165] As explained above, AMIGO2 is a protein with six LRR domains that bind homologous proteins with LRR domains. This ECM reorganization could be a chemotactic stimulus for SVPs that have acquired the migratory phenotype and are able to tightly bind the proteoglycans into the matrix by AMIGO2.

Future studies should validate the *in vitro* data on AMIGO2 antiapoptotic and promigratory function in SVPs. It would be worth also to attempting to correlate the relationship between migratory phenotype and subendothelial proteoglycan distribution, shedding light on one of the triggering events of IH. More in-depth information about AMIGO2 activation and functionsin vascular context could make a prognostic difference in the progression of IH.

LIST OF REFERENCES

1. Kumar, V., Abul K. Abbas, Nelson Fausto, Stanley L. Robbins, and Ramzi S. Cotran., *Robbins and Cotran Pathologic Basis of Disease*. 2005.

2. Virmani, R., et al., Lessons from sudden coronary death: a comprehensive morphological classification scheme for atherosclerotic lesions. Arterioscler Thromb Vasc Biol, 2000. **20**(5): p. 1262-75.

3. Stary, H.C., et al., A definition of advanced types of atherosclerotic lesions and a histological classification of atherosclerosis. A report from the Committee on Vascular Lesions of the Council on Arteriosclerosis, American Heart Association. Arterioscler Thromb Vasc Biol, 1995. **15**(9): p. 1512-31.

4. Lipinski, M., et al., What percent luminal stenosis should be used to define angiographic coronary artery disease for noninvasive test evaluation? Ann Noninvasive Electrocardiol, 2002. **7**(2): p. 98-105.

5. Hillis, L.D., et al., 2011 ACCF/AHA Guideline for Coronary Artery Bypass Graft Surgery. A report of the American College of Cardiology Foundation/American Heart Association Task Force on Practice Guidelines. Developed in collaboration with the American Association for Thoracic Surgery, Society of Cardiovascular Anesthesiologists, and Society of Thoracic Surgeons. J Am Coll Cardiol, 2011. **58**(24): p. e123-210.

6. Rihal, C.S., et al., Indications for coronary artery bypass surgery and percutaneous coronary intervention in chronic stable angina: review of the evidence and methodological considerations. Circulation, 2003. **108**(20): p. 2439-45.

7. QualityWatch, Indicator: International comparisons of surgical procedures, N.T.H. Foundation, Editor. 2015.

8. Galbut, D.L., et al., Bilateral internal thoracic artery grafting improves long-term survival in patients with reduced ejection fraction: a propensity-matched study with 30-year follow-up. J Thorac Cardiovasc Surg, 2012. **143**(4): p. 844-853 e4.

9. Lytle, B.W., et al., The effect of bilateral internal thoracic artery grafting on survival during 20 postoperative years. Ann Thorac Surg, 2004. **78**(6): p. 2005-12; discussion 2012-4.

10. Harskamp, R.E., et al., Saphenous vein graft failure and clinical outcomes: toward a surrogate end point in patients following coronary artery bypass surgery? Am Heart J, 2013. **165**(5): p. 639-43.

11. Cohn, L.H., Use of the Internal Mammary Artery Graft and In-Hospital Mortality and Other Adverse Outcomes Associated With Coronary Artery Bypass Surgery. Circulation, 2001. **103**: p. 483-484.

12. Loop, F.D., et al., Influence of the internal-mammary-artery graft on 10-year survival and other cardiac events. N Engl J Med, 1986. **314**(1): p. 1-6.

13. Edwards, F.H., R.E. Clark, and M. Schwartz, Impact of internal mammary artery conduits on operative mortality in coronary revascularization. Ann Thorac Surg, 1994. **57**(1): p. 27-32.

14. Taggart, D.P., Current status of arterial grafts for coronary artery bypass grafting. Ann Cardiothorac Surg, 2013. **2**(4): p. 427-30.

15. Souza, D.S., et al., Harvesting the saphenous vein with surrounding tissue for CABG provides long-term graft patency comparable to the left internal thoracic artery: results of a randomized longitudinal trial. J Thorac Cardiovasc Surg, 2006. **132**(2): p. 373-8.

16. Sabik, J.F., 3rd, et al., Comparison of saphenous vein and internal thoracic artery graft patency by coronary system. Ann Thorac Surg, 2005. **79**(2): p. 544-51; discussion 544-51.

17. Samano, N., et al., The no-touch saphenous vein for coronary artery bypass grafting maintains a patency, after 16 years, comparable to the left internal thoracic artery: A randomized trial. J Thorac Cardiovasc Surg, 2015. **150**(4): p. 880-8.

18. Carpentier, A., et al., The aorta-to-coronary radial artery bypass graft. A technique avoiding pathological changes in grafts. Ann Thorac Surg, 1973. **16**(2): p. 111-21.

19. Carpentier, A., Discussion of Geha AS, Krone RJ, Mc-Cormick JR: selection of coronary bypass: anatomic, physiologic, and angiographic considerations of vein and mammary artery grafts. J Thorac Cardiovasc Surg, 1975. **70** p. 414-431.

20. Tatoulis, J., B.F. Buxton, and J.A. Fuller, *Patencies of 2127 arterial to coronary conduits over 15 years.* Ann Thorac Surg, 2004. **77**(1): p. 93-101.

21. Bakaeen, F.G., M.A. Zenati, and D.L. Bhatt, *Conduits in coronary artery bypass grafting.* Semin Thorac Cardiovasc Surg, 2013. **25**(4): p. 273-9.

22. Hayward, P.A., et al., Comparable patencies of the radial artery and right internal thoracic artery or saphenous vein beyond 5 years: results from the Radial Artery Patency

and Clinical Outcomes trial. J Thorac Cardiovasc Surg, 2010. **139**(1): p. 60-5; discussion 65-7.

23. Perrault, L.P., et al., Clinical experience with the right gastroepiploic artery in coronary artery bypass grafting. Ann Thorac Surg, 1993. **56**(5): p. 1082-4.

24. Mukherjee, D., et al., How does the right gastroepiploic artery compare with the saphenous vein for revascularization of the right coronary artery? Interact Cardiovasc Thorac Surg, 2012. **15**(5): p. 888-92.

25. Captur, G., *Memento for Rene Favaloro.* Tex Heart Inst J, 2004. **31**(1): p. 47-60.

26. Diodato, M. and E.G. Chedrawy, Coronary artery bypass graft surgery: the past, present, and future of myocardial revascularisation. Surg Res Pract, 2014. **2014**: p. 726158.

27. Raja, S.G., et al., *Saphenous vein grafts: to use or not to use?* Heart Lung Circ, 2004. **13**(2): p. 150-6.

28. Malone, J.M., C.W. Kischer, and W.S. Moore, Changes in venous endothelial fibrinolytic activity and histology with in vitro venous distention and arterial implantation. Am J Surg, 1981. **142**(2): p. 178-82.

29. Lemson, M.S., et al., *Intimal hyperplasia in vascular grafts.* Eur J Vasc Endovasc Surg, 2000. **19**(4): p. 336-50.

30. de Vries, M.R., et al., *Vein graft failure: from pathophysiology to clinical outcomes.* Nat Rev Cardiol, 2016. **13**(8): p. 451-70.

31. Dreifaldt, M., et al., The no-touch saphenous vein as the preferred second conduit for coronary artery bypass grafting. Ann Thorac Surg, 2013. **96**(1): p. 105-11.

32. Johansson, B., et al., *No touch vein harvesting technique for CABG improves the long-term clinical outcome.* Scandinavian Cardiovascular Journal, 2009. **43**(1): p. 63-68.

33. Rueda, F., et al., Novel no-touch technique of harvesting the saphenous vein for coronary artery bypass grafting. Arq Bras Cardiol, 2008. **90**(6): p. 356-62.

34. Souza, D.S., et al., High early patency of saphenous vein graft for coronary artery bypass harvested with surrounding tissue. Ann Thorac Surg, 2001. **71**(3): p. 797-800.

35. Dashwood, M.R. and J.C. Tsui, 'No-touch' saphenous vein harvesting improves graft performance in patients undergoing coronary artery bypass surgery: a journey from bedside to bench. Vascul Pharmacol, 2013. **58**(3): p. 240-50.

36. Meissner, M.H., et al., *The hemodynamics and diagnosis of venous disease.* J Vasc Surg, 2007. **46 Suppl S**: p. 4S-24S.

37. Haruguchi, H. and S. Teraoka, Intimal hyperplasia and hemodynamic factors in arterial bypass and arteriovenous grafts: a review. J Artif Organs, 2003. **6**(4): p. 227-35.

38. Kwei, S., et al., Early adaptive responses of the vascular wall during venous arterialization in mice. Am J Pathol, 2004. **164**(1): p. 81-9.

39. Baldwin, Z.K., et al., Slower onset of low shear stress leads to less neointimal thickening in experimental vein grafts. Ann Vasc Surg, 2006. **20**(1): p. 106-13.

40. Liu, S.Q., et al., A possible role of initial cell death due to mechanical stretch in the regulation of subsequent cell proliferation in experimental vein grafts. Biomech Model Mechanobiol, 2002. **1**(1): p. 17-27.

41. Carrel A, G.C., *Uniterminal and Bitenninal Venous Transpositions.* Surgery, Gynecology & Obstetrics, 1906. **2**: p. 266-286.

42. Kipshidze, N., et al., Role of the endothelium in modulating neointimal formation: vasculoprotective approaches to attenuate restenosis after percutaneous coronary interventions. J Am Coll Cardiol, 2004. **44**(4): p. 733-9.

43. Patel, S.D., et al., The role of endothelial cells and their progenitors in intimal hyperplasia. Ther Adv Cardiovasc Dis, 2010. **4**(2): p. 129-41.

44. Caro, C., et al., The geometry of unstented and stented pig common carotid artery bypass grafts. Biorheology, 2002. **39**(3-4): p. 507-12.

45. Shukla, N. and J.Y. Jeremy, Pathophysiology of saphenous vein graft failure: a brief overview of interventions. Curr Opin Pharmacol, 2012. **12**(2): p. 114-20.

46. Garg, U.C. and A. Hassid, Nitric oxide-generating vasodilators and 8-bromo-cyclic guanosine monophosphate inhibit mitogenesis and proliferation of cultured rat vascular smooth muscle cells. J Clin Invest, 1989. **83**(5): p. 1774-7.

47. Gerrity, R.G., The role of the monocyte in atherogenesis: I. Transition of blood-borne monocytes into foam cells in fatty lesions. Am J Pathol, 1981. **103**(2): p. 181-90.

48. Wainwright, C.L., A.M. Miller, and R.M. Wadsworth, *Inflammation as a key event in the development of neointima following vascular balloon injury.* Clin Exp Pharmacol Physiol, 2001. **28**(11): p. 891-5.

49. Mitra, A.K., D.M. Gangahar, and D.K. Agrawal, Cellular, molecular and immunological mechanisms in the pathophysiology of vein graft intimal hyperplasia. Immunol Cell Biol, 2006. **84**(2): p. 115-24.

50. Newby, A.C., Dual role of matrix metalloproteinases (matrixins) in intimal thickening and atherosclerotic plaque rupture. Physiol Rev, 2005. **85**(1): p. 1-31.

51. Yuan, S.M., alpha-Smooth Muscle Actin and ACTA2 Gene Expressions in Vasculopathies. Braz J Cardiovasc Surg, 2015. **30**(6): p. 644-9.

52. Jiang, Z., et al., Established neointimal hyperplasia in vein grafts expands via TGF-beta-mediated progressive fibrosis. Am J Physiol Heart Circ Physiol, 2009. **297**(4): p. H1200-7.

53. Zalewski, A., Y. Shi, and A.G. Johnson, Diverse origin of intimal cells: smooth muscle cells, myofibroblasts, fibroblasts, and beyond? Circ Res, 2002. **91**(8): p. 652-5.

54. Li, D.Y., et al., Elastin is an essential determinant of arterial morphogenesis. Nature, 1998. **393**(6682): p. 276-80.

55. Galis, Z.S. and J.J. Khatri, Matrix metalloproteinases in vascular remodeling and atherogenesis: the good, the bad, and the ugly. Circ Res, 2002. **90**(3): p. 251-62.

56. Kallenbach, K., et al., Inhibition of smooth muscle cell migration and neointima formation in vein grafts by overexpression of matrix metalloproteinase-3. J Vasc Surg, 2009. **49**(3): p. 750-8.

57. Southgate, K.M., et al., Increased secretion of basement membrane-degrading metalloproteinases in pig saphenous vein into carotid artery interposition grafts. Arterioscler Thromb Vasc Biol, 1999. **19**(7): p. 1640-9.

58. Thatte, H.S. and S.F. Khuri, The coronary artery bypass conduit: I. Intraoperative endothelial injury and its implication on graft patency. Ann Thorac Surg, 2001. **72**(6): p. S2245-52; discussion S2267-70.

59. Noonan, D.M., et al., The complete sequence of perlecan, a basement membrane heparan sulfate proteoglycan, reveals extensive similarity with laminin A chain, low density

lipoprotein-receptor, and the neural cell adhesion molecule. J Biol Chem, 1991. **266**(34): p. 22939-47.

60. Dashwood, M.R., et al., Effect of vein graft harvesting on endothelial nitric oxide synthase and nitric oxide production. Ann Thorac Surg, 2005. **80**(3): p. 939-44.

61. Tineli, R.A., et al., Mechanical forces and human saphenous veins: coronary artery bypass graft implications. Rev Bras Cir Cardiovasc, 2007. **22**(1): p. 87-95.

62. Castier, Y., et al., *Role of NF-kappaB in flow-induced vascular remodeling.* Antioxid Redox Signal, 2009. **11**(7): p. 1641-9.

63. Wagenseil, J.E. and R.P. Mecham, *Vascular extracellular matrix and arterial mechanics.* Physiol Rev, 2009. **89**(3): p. 957-89.

64. Travo, P., K. Weber, and M. Osborn, Co-existence of vimentin and desmin type intermediate filaments in a subpopulation of adult rat vascular smooth muscle cells growing in primary culture. Exp Cell Res, 1982. **139**(1): p. 87-94.

65. Johnson, J.L., et al., Injury induces dedifferentiation of smooth muscle cells and increased matrix-degrading metalloproteinase activity in human saphenous vein. Arterioscler Thromb Vasc Biol, 2001. **21**(7): p. 1146-51.

66. Ye, G.J., A.P. Nesmith, and K.K. Parker, The role of mechanotransduction on vascular smooth muscle myocytes' [corrected] cytoskeleton and contractile function. Anat Rec (Hoboken), 2014. **297**(9): p. 1758-69.

67. Kalra, M. and V.M. Miller, Early remodeling of saphenous vein grafts: proliferation, migration and apoptosis of adventitial and medial cells occur simultaneously with changes in graft diameter and blood flow. J Vasc Res, 2000. **37**(6): p. 576-84.

68. Shi, Y., et al., Remodeling of autologous saphenous vein grafts. The role of perivascular myofibroblasts. Circulation, 1997. **95**(12): p. 2684-93.

69. Majesky, M.W., et al., *The adventitia: a dynamic interface containing resident progenitor cells.* Arterioscler Thromb Vasc Biol, 2011. **31**(7): p. 1530-9.

70. Kopjar, T. and M.R. Dashwood, Endoscopic Versus "No-Touch" Saphenous Vein Harvesting for Coronary Artery Bypass Grafting: A Trade-Off Between Wound Healing and Graft Patency. Angiology, 2016. **67**(2): p. 121-32.

71. Dashwood, M.R. and A. Loesch, The saphenous vein as a bypass conduit: the potential role of vascular nerves in graft performance. Curr Vasc Pharmacol, 2009. **7**(1): p. 47-57.

72. Dashwood, M.R., et al., Retaining perivascular tissue of human saphenous vein grafts protects against surgical and distension-induced damage and preserves endothelial nitric oxide synthase and nitric oxide synthase activity. J Thorac Cardiovasc Surg, 2009. **138**(2): p. 334-40.

73. Souza, D.S., et al., "No-touch" technique using saphenous vein harvested with its surrounding tissue for coronary artery bypass grafting maintains an intact endothelium. Scand Cardiovasc J, 1999. **33**(6): p. 323-9.

74. Momin, A.U., et al., Leptin is an endothelial-independent vasodilator in humans with coronary artery disease: Evidence for tissue specificity of leptin resistance. Eur Heart J, 2006. **27**(19): p. 2294-9.

75. Wang, Z., M.R. Castresana, and W.H. Newman, *NF-kappaB is required for TNF-alpha-directed smooth muscle cell migration.* FEBS Lett, 2001. **508**(3): p. 360-4.

76. Kim, H.M., et al., Inhibitory role of magnolol on proliferative capacity and matrix metalloproteinase-9 expression in TNF-alpha-induced vascular smooth muscle cells. Int Immunopharmacol, 2007. **7**(8): p. 1083-91.

77. Fernandez-Alfonso, M.S., et al., Commentary: Perivascular Fat and Improved Vein Graft Patency in Patients Undergoing Coronary Artery Bypass Surgery. Curr Vasc Pharmacol, 2016. **14**(4): p. 308-12.

78. Dreifaldt, M., et al., The vasa vasorum and associated endothelial nitric oxide synthase is more important for saphenous vein than arterial bypass grafts. Angiology, 2013. **64**(4): p. 293-9.

79. Maurice, G., et al., [Modeling of elastic deformation and vascular resistance of arterial and venous vasa vasorum]. J Mal Vasc, 1998. **23**(4): p. 282-8.

80. Dashwood, M.R., et al., Hypothesis: a potential role for the vasa vasorum in the maintenance of vein graft patency. Angiology, 2004. **55**(4): p. 385-95.

81. Campagnolo, P., et al., Human adult vena saphena contains perivascular progenitor cells endowed with clonogenic and proangiogenic potential. Circulation, 2010. **121**(15): p. 1735-45.

82. Prandi, F., et al., Adventitial vessel growth and progenitor cells activation in an ex vivo culture system mimicking human saphenous vein wall strain after coronary artery bypass grafting. PLoS One, 2015. **10**(2): p. e0117409.

83. Shepro, D. and N.M. Morel, *Pericyte physiology.* FASEB J, 1993. **7**(11): p. 1031-8.

84. Betsholtz, C., P. Lindblom, and H. Gerhardt, *Role of pericytes in vascular morphogenesis.* EXS, 2005(94): p. 115-25.

85. Kovacic, J.C. and M. Boehm, Resident vascular progenitor cells: an emerging role for non-terminally differentiated vessel-resident cells in vascular biology. Stem Cell Res, 2009. **2**(1): p. 2-15.

86. Hellstrom, M., et al., Lack of pericytes leads to endothelial hyperplasia and abnormal vascular morphogenesis. J Cell Biol, 2001. **153**(3): p. 543-53.

87. Crisan, M., et al., *Perivascular cells for regenerative medicine.* J Cell Mol Med, 2012. **16**(12): p. 2851-60.

88. Allt, G. and J.G. Lawrenson, *Pericytes: cell biology and pathology.* Cells Tissues Organs, 2001. **169**(1): p. 1-11.

89. Armulik, A., G. Genove, and C. Betsholtz, Pericytes: developmental, physiological, and pathological perspectives, problems, and promises. Dev Cell, 2011. **21**(2): p. 193-215.

90. Gerhardt, H. and C. Betsholtz, *Endothelial-pericyte interactions in angiogenesis.* Cell Tissue Res, 2003. **314**(1): p. 15-23.

91. Gerhardt, H., H. Wolburg, and C. Redies, N-cadherin mediates pericytic-endothelial interaction during brain angiogenesis in the chicken. Dev Dyn, 2000. **218**(3): p. 472-9.

92. Diaz-Flores, L., et al., Pericytes. Morphofunction, interactions and pathology in a quiescent and activated mesenchymal cell niche. Histol Histopathol, 2009. **24**(7): p. 909-69.

93. Winkler, E.A., R.D. Bell, and B.V. Zlokovic, *Central nervous system pericytes in health and disease.* Nat Neurosci, 2011. **14**(11): p. 1398-1405.

94. Rojas, A., et al., The role played by perivascular cells in kidney interstitial injury. Clin Nephrol, 2012. **77**(5): p. 400-8.

95. Montagne, A., et al., Blood-brain barrier breakdown in the aging human hippocampus. Neuron, 2015. **85**(2): p. 296-302.

96. Vono, R., et al., Activation of the Pro-Oxidant PKCbetaII-p66Shc Signaling Pathway Contributes to Pericyte Dysfunction in Skeletal Muscles of Patients With Diabetes With Critical Limb Ischemia. Diabetes, 2016. **65**(12): p. 3691-3704.

97. Maeda, S., et al., Sulforaphane inhibits advanced glycation end product-induced pericyte damage by reducing expression of receptor for advanced glycation end products. Nutr Res, 2014. **34**(9): p. 807-13.

98. Nayak, R.C., et al., A monoclonal antibody (3G5)-defined ganglioside antigen is expressed on the cell surface of microvascular pericytes. J Exp Med, 1988. **167**(3): p. 1003-15.

99. Helmbold, P., et al., Human dermal pericytes express 3G5 ganglioside--a new approach for microvessel histology in the skin. J Cutan Pathol, 2001. **28**(4): p. 206-10.

100. Gushi, A., et al., The 3G5 antigen is expressed in dermal mast cells but not pericytes. J Cutan Pathol, 2008. **35**(3): p. 278-84.

101. Cho, H., et al., Pericyte-specific expression of Rgs5: implications for PDGF and EDG receptor signaling during vascular maturation. FASEB J, 2003. **17**(3): p. 440-2.

102. Murfee, W.L., T.C. Skalak, and S.M. Peirce, Differential arterial/venous expression of NG2 proteoglycan in perivascular cells along microvessels: identifying a venule-specific phenotype. Microcirculation, 2005. **12**(2): p. 151-60.

103. Boado, R.J. and W.M. Pardridge, Differential expression of alpha-actin mRNA and immunoreactive protein in brain microvascular pericytes and smooth muscle cells. J Neurosci Res, 1994. **39**(4): p. 430-5.

104. Crisan, M., et al., A perivascular origin for mesenchymal stem cells in multiple human organs. Cell Stem Cell, 2008. **3**(3): p. 301-13.

105. Stewart, P.A. and M.J. Wiley, Developing nervous tissue induces formation of blood-brain barrier characteristics in invading endothelial cells: a study using quail--chick transplantation chimeras. Dev Biol, 1981. **84**(1): p. 183-92.

106. Sa-Pereira, I., D. Brites, and M.A. Brito, *Neurovascular unit: a focus on pericytes.* Mol Neurobiol, 2012. **45**(2): p. 327-47.

107. Daneman, R., et al., Pericytes are required for blood-brain barrier integrity during embryogenesis. Nature, 2010. **468**(7323): p. 562-6.

108. Liebner, S., et al., Wnt/beta-catenin signaling controls development of the blood-brain barrier. J Cell Biol, 2008. **183**(3): p. 409-17.

109. Luissint, A.C., et al., Tight junctions at the blood brain barrier: physiological architecture and disease-associated dysregulation. Fluids Barriers CNS, 2012. **9**(1): p. 23.

110. Dohgu, S., et al., Brain pericytes contribute to the induction and up-regulation of blood-brain barrier functions through transforming growth factor-beta production. Brain Res, 2005. **1038**(2): p. 208-15.

111. Hori, S., et al., A pericyte-derived angiopoietin-1 multimeric complex induces occludin gene expression in brain capillary endothelial cells through Tie-2 activation in vitro. J Neurochem, 2004. **89**(2): p. 503-13.

112. Carmeliet, P. and R.K. Jain, *Molecular mechanisms and clinical applications of angiogenesis.* Nature, 2011. **473**(7347): p. 298-307.

113. Ribatti, D., B. Nico, and E. Crivellato, *The role of pericytes in angiogenesis.* Int J Dev Biol, 2011. **55**(3): p. 261-8.

114. Hall, A.P., Review of the pericyte during angiogenesis and its role in cancer and diabetic retinopathy. Toxicol Pathol, 2006. **34**(6): p. 763-75.

115. Dalkara, T., Y. Gursoy-Ozdemir, and M. Yemisci, *Brain microvascular pericytes in health and disease.* Acta Neuropathol, 2011. **122**(1): p. 1-9.

116. Kotecki, M., et al., Calpain- and talin-dependent control of microvascular pericyte contractility and cellular stiffness. Microvasc Res, 2010. **80**(3): p. 339-48.

117. Rucker, H.K., H.J. Wynder, and W.E. Thomas, *Cellular mechanisms of CNS pericytes.* Brain Res Bull, 2000. **51**(5): p. 363-9.

118. Davis, G.E., W. Koh, and A.N. Stratman, Mechanisms controlling human endothelial lumen formation and tube assembly in three-dimensional extracellular matrices. Birth Defects Res C Embryo Today, 2007. **81**(4): p. 270-85.

119. Stratman, A.N., et al., Pericyte recruitment during vasculogenic tube assembly stimulates endothelial basement membrane matrix formation. Blood, 2009. **114**(24): p. 5091-5101.

120. Stratman, A.N. and G.E. Davis, Endothelial cell-pericyte interactions stimulate basement membrane matrix assembly: influence on vascular tube remodeling, maturation, and stabilization. Microsc Microanal, 2012. **18**(1): p. 68-80.

121. Corselli, M., et al., Identification of perivascular mesenchymal stromal/stem cells by flow cytometry. Cytometry A, 2013. **83**(8): p. 714-20.

122. Birbrair, A., et al., Skeletal muscle neural progenitor cells exhibit properties of NG2-glia. Exp Cell Res, 2013. **319**(1): p. 45-63.

123. Krautler, N.J., et al., Follicular dendritic cells emerge from ubiquitous perivascular precursors. Cell, 2012. **150**(1): p. 194-206.

124. Balabanov, R., et al., CNS microvascular pericytes express macrophage-like function, cell surface integrin alpha M, and macrophage marker ED-2. Microvasc Res, 1996. **52**(2): p. 127-42.

125. Sakuma, R., et al., Brain pericytes serve as microglia-generating multipotent vascular stem cells following ischemic stroke. J Neuroinflammation, 2016. **13**(1): p. 57.

126. Dellavalle, A., et al., Pericytes of human skeletal muscle are myogenic precursors distinct from satellite cells. Nat Cell Biol, 2007. **9**(3): p. 255-67.

127. Chen, W.C., et al., Human myocardial pericytes: multipotent mesodermal precursors exhibiting cardiac specificity. Stem Cells, 2015. **33**(2): p. 557-73.

128. Paquet-Fifield, S., et al., A role for pericytes as microenvironmental regulators of human skin tissue regeneration. J Clin Invest, 2009. **119**(9): p. 2795-806.

129. Mangialardi, G., A. Cordaro, and P. Madeddu, *The bone marrow pericyte: an orchestrator of vascular niche.* Regen Med, 2016. **11**(8): p. 883-895.

130. Tormin, A., et al., CD146 expression on primary nonhematopoietic bone marrow stem cells is correlated with in situ localization. Blood, 2011. **117**(19): p. 5067-77.

131. Covas, D.T., et al., Multipotent mesenchymal stromal cells obtained from diverse human tissues share functional properties and gene-expression profile with CD146+ perivascular cells and fibroblasts. Exp Hematol, 2008. **36**(5): p. 642-54.

132. Collett, G.D. and A.E. Canfield, *Angiogenesis and pericytes in the initiation of ectopic calcification.* Circ Res, 2005. **96**(9): p. 930-8.

133. Gubernator, M., et al., Epigenetic profile of human adventitial progenitor cells correlates with therapeutic outcomes in a mouse model of limb ischemia. Arterioscler Thromb Vasc Biol, 2015. **35**(3): p. 675-88.

134. Kuja-Panula, J., et al., AMIGO, a transmembrane protein implicated in axon tract development, defines a novel protein family with leucine-rich repeats. J Cell Biol, 2003. **160**(6): p. 963-73.

135. Musacchio, M. and N. Perrimon, The Drosophila kekkon genes: novel members of both the leucine-rich repeat and immunoglobulin superfamilies expressed in the CNS. Dev Biol, 1996. **178**(1): p. 63-76.

136. Ashburner, M., et al., An exploration of the sequence of a 2.9-Mb region of the genome of Drosophila melanogaster: the Adh region. Genetics, 1999. **153**(1): p. 179-219.

137. Kajava, A.V., *Structural diversity of leucine-rich repeat proteins.* J Mol Biol, 1998. **277**(3): p. 519-27.

138. Kamiguchi, H. and V. Lemmon, Neural cell adhesion molecule L1: signaling pathways and growth cone motility. J Neurosci Res, 1997. **49**(1): p. 1-8.

139. Martinek, S. and U. Gaul, *Neural development: how cadherins zipper up neural circuits.* Curr Biol, 1997. **7**(11): p. R712-5.

140. Rothberg, J.M., et al., slit: an extracellular protein necessary for development of midline glia and commissural axon pathways contains both EGF and LRR domains. Genes Dev, 1990. **4**(12A): p. 2169-87.

141. Schwab, M.E., Functions of Nogo proteins and their receptors in the nervous system. Nat Rev Neurosci, 2010. **11**(12): p. 799-811.

142. Ng, A. and R.J. Xavier, Leucine-rich repeat (LRR) proteins: integrators of pattern recognition and signaling in immunity. Autophagy, 2011. **7**(9): p. 1082-4.

143. Li, Z., et al., AMIGO2 modulates T cell functions and its deficiency in mice ameliorates experimental autoimmune encephalomyelitis. Brain Behav Immun, 2017. **62**: p. 110-123.

144. Benedetti, G., et al., IL-17A and TNF-alpha Increase the Expression of the Antiapoptotic Adhesion Molecule Amigo-2 in Arthritis Synoviocytes. Front Immunol, 2016. **7**: p. 254.

145. Shen, S., T. Gui, and C. Ma, Identification of molecular biomarkers for pancreatic cancer with mRMR shortest path method. Oncotarget, 2017. **8**(25): p. 41432-41439.

146. Rabenau, K.E., et al., DEGA/AMIGO-2, a leucine-rich repeat family member, differentially expressed in human gastric adenocarcinoma: effects on ploidy, chromosomal stability, cell adhesion/migration and tumorigenicity. Oncogene, 2004. **23**(29): p. 5056-67.

147. Kanda, Y., et al., Amigo2-upregulation in Tumour Cells Facilitates Their Attachment to Liver Endothelial Cells Resulting in Liver Metastases. Sci Rep, 2017. **7**: p. 43567.

148. Hossain, S., et al., *Expressions and Roles of AMIGO Gene Family in Vascular Endothelial Cells.* International Journal of Bioscience, Biochemistry and Bioinformatics, 2012. **2**(1): p. 1-5.

149. Park, H., et al., AMIGO2, a novel membrane anchor of PDK1, controls cell survival and angiogenesis via Akt activation. J Cell Biol, 2015. **211**(3): p. 619-37.

150. Ono, T., et al., Alivin 1, a novel neuronal activity-dependent gene, inhibits apoptosis and promotes survival of cerebellar granule neurons. J Neurosci, 2003. **23**(13): p. 5887-96.

151. Martin, M., Cutadapt removes adapter sequences from high-throughput sequencing reads.2011. **17**(1).

152. Dobin, A., et al., *STAR: ultrafast universal RNA-seq aligner.*Bioinformatics, 2012. **29**(1): p. 15-21.

153. Love, M.I., W. Huber, and S. Anders, Moderated estimation of fold change and dispersion for RNA-seq data with DESeq2. Genome Biol, 2014. **15**(12): p. 550.

154. Anders, S., P.T. Pyl, and W. Huber, *HTSeq--a Python framework to work with high-throughput sequencing data.* Bioinformatics, 2014. **31**(2): p. 166-9.

155. Vladar, E.K., D. Antic, and J.D. Axelrod, *Planar cell polarity signaling: the developing cell's compass.* Cold Spring Harb Perspect Biol, 2009. **1**(3): p. a002964.

156. Peng, H., et al., Characterization of the human nicotinic acetylcholine receptor subunit alpha (alpha) 9 (CHRNA9) and alpha (alpha) 10 (CHRNA10) in lymphocytes. Life Sci, 2004. **76**(3): p. 263-80.

157. Fournier, P.G., et al., The TGF-beta Signaling Regulator PMEPA1 Suppresses Prostate Cancer Metastases to Bone. Cancer Cell, 2015. **27**(6): p. 809-21.

158. Chen, X., et al., *STEAP4 and insulin resistance.* Endocrine, 2014. **47**(2): p. 372-9.

159. Puig-Oliveras, A., et al., Expression-based GWAS identifies variants, gene interactions and key regulators affecting intramuscular fatty acid content and composition in porcine meat. Sci Rep, 2016. **6**: p. 31803.

160. Canham, P.B., H.M. Finlay, and D.R. Boughner, Contrasting structure of the saphenous vein and internal mammary artery used as coronary bypass vessels. Cardiovasc Res, 1997. **34**(3): p. 557-67.

161. Halka, A.T., et al., The effects of stretch on vascular smooth muscle cell phenotype in vitro. Cardiovasc Pathol, 2008. **17**(2): p. 98-102.

162. Predel, H.G., et al., Implications of pulsatile stretch on growth of saphenous vein and mammary artery smooth muscle. Lancet, 1992. **340**(8824): p. 878-9.

163. Asnacios, A. and O. Hamant, *The mechanics behind cell polarity.* Trends Cell Biol, 2012. **22**(11): p. 584-91.

164. Scott, L., et al., Subendothelial proteoglycan synthesis and transforming growth factor beta distribution correlate with susceptibility to atherosclerosis. J Vasc Res, 1997. **34**(5): p. 365-77.

165. Lee, R.T., et al., Mechanical strain induces specific changes in the synthesis and organization of proteoglycans by vascular smooth muscle cells. J Biol Chem, 2001. **276**(17): p. 13847-51.

ACKNOWLEDGMENTS

I would like to thank the many people who have contributed to the work of this thesis and have supported me during these years.

A special appreciation and thanks to my supervisors Professor Gianfranco Pintus and Dr Gaia Spinetti for all their support and guidance throughout my PhD project. I am also very grateful to Professor Paolo Madedduwho gave me the opportunity to spend the last yearof my PhD at the Bristol Heart Institute.

I would like to thank all my colleagues and friends at MultiMedica who have supported me, helping me to grow as a person and giving me an extraordinary time in my life. Thanks to Rossella, Elena, Emanuela, Chiara and Cristina and all of the MultiMedica Pathology Anatomy department.

I would also like to thank all of the staff in level 7 of the Bristol Royal Infirmary. The support and enthusiasm they have shown me will never be forgotten. Thanks to Eva for all she has taught me. Thanks to Elisa for her support.Thanks toGraciella and her patience. Thanks to David, Ashton, Michele, Marie, Alex, Sadie, Will and Valeria.

Thanks to Vanessa, Maria Francesco and Kiyan who have made this experience in Bristol so special.

None of this would have been possible without the constant support and encouragement of my friends and especially of my family who have been a constant source of support and strength throughout.